CHEMISTRY OF GOLD IN SOME WESTERN AUSTRALIAN SOILS

D.J. Gray, M.J. Lintern and G.D. Longman

CRC LEME OPEN FILE REPORT 68

February 1999

CHEMISTRY OF GOLD IN SOME WESTERN AUSTRALIAN SOILS

D.J. Gray, M.J. Lintern and G.D Longman

CRC LEME OPEN FILE REPORT 68

February 1999

RESEARCH ARISING FROM CSIRO/AMIRA REGOLITH GEOCHEMISTRY PROJECTS 1987-1993

In 1987, CSIRO commenced a series of multi-client research projects in regolith geology and geochemistry which were sponsored by companies in the Australian mining industry, through the Australian Mineral Industries Research Association Limited (AMIRA). The initial research program, "Exploration for concealed gold deposits, Yilgarn Block, Western Australia" (1987-1993) had the aim of developing improved geological, geochemical and geophysical methods for mineral exploration that would facilitate the location of blind, buried or deeply weathered gold deposits. The program included the following projects:

P240: Laterite geochemistry for detecting concealed mineral deposits (1987-1991). Leader: Dr R.E. Smith.
Its scope was development of methods for sampling and interpretation of multi-element laterite geochemistry data and application of multi-element techniques to gold and polymetallic mineral exploration in weathered terrain. The project emphasised viewing laterite geochemical dispersion patterns in their regolith-landform context at local and district scales. It was supported by 30 companies.

P241: Gold and associated elements in the regolith - dispersion processes and implications for exploration (1987-1991). Leader: Dr C.R.M. Butt.
The project investigated the distribution of ore and indicator elements in the regolith. It included studies of the mineralogical and geochemical characteristics of weathered ore deposits and wall rocks, and the chemical controls on element dispersion and concentration during regolith evolution. This was to increase the effectiveness of geochemical exploration in weathered terrain through improved understanding of weathering processes. It was supported by 26 companies.

These projects represented "an opportunity for the mineral industry to participate in a multi-disciplinary program of geoscience research aimed at developing new geological, geochemical and geophysical methods for exploration in deeply weathered Archaean terrains". This initiative recognised the unique opportunities, created by exploration and open-cut mining, to conduct detailed studies of the weathered zone, with particular emphasis on the near-surface expression of gold mineralisation. The skills of existing and specially recruited research staff from the Floreat Park and North Ryde laboratories (of the then Divisions of Minerals and Geochemistry, and Mineral Physics and Mineralogy, subsequently Exploration Geoscience and later Exploration and Mining) were integrated to form a task force with expertise in geology, mineralogy, geochemistry and geophysics. Several staff participated in more than one project. Following completion of the original projects, two continuation projects were developed.

P240A: Geochemical exploration in complex lateritic environments of the Yilgarn Craton, Western Australia (1991-1993). Leaders: Drs R.E. Smith and R.R. Anand.
The approach of viewing geochemical dispersion within a well-controlled and well-understood regolith-landform and bedrock framework at detailed and district scales continued. In this extension, focus was particularly on areas of transported cover and on more complex lateritic environments typified by the Kalgoorlie regional study. This was supported by 17 companies.

P241A: Gold and associated elements in the regolith - dispersion processes and implications for exploration. Leader: Dr. C.R.M. Butt.
The significance of gold mobilisation under present-day conditions, particularly the important relationship with pedogenic carbonate, was investigated further. In addition, attention was focussed on the recognition of primary lithologies from their weathered equivalents. This project was supported by 14 companies.

Although the confidentiality periods of the research reports have expired, the last in December 1994, they have not been made public until now. Publishing the reports through the CRC LEME Report Series is seen as an appropriate means of doing this. By making available the results of the research and the authors' interpretations, it is hoped that the reports will provide source data for future research and be useful for teaching. CRC LEME acknowledges the Australian Mineral Industries Research Association and CSIRO Division of Exploration and Mining for authorisation to publish these reports. It is intended that publication of the reports will be a substantial additional factor in transferring technology to aid the Australian Mineral Industry.

Chemistry of Gold in some Western Australian Soils

Report to AMIRA Project 241

CSIRO/AMIRA Weathering Processes Group

D.J. Gray, M.J. Lintern and G.D. Longman

November 1990

CSIRO Division of Exploration Geoscience
Floreat Park WA

PREFACE

Soil sampling is extensively employed in modern-day Au exploration. A major part of the activity of the Weathering Processes group has been to examine the distribution of Au in soils, with regard to improving soil sampling techniques. This report details work on the chemistry of Au in southern Yilgarn soils, with the goal of understanding how Au is associated with the soil constituents. This subject is important for our understanding of the mechanisms of soil Au anomaly formation and deciding how to most effectively use soil as an exploration medium. Specifically, the study:

    (i)   demonstrates the high solubility of Au in soils;

    (ii)   indicates that, contrary to expectations, Au in the carbonate horizon is more soluble than Au in the other horizons;

    (iii)   demonstrates the lesser solubility of Au in Fe oxide dominated soils;

    (iv)   suggests that Au in carbonate-rich soils is highly extractable, with at least two forms: Au associated with organic matter in surface horizons; and Au associated with carbonate surfaces;

    (v)   suggests that Au distribution in soils is controlled by physical rather than chemical factors: specifically that the Au/carbonate association is due to Au being precipitated via evaporative processes.

This investigation is complementary to other investigations of Au chemistry and studies of the nature and surface expression of gold mineralization. Together they address many of the principal objectives of the Project.

C.R.M. Butt,
Project Leader.
November, 1990

ABSTRACT

The chemistry of Au in sample soils from the southern Yilgarn, W.A. was investigated by a variety of experiments. Soil solution and incubation studies implied that in carbonate-rich soils dolomite was forming as a result of evaporative processes, with the soil solution in the carbonate horizon being more saline than elsewhere, and containing high concentrations of Na and Mg. The dolomite appears to be coating the surfaces of other minerals, and will therefore dominate the chemistry of this zone.

Shaking $AuCl_4^-$ solutions with various soil samples showed that the samples least likely to adsorb $AuCl_4^-$ over one day are those enriched in carbonates and low in organic matter. This may reflect poor adsorption of anionic Au complexes at the higher pH of the carbonate dominated materials

Selective extraction data suggested that various forms of Au exist in the soils tested. In the upper part of the profile where organic matter is high, Au appears to be associated with this phase. Lower in the profile, Au associated with the Fe oxides or other non-carbonate materials generally has a moderate extractability, which is considerably lower for samples that are merely crushed to < 10 mm, relative to those pulverized to < 75 μm, suggesting that the Au occurs within solid phases or is otherwise not available to solution. Gold associated with carbonates is very soluble, even in crushed samples, suggesting that a substantial part of the Au associated with carbonates is on surfaces or in environments that are readily accessible to the solution.

Soil incubation experiments were performed on three samples from various depths down a carbonate-rich soil profile. Shaking the samples with deionized water resulted in significant dissolution of about 10 μg/L Au over one week for all three samples. This dissolution was suppressed by CO_2 bubbling. The dissolved Au then reprecipitated in the mixtures with the two samples that occurred closer to the soil surface. Reprecipitation was prevented by irradiation of the mixtures, indicating it to be a result of biological activity. The deeper, carbonate-rich sample differed in that Au dissolution increased with time and was not suppressed by CO_2 bubbling.

When the soil samples were shaken with a solution containing $AuCl_4^-$ the Au precipitated from solution. After several weeks exposure, there was major redissolution of the Au (up to 2.3 mg/L) in the mixtures with the two samples closer to the surface. This redissolution was completely repressed by CO_2 bubbling and strongly reduced by irradiation. The redissolution carbonate-rich sample showed a sustained redissolution, that was less strongly affected by CO_2 bubbling or irradiation.

Thus, the incubation experiments indicated that the soil samples tested had the capacity to dissolve major concentrations of Au. Results suggested that Au dissolved more readily from the carbonate-rich sample than from samples further up in the profile.

Results to date suggest that, contrary to expectations, Au is less strongly adsorbed by, and more soluble from, carbonate-rich horizons than other soil zones. The mechanism for Au concentration in this zone is suggested to be evaporative concentration, rather than through chemical factors. This hypothesis may have important applications for the use of soil as an exploration tool north of the Menzies line.

TABLE OF CONTENTS

LIST OF FIGURES

LIST OF TABLES

LIST OF ABBREVIATIONS

OC: organic carbon
SI: saturation index
TDS: total dissolved solids
TMF: Telfer mill feed sample
XRD: X-ray diffraction

LIST OF COMPOUNDS

CN^-:   cyanide
HCl: hydrochloric acid
HS^-:   hydrogen sulphide
I^-:   iodide
KCN: potassium cyanide
NaOH: sodium hydroxide
SCN^-:   thiocyanate
$S_2O_3^{2-}$:   thiosulphate

LIST OF MINERALS

Calcite: $CaCO_3$
Dolomite: $CaMg(CO_3)_2$
Fe oxides: generic term for iron oxides, oxyhydroxides and hydroxides
Halite: NaCl
Siderite: $FeCO_3$

1.   Introduction

This report describes experiments investigating the mobility of gold in soils. These studies are being run parallel to investigations on the hydrogeochemistry of Au within surface and deeper groundwaters, in order to obtain information on Au mobility for weathering environments of importance within the Yilgarn Block. Soils are commonly the most convenient and cheapest medium for Au exploration. However several problems are encountered in investigating their characteristics:

(i) Soils are generally highly weathered, and minerals of interest are generally small grained, often poorly crystalline and/or of varying chemical composition. The most chemically active phases, such as fine hydrated Fe or Mn oxides or organic matter, are generally very hard to investigate by direct instrumental techniques such as thin-section studies, X-ray diffraction (XRD) or electron microprobe;

(ii) Complex biological reactions within the soil may be of major importance for element mobilities. This is because biological processes may control the pH/Eh characteristics of a soil, may produce important ligands (such as cyanide, amino acids, sulphur compounds or humic/fulvic acids), or may create important sites for sorption (such as solid organic matter, oxides precipitated via biological reactions, or cell walls). These factors may be of particular importance to Au, due to its very high affinity for organic derived ligands (Gray, 1988) such as those mentioned above. These biological reactions are extremely complex and very difficult to model, or to extrapolate results from one site or set of conditions to another.

(iii) Soil solutions are difficult to separate. In addition, soils within the Yilgarn block are commonly very dry. It is possible that major chemical redistributions occur during periods of higher water content, *i.e.*, after rain.

In general the distribution and chemistry of trace elements in soils is most effectively investigated using chemical techniques such as selective extraction or incubation studies. Though it is generally recognized that such techniques may not provide absolute answers, they may provide very useful insights into the chemistry of elements in soils.

The present study involved a number of specific techniques, namely:

   (i)   soil incubations;
  (ii)   soil solution studies;
 (iii)   sorption tests;
 (iv)   extraction tests.

Results from soil incubation experiments on samples from a gold rich profile in the southern Yilgarn (Section 3) implied a number of fundamental changes to the initial assumptions on the behaviour of Au in these soils. This experiment was restricted to a limited suite of samples, and further, shorter, experiments were therefore conducted on a wider range of materials (Sections 4-6). Section 7 explores some general principles that may be distinguished from this work. These experiments have led to previously unexpected hypotheses on the redistribution of Au in soil, that may ultimately be of importance in the use of soil as an exploration medium.

## 2.	Soil Materials

Soil samples from three soil profiles (A,B and C) were selected from a gold deposit located in an area east of Hyden in Western Australia. The samples were selected primarily because they satisfied the following criteria:

(i)	they were situated directly over (profile A), within 5 m of (on hanging wall; profile B), and within 400 m of (with possible quartz stringers close by; profile C) known mineralization, and all contained readily detectable amounts of Au (several hundred µg/kg);

(ii)	they are examples of two commonly found semi-arid soil profiles that occur throughout the southern Yilgarn. These are a clay-rich type (Profiles A and B) consisting, predominantly, of deep, kaolinite clay infused near the surface with pedogenic carbonate, and a sandy lateritic type comprised of ferruginous nodules (Profile C).

Of particular interest in two of the profiles (A and B) was the close association of Au with pedogenic carbonate. This phenomenon has recently been reported from a variety of locations within the Yilgarn block (e.g., Lintern, 1989; Lintern and Scott, 1990).

The geology of the area consists of a sequence of metamorphosed volcanic and sedimentary rocks. Specifically, the area is dominated by a flow sequence of mafic (tholeiitic basalt, dolerite and gabbro), ultramafic (peridotitic komatiite, dunite and talcose schists) and chemical sediments (cherts, siltstone and sandstone). Mineralization is hosted primarily by a steeply dipping, semi-conformable shear system comprised of BIF-chert units near the contact of a mafic intrusive and the ultramafic flow sequence.

The major landform of the area is an undulating plain averaging about 440 m above sea level with local relief from 25-50 m. The uplands are often mantled by a relict regolith of lateritic origin. There has been extensive, though incomplete, stripping of the lateritic material along the valley floors and flanking slopes, and many of these areas are now mantled by deep, red clay-rich material, infused near the surface with pedogenic carbonate.

The nature and density of the vegetation is largely controlled by soil type and topographic location and consists of a mosaic of plant communities. Over the deep red clays, scelerophyll woodland is dominant, consisting of a eucalypt canopy (up to 10m in height) with occasional larger salmon gums and a lower semi-continuous shrubby horizon up to 1-2m high where tea-tree is dominant. On the lateritic uplands and adjacent sand plain, broombush thickets and heathland is dominant and consists of a large variety of genera including acacias, casuarinas, hakeas and occasional mallee eucalypt.

The main features of the climate at Hyden are cool winters, hot summers and winter rainfall. Summer maximum and minimum temperatures are 31°C and 14°C, respectively; winter maximum and minimum temperatures are 15°C and 5°C, respectively. Extremes recorded for Hyden are 45°C and -3°C. Annual evaporation is about 2200 mm. Rains are mainly from cold fronts associated with sub-Antarctic lows. Falls from cold fronts rarely exceed 10 mm but may reach 40 mm or more if supplemented by moist air emanating from north-west, tropical rain-bearing depressions. Rain occasionally falls (up to 50 mm) from thunderstorms associated with troughs moving in from the west (Anon, 1981).

2.1. Profile A

The major and minor element geochemistry of Profile A samples are given in Table 1.

Table 1: Elemental Compositions* of Samples from Profile A.

	Method	1467	1468	1470
Depth (cm)	-	5-15	15-25	60-80
OC		0.95	0.57	0.18
SiO_2	ICP	64.23	47.54	24.96
Al_2O_3	ICP	12.22	13.05	9.53
Fe_2O_3	ICP	8.88	14.57	11.08
MgO	ICP	1.28	1.86	8.86
CaO	ICP	0.64	3.63	14.37
Na_2O	ICP	0	0.03	0.27
TiO_2	ICP	0.47	0.51	0.36
P_2O_5	ICP	0.03	0	0
As	NAA	14.5	28.5	25.7
Au	NAA	0.9	2.93	4.26
Ba	ICP	94	155	168
Be	ICP	0	0.48	3.52
Ce	NAA	26.3	25.3	15.6
Co	ICP	27.5	26	9.11
Co	NAA	24.5	22.1	15.7
Cr	ICP	521	953	805
Cr	NAA	575	1030	840
Cu	ICP	44.1	78.7	80.3
La	NAA	15.3	15.1	10.1
Mn	ICP	414	430	295
Mo	NAA	3.6	4.4	4.1
Ni	ICP	156	152	88.3
Sb	NAA	0.55	1.58	0.42
V	ICP	155	283	251
W	NAA	3.1	3.7	3.3
Zr	ICP	103	101	61

* All oxides, and organic carbon (OC) in %, all other elements in mg/kg (ppm)

The mineralogy of these samples, as determined by XRD, is given in Table 2.

Measurement of shifts of the calcite reflections in the XRD patterns of the carbonate containing samples indicated the calcite to contain less than 5% Mg.

The soils can be loosely described as:

1467: Organic rich

1468: Iron oxide rich

1470: Carbonate rich

Table 2: Semi-quantitative Mineralogy of Samples from Profile A.

Mineral	1467	1468	1470
Smectite	xxx	xxx	-
Kaolin	xxx	xxx	xx
Quartz	xxx	xx	x
Goethite	x	xx	x
Hematite	?	?	?
Anatase	x	?	-
Rutile	x	?	-
Calcite	-	xx	x
Dolomite	-	x	xxx
Feldspar	-	-	x

xxx	major component	?	possible component
xx	minor component	-	below detection
x	trace component		

2.2. Profile B

Data for samples from Profile B are given in Tables 3 and 4.

Table 3: Elemental Compositions* for Profile B Samples.

	Sample												
	1214	1202	1203	1204	1205	1206	1207	1208	1209	1210	1211	1212	1213
Depth (m)	0.005	0.025	0.075	0.125	0.175	0.250	0.350	0.450	0.600	0.800	1.000	1.450	1.800
pH		6.8	6.9	7.0	6.9	6.5	6.5	6.6	7.0	7.1	6.7	6.2	6.1
OC	2.70	1.66	1.36	1.03	0.48	0.28	0.17	0.16	0.14	0.25	0.12	0.10	0.05
SiO_2	70.1	66.7	60.9	50.6	42.2	41.7	45.4	49.2	53.1	55.9	63.4	70.9	72.6
TiO_2	0.40	0.39	0.39	0.32	0.30	0.32	0.37	0.41	0.44	0.46	0.52	0.55	0.52
Al_2O_3	8.78	8.94	9.05	7.88	7.68	8.32	9.31	10.30	11.30	11.80	13.20	14.00	14.30
Fe_2O_3	6.23	5.98	5.72	4.04	4.28	4.07	4.93	5.27	5.49	5.50	6.07	6.49	5.92
MgO	1.72	2.04	2.60	4.97	7.25	8.46	6.91	6.62	5.90	5.29	3.36	1.23	0.95
CaO	3.15	5.33	7.47	11.20	13.20	13.00	9.13	8.58	7.42	6.33	3.15	0.11	0.06
Au	0.136	0.240	0.260	0.680	0.830	0.780	0.580	0.540	0.600	0.520	0.530	0.072	0.004
Ba	103	105	106	108	140	258	218	273	212	177	181	182	157
Be	1.20	0.00	0.00	0.00	0.00	0.00	0.00	0.00	0.00	0.00	0.0⌐	0.00	0.00
Cr	268	213	294	160	167	172	198	217	238	241	279	331	342
Cu	23	30	50	40	54	47	48	51	54	53	62	76	60
Mn	848	652	629	488	428	458	439	478	437	439	490	415	114
Ni	66	68	76	63	59	66	70	75	74	77	87	104	66
V	102	102	103	71	94	131	154	141	110	107	115	123	109
Zr	83	97	100	76	65	70	85	89	95	103	112	116	102

* All oxides, and OC in %, all other elements in mg/kg.

Table 4: Semi-quantitative Mineralogy, as based on XRD Analysis, of Profile B Samples.

	Sample												
	1214	1202	1203	1204	1205	1206	1207	1208	1209	1210	1211	1212	1213
Depth (m)	0.005	0.025	0.075	0.125	0.175	0.250	0.350	0.450	0.600	0.800	1.000	1.450	1.800
Kaolin	x	xxx	xxx	xxx	xxx	xxx	xxx	xxx	xxx	xxx	xxx	xxx	xxx
Quartz	xxx	xxx	xxx	xxx	xxx	xxx	xxx	xxx	xxx	xxx	xxx	xxx	xxx
Hematite	x	x	x	x	x	x	?	?	?	?	x	x	x
Goethite	-	-	-	-	-	-	-	-	-	?	?	x	x
Calcite	x	xx	xxx	xx	xx	x	-	-	-	-	-	-	-
Dolomite	x	x	xx	xxx	xxx	xxx	xxx	xxx	xxx	xxx	xxx	xx	-
Gypsum	-	-	-	-	-	-	-	-	-	-	-	x	x
Anatase	x	-	-	-	-	x	-	-	-	x	x	x	x
Rutile	?	-	-	-	-	x	-	-	-	x	x	x	x

xxx	major component	?	possible component
xx	minor component	-	below detection
x	trace component	nd	not determined

This profile is strongly enriched in calcite and dolomite. The most carbonate-rich zone occurs at about 0.15 to 0.3 m, which corresponds to the zone of highest Au (Fig. 1). As expected, organic carbon is highest in the uppermost part of the soil profile. Total carbonate is highest at about 0.2 m depth, and it steadily decreases with depth to about zero at 1.5 m. Dolomite is generally the dominant carbonate mineral, with calcite being dominant only at the top 0.1 m of the profile (Table 4).
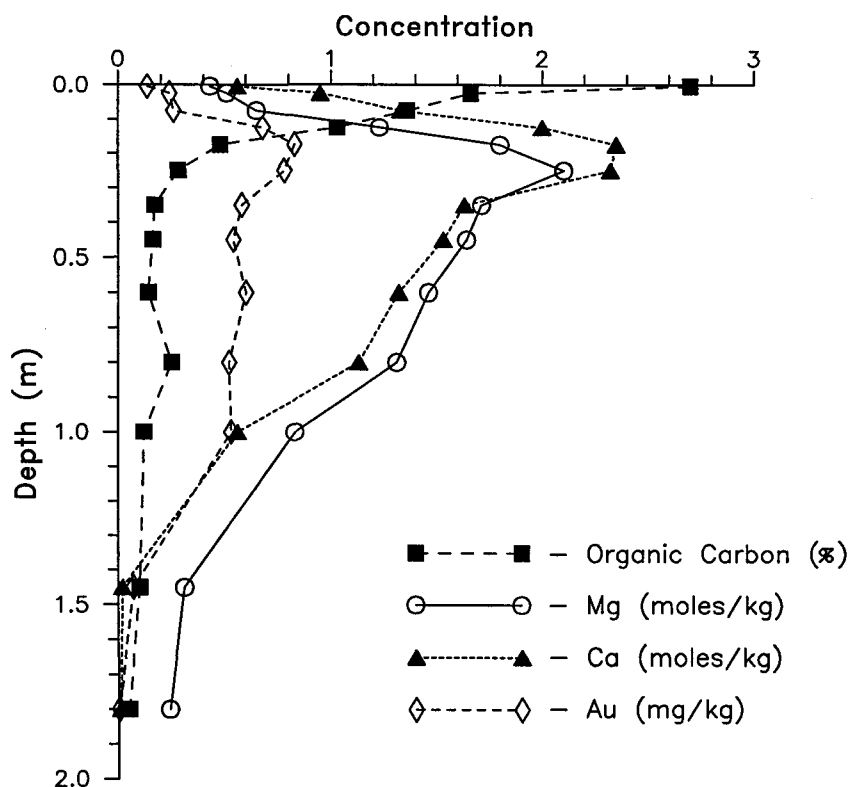
Figure 1: Organic Carbon, Mg, Ca and Au vs. Depth for Profile B.

2.3. Profile C

Data for samples from Profile C are shown in Tables 5 and 6.

Table 5: Elemental Compositions* for Profile C Samples.

| | Sample | | | | | | |
	1239	1241	1243	1245	1247	1249	1251
Depth (m)	0.025	0.125	0.250	0.450	0.650	0.850	1.300
pH	4.6	4.6	4.4	4.3	4.2	4.3	4.4
OC	1.30	0.46	0.24	0.14	0.07	0.07	0.02
SiO_2	59.4	47.4	38.5	31.0	32.4	34.4	24.3
TiO_2	0.44	0.47	0.50	0.55	0.53	0.57	0.45
Al_2O_3	11.40	12.90	19.90	19.90	20.50	17.60	13.70
Fe_2O_3	20.40	32.10	30.60	36.30	37.50	36.30	48.90
MgO	0.08	0.07	0.06	0.06	0.07	0.06	0.05
CaO	0.06	0.06	0.05	0.04	0.05	0.04	0.05
Au	0.170	0.240	0.160	0.221	0.170	0.490	0.990
Ba	24	11	9	3	0	1	0
Be	0.00	0.00	0.00	0.00	0.00	0.00	0.00
Cr	921	1156	1506	1617	1352	1417	1079
Cu	51	74	137	193	208	205	265
Mn	43	59	42	48	51	67	73
Ni	44	57	65	69	68	62	74
V	353	434	480	702	571	830	597
Zr	139	161	180	180	168	156	146

*   All oxides, and OC in %, all other elements in mg/kg

Table 6: Semi-quantitative Mineralogy, as based on XRD Analysis, for Profile C Samples.

| | Sample | | | | | | |
	1239	1241	1243	1245	1247	1249	1251
Depth (m)	0.025	0.125	0.250	0.450	0.650	0.850	1.300
Kaolin	xxx	xxx	xxx	xxx	xxx	xxx	xxx
Quartz	xxx	xxx	xxx	xxx	xxx	xxx	xxx
Hematite	xx	xxx	xx	xx	xx	xx	xxx
Goethite	x	xx	xxx	xxx	xxx	xxx	xxx
Calcite	-	-	-	-	-	-	-
Dolomite	-	-	-	-	-	-	-

xxx   major component   x   trace component
xx   minor component   -   below detection

As can be observed, this profile is considerably enriched in the Fe oxide minerals hematite and goethite, with no carbonate observed. Gold distribution differs significantly from that in the carbonate-rich Profile B, remaining approximately constant at about 0.2 mg/kg down to 0.7 m, and then increasing rapidly with depth (Fig. 2). There is little correlation between Au and either organic carbon or Fe content.
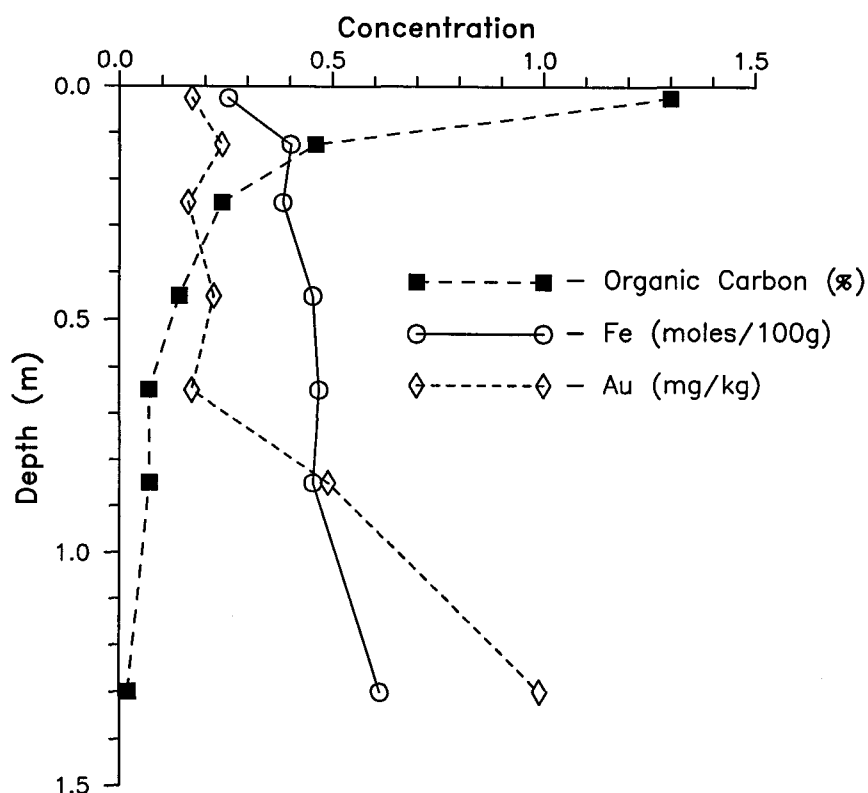
Figure 2: Organic Carbon, Fe and Au vs. Depth for Profile C.

2.4.   Single Samples

The three other samples investigated were standard 7 (Std. 7), standard 11 (Std. 11) and a Mill Feed sample from Telfer Mine (TMF). Standard 7 was a bulk sample of surface lateritic gravel obtained from a bulldozed slope near Holleton. Standard 11 was a bulk sample of lateritic duricrust obtained from a pit at Mt. Gibson Gold Mine, at least one metre below the natural surface. Telfer Mill Feed sample was a standard mill feed sample. The chemistry and mineralogy of these samples are shown in Table 7.

Standard 7 and Std. 11 have very similar chemical compositions and mineralogies, differing mainly in that Std. 7 contains significantly more organic matter, consistent with it being a surface sample. TMF shows the standard mineralogy of a saprolitic or mottled zone material.

Table 7: Chemistry and Mineralogy of Samples Std. 7, Std. 11 and TMF.

	Std. 7	Std. 11	TMF
Description	Lateritic Material	Lateritic Duricrust	Saprolite
pH	4.7	6.7	8.1
OC	1.22	0.04	0.02
SiO_2	45.6	42.8	76.3
TiO_2	1.48	1.62	0.98
Al_2O_3	17.5	19.1	11.3
Fe_2O_3	28.6	27.0	6.1
MgO	0.16	0.05	0.22
CaO	0.19	0.02	0.17
Au	0.59	3.15	nd
Ba	23	590	210
Be	0.7	0.7	0.2
Cr	410	460	100
Cu	42	35	197
Mn	170	95	73
Ni	35	22	0
V	790	1620	75
Zr	180	270	370
Mineralogy	Hematite, Kaolinite, Quartz, Goethite (trace), Mica	Kaolinite, Hematite, Quartz, Goethite, Mica	Quartz, Kaolinite (well ordered), Muscovite mica, Goethite (trace)

nd: not determined

3.   Soil Incubations

3.1.   Introduction

The object of the incubation experiments was to test the capacity of the soils to dissolve or precipitate Au. This would presumably involve the interaction of a number of factors, such as the form of the Au in the soil, potential Au ligands present, and changes in the soil solution characteristics over time. Results from these experiments are complex and difficult to interpret unambiguously in the absence of other work. However, these experiments proved invaluable to the conceptual modelling of Au transport in soils (Section 3.4), and provided for further experimentation to test the models proposed (as detailed in Sections 4 to 6).

3.2.   Methodology

The samples used for this set of experiments were those from Profile A. The elemental compositions and mineralogies of these samples are given in Tables 1 and 2. Sample preparation involved crushing to < 10 mm (which was virtually unnecessary, due to the highly friable nature of these samples). The samples were investigated by batch experiments as follows:

Four differing solutions were mixed with each of the soils at a ratio of 50 g soil to 100 mL water:

(i)   deionized water only;
(ii) deionized water/CO_2 bubbled into the slurry;
(iii) deionized water/5 mg/L $AuCl_4^-$;
(iv) deionized water/5 mg/L $AuCl_4^-$/CO_2 bubbled into the slurry.

Four 350 mL glass bottles were set up for each soil-solution combination, giving a total of (4 differing solutions) x (3 different samples) x 4 = 48 samples. These were sealed and shaken in the dark, and then removed at the following time intervals:

(i)   one day;
(ii) one week;
(iii) one month;
(iv) six months.

The slurries were then centrifuged at 4000 revolutions per minute (rpm) for 15 min. An aliquot of the supernatant was used for alkalinity titration (to give HCO_3^- concentration) and pH measurements, with the remainder filtered through 0.45 µm membrane filter. A sub-sample was analysed by Ion Chromatography, for Cl^-, Br^-, SO_4^{2-} and NO_3^- [1], using a DIONEX AS4A column under standard eluent conditions with a conductivity detector, and for I^- using a DIONEX AS5 column under standard eluent conditions with an electrochemical detector (Dionex, 1985). Another sub-sample was acidified and analysed for Na, K, Ca and Mg by flame AAS on a Varian AA875, and a further sub-sample was analysed for Au by ICP-MS.

In an additional experiment two differing solutions [analogous to solutions (i) and (iii) in the first batch experiment] were mixed with the soils at a ratio of 50 g soil to 100 ml water:

(i)   deionized water
(ii) deionized water/5 mg/L $AuCl_4^-$

Two 350 ml bottles were set up for each soil-solution combination, giving a total of (2 differing solutions) x (3 different soil samples) x 2 = 12 samples. These were sealed, and then sterilized by irradiation with 4 megarads for 8 hrs on a GC220 Irradiater, with a Co^{60} source [2], and shaken in the dark. Irradiation was used in this experiment, rather than heating or treating with oxidative solutions, because it prevented biological activity, with the minimum of change to the chemistry of the soil. One set of the bottles was taken off the shaker at three months, and a 10 mL liquid sample filtered and collected as described above. Following this, 10 mL of deionized water and one gram of UNTREATED soil sample was added to the bottle, thus allowing the mixture to be "inoculated" with the normal soil organisms. The bottle was then returned to the shaker.

Three months later (*i.e.*, six months after the irradiation) the inoculated mixtures, and the mixtures that had been irradiated and then shaken for six months, were taken off the shaker, and solutions analysed for Au as described above.

---

[1] Note that the cations are analysed as the element (*e.g.*, Na), whereas ion chromatography analysed for the particular ion (*e.g.*, Cl^-), and this is reflected in how the elements are denoted in the text.

[2] Courtesy of WA Department of Agriculture.

All incubations were done in glass bottles, to ensure that plasticisers (or other additives to plastics) were not present, and that there were no plastic surfaces for Au precipitation.

3.3. Results

3.3.1. Tabulated Results

The elemental information was used for thermodynamic speciation of the solutions, using the computer program PHREEQE (Parkhurst *et al.*, 1980). This program has been used extensively in other reports (Gray, 1990a, b) and reference should be made to these reports for further details. Parameters derived from speciation analysis relevant to this experiment are gold solution speciation and degree of saturation with respect to various minerals. The latter parameter is quantified in terms of a saturation index (SI). If the SI for a solid phase is calculated as 0 then the solution is saturated with respect to the mineral concerned, while a value less than 0 implies the solution is undersaturated and a value greater than 0 implies the solution is oversaturated and precipitation of that solid should occur.

The SI data for the solids calcite, dolomite and magnesite are illustrated diagrammatically in Fig. 3. The SI values for each different solution type (as given in the key) are each plotted for each sampling time: thus the first four points of Fig. 3a are the plotted SI values for calcite for the 1467/water mixtures sampled at one day, one week, one month and 6 months; the next four points are the plotted SI values for calcite for the $1467/AuCl_4^-$/water mixtures, and so on. Analysis of the raw data showed that the solutions were just saturated to significantly oversaturated with respect to the carbonate minerals.

The SI values for Au were also calculated, and in all cases Au appeared to be strongly over-saturated with respect to Au metal. However the SI results for Au may be incorrect for several reasons:

(i) small concentrations of molecules such as cyanide (CN^-), sulphide or amino acids could have a strong effect on Au solubility;

(ii) the solid Au phase in the soils that is interacting with the solution is very possibly <u>NOT</u> Au metal, but instead could be a complexed and/or adsorbed form of Au;

(iii) opening the bottles for sampling may fundamentally affect solution parameters, such as the oxidation potential, that have a major effect on Au solubility.

One species that may have a major effect on Au solubility is thiosulphate ($S_2O_3^{2-}$). This was analysed for, but was below the detection limit (<0.002 mg/L) in all samples tested.
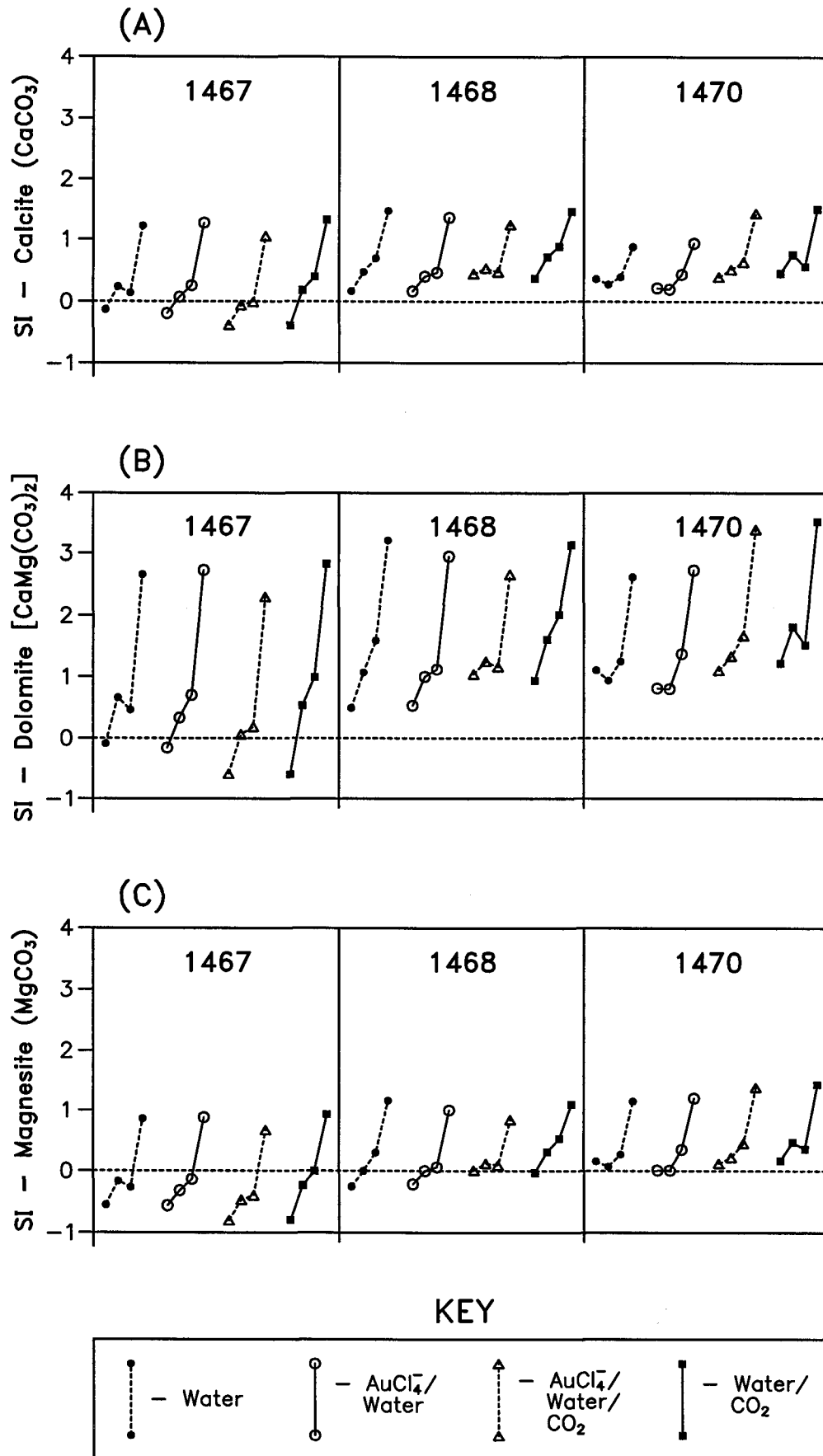
Figure 3: SI Values for Incubation Solutions (see Section 3.3.1 for details).

Results for the major elements are plotted in Figs. 4 to 15, and compiled in Appendix 1. In addition to the plots of element concentration vs time, the major element data can be plotted using ternary plots. In this method, the concentrations of the major anions and cations are recalculated as their charge equivalents. The % equivalents of the ions are then plotted on ternary diagrams for the cations and anions (Figs. 16 to 18), with the arrows representing the direction of changes in the chemistry of the solutions over time.

3.3.2.   General Chemistry

Solution acidity (pH) will clearly have a major effect on the geochemistry of gold and other elements. For the treatments that did not involve CO_2 bubbling, the measured pH for the various mixtures increased in the order 1467 < 1468 < 1470. This is presumably because of the higher concentration of humic material close to the surface (*i.e.*, sample 1467), which can often be associated with acid production, and the higher level of carbonate at depth (*i.e.*, sample 1470), which will generally be associated with alkaline conditions. The measured pH data (Fig. 4) shows a general decline in pH for one month, followed by an increase in pH by six months. This result is surprising, as pH is expected to generally decrease due to oxidation of organic matter:

$$(CH_2O) + O_2 \Rightarrow H^+ + HCO_3^- \qquad \qquad ...(1)$$

Additionally, speciation analysis (Fig. 3) showed that the six month solutions were particularly oversaturated with respect to calcite and dolomite: *i.e.*, there was more Ca and Mg or, alternatively, pH is too high, than would be allowed if the solution were in equilibrium with calcite or dolomite. This result is not feasible if, as is highly possible, the source of the Ca and Mg is these minerals .

One explanation of these results is that indeed the pH has been declining and CO_2 and HCO_3^- has been produced due to organic matter oxidation. The concentrations of dissolved CO_2 may have become particularly high in the six month samples, resulting in degassing and increase in pH, following opening of the bottles and centrifugation of the slurries:

$$HCO_3^- + H^+ \Rightarrow H_2O + CO_{2(g)} \qquad \qquad ...(2)$$

As the pH increases due to degassing, the solution becomes oversaturated with respect to the carbonate minerals. This hypothesis is supported by the observation of precipitated calcite in a number of the filtered six month solutions that were allowed to stand.

Solution concentrations of Ca and Mg are, as suggested above, dependent on equilibration with the carbonate minerals calcite and dolomite. The concentrations of these elements in the initial solutions (Figs. 5 and 6) are increased either by the addition of the gold standard (which contains acid) or CO_2 (which reacts with the solution as the acid H_2CO_3). This is consistent with dissolution of carbonate minerals with acid:

$$CaCO_3 + H^+ \Rightarrow Ca^{2+} + HCO_3^- \qquad \qquad ...(3)$$
$$\text{(calcite)}$$

(A)

(B)

(C)
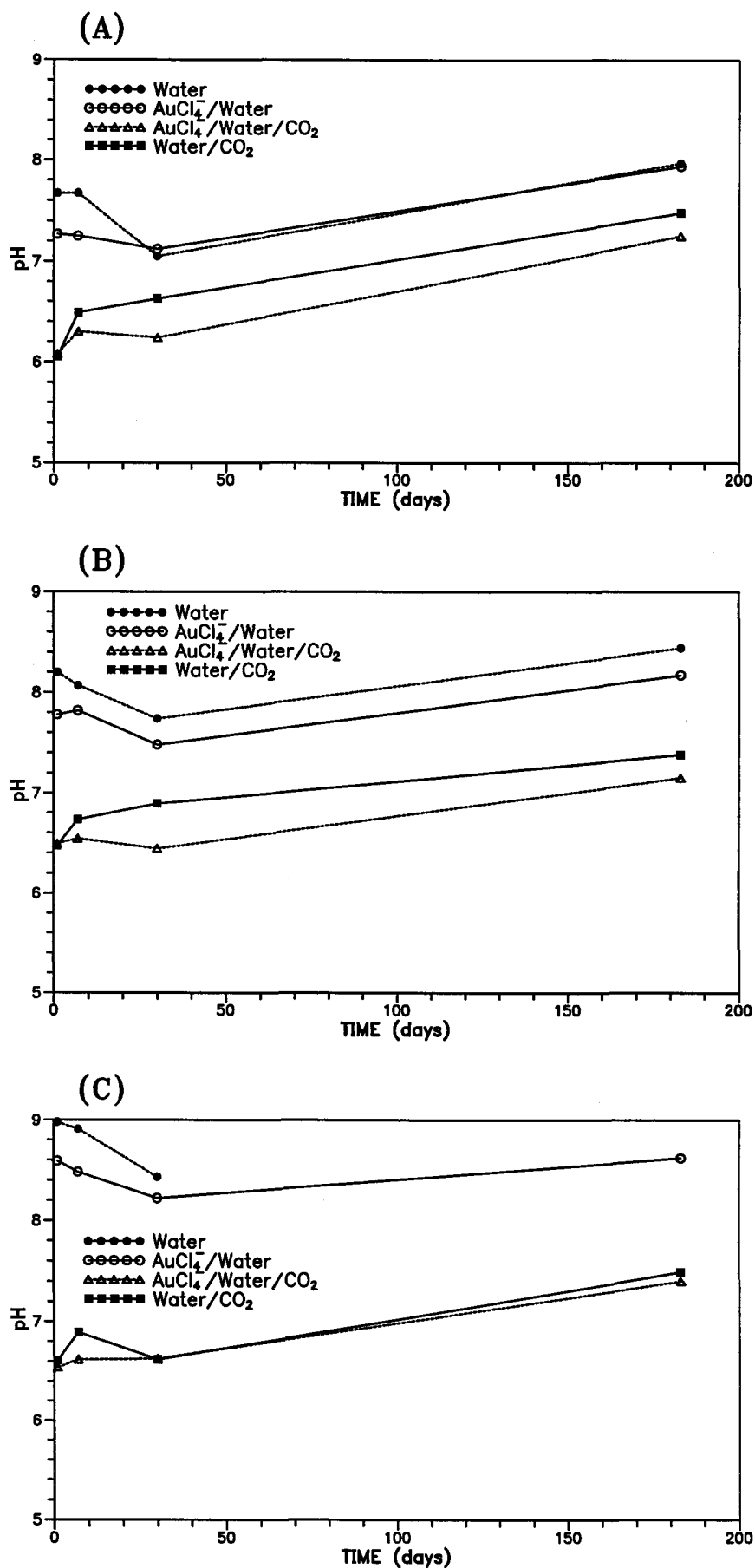
Figure 4: pH vs. Time for (a) Sample 1467, (b) Sample 1468, and (c) Sample 1470.
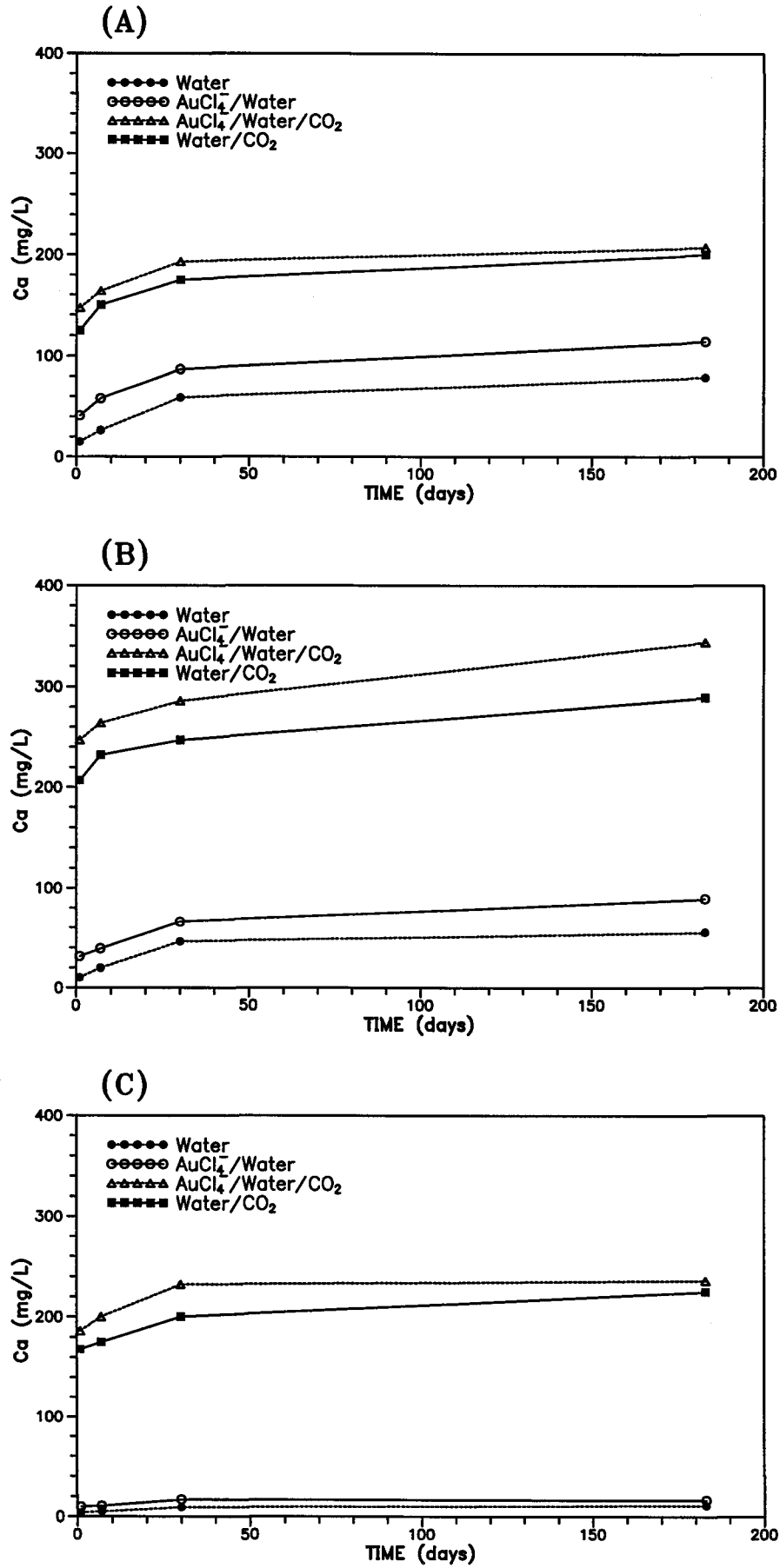
Figure 5: Ca vs. Time for (a) Sample 1467, (b) Sample 1468, and (c) Sample 1470.
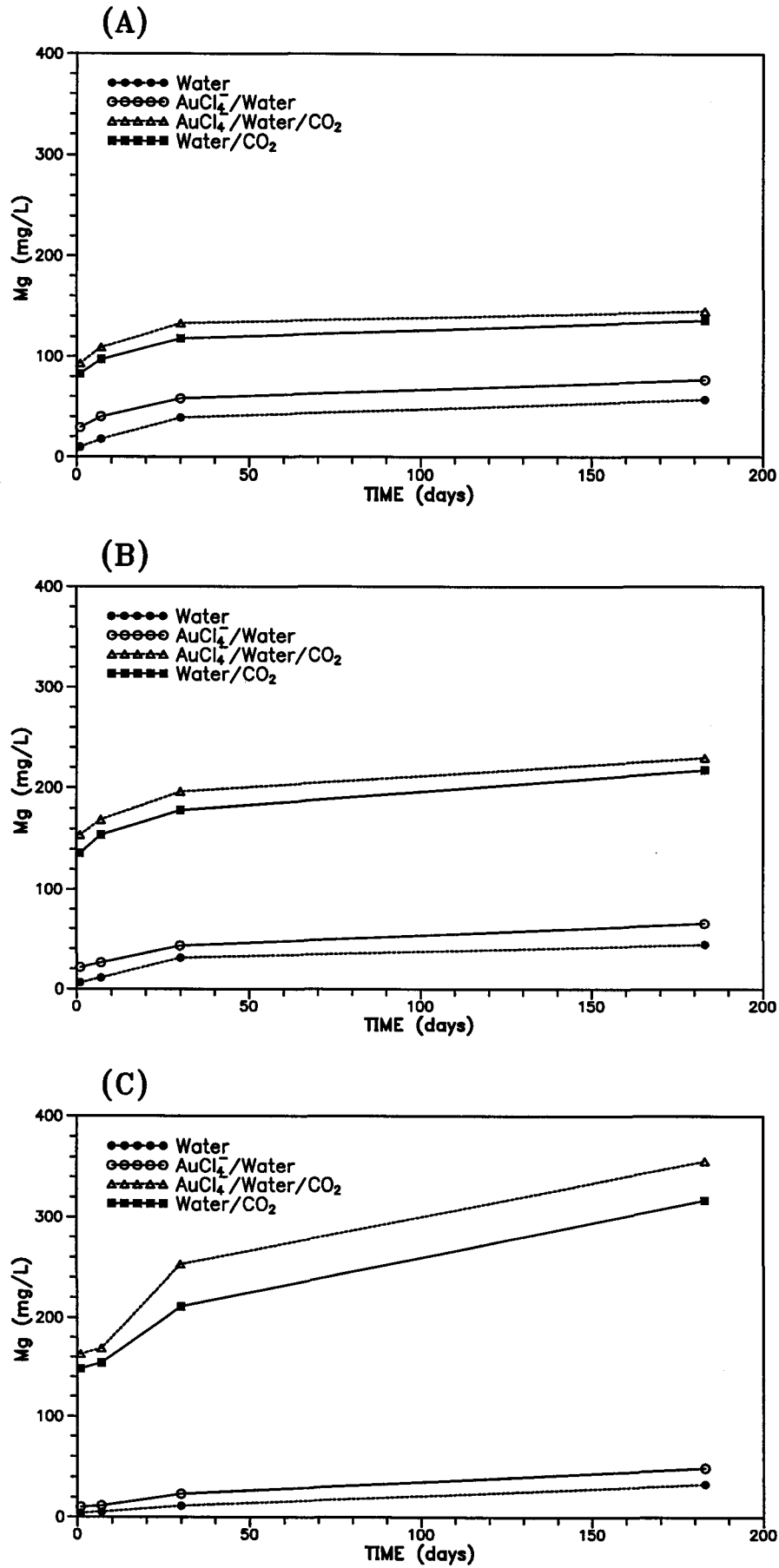
Figure 6: Mg vs. Time for (a) Sample 1467, (b) Sample 1468, and (c) Sample 1470.

(A)

(B)

(C)
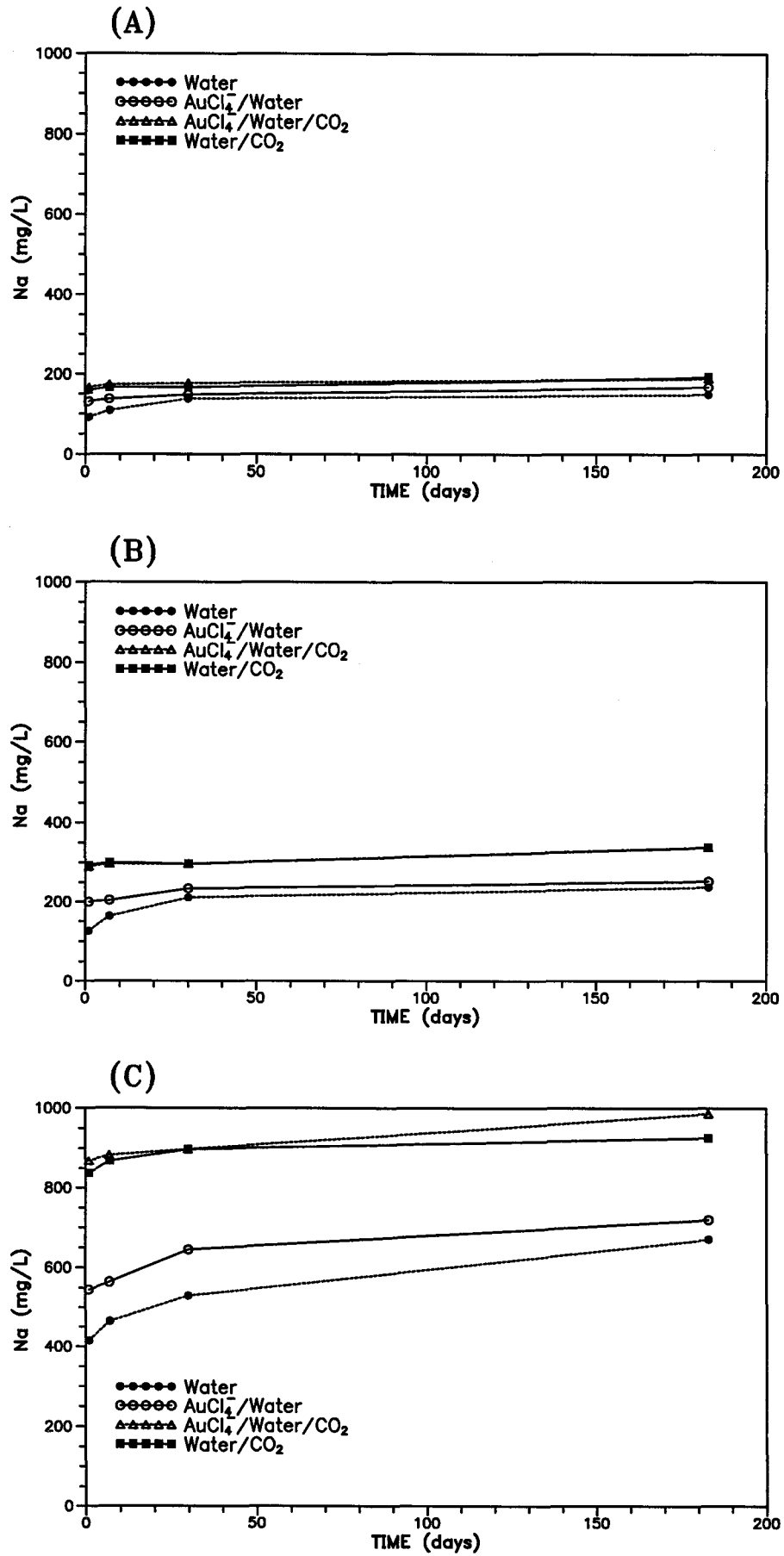
Figure 7: Na vs. Time for (a) Sample 1467, (b) Sample 1468, and (c) Sample 1470

(A)

(B)

(C)
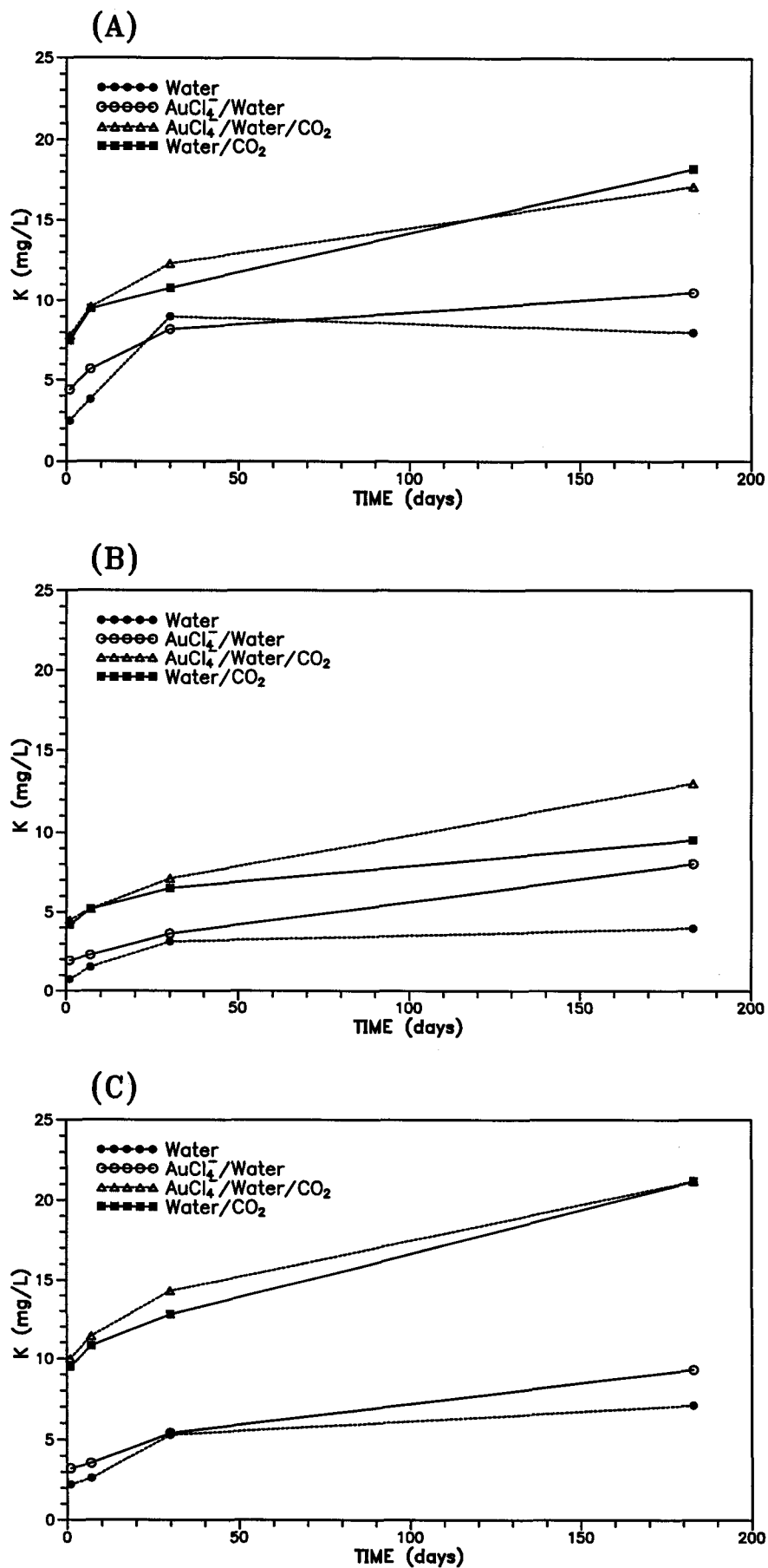
Figure 8: K vs. Time for (a) Sample 1467, (b) Sample 1468, and (c) Sample 1470

(A)

(B)

(C)
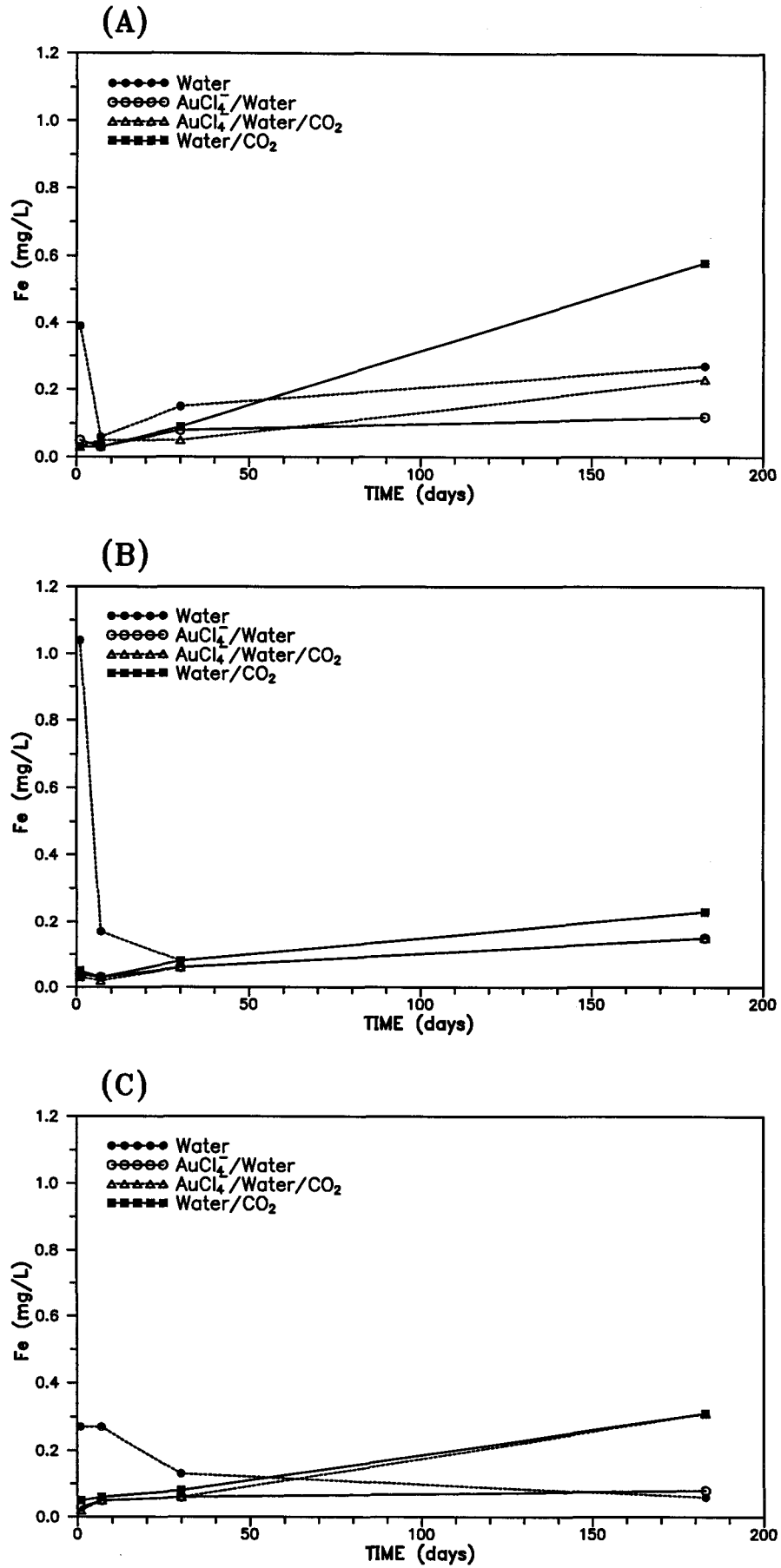
Figure 9: Fe vs. Time for (a) Sample 1467, (b) Sample 1468, and (c) Sample 1470.

(A)

(B)

(C)
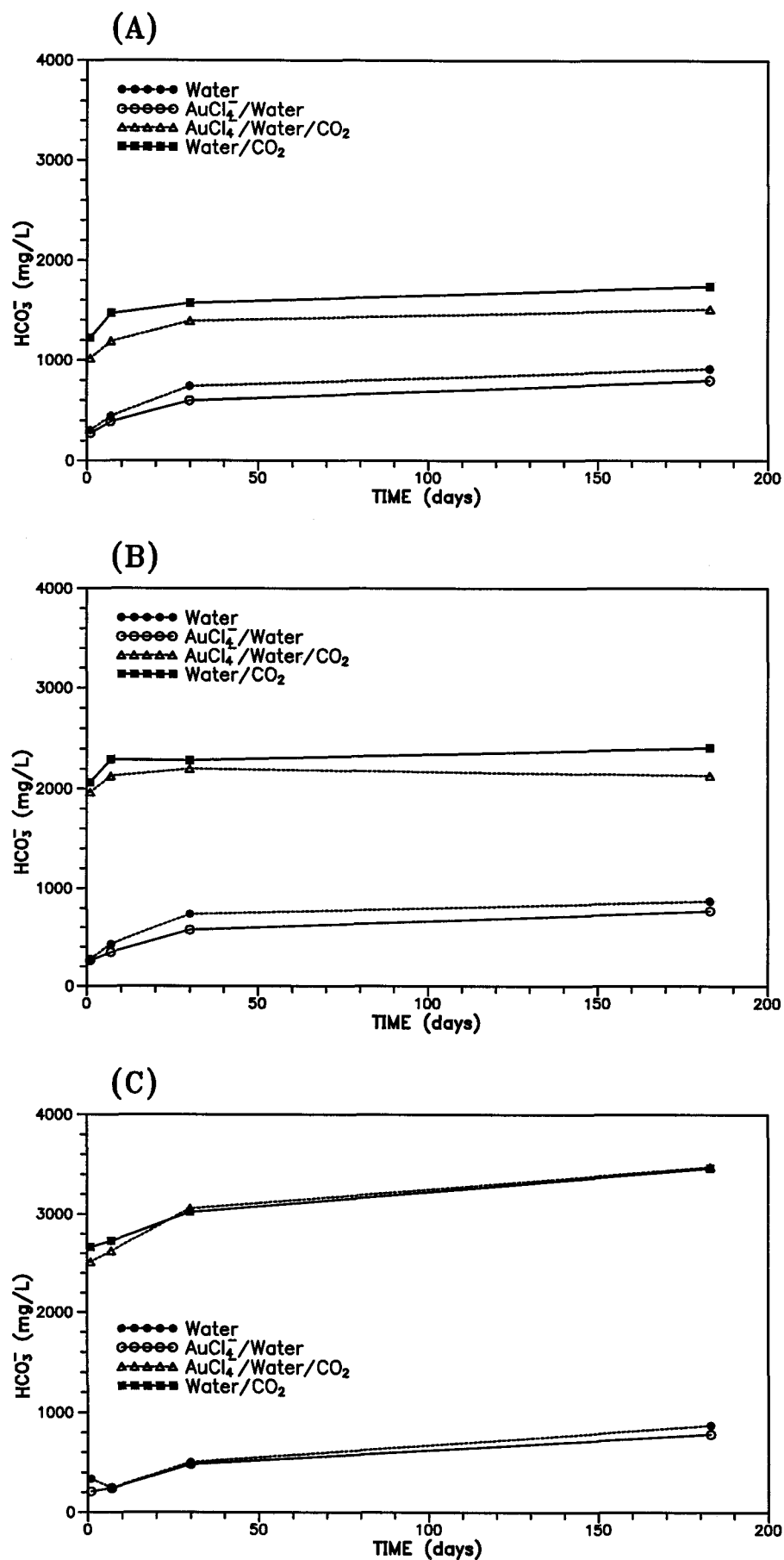
Figure 10: HCO_3^- vs. Time for (a) Sample 1467, (b) Sample 1468, and (c) Sample 1470.
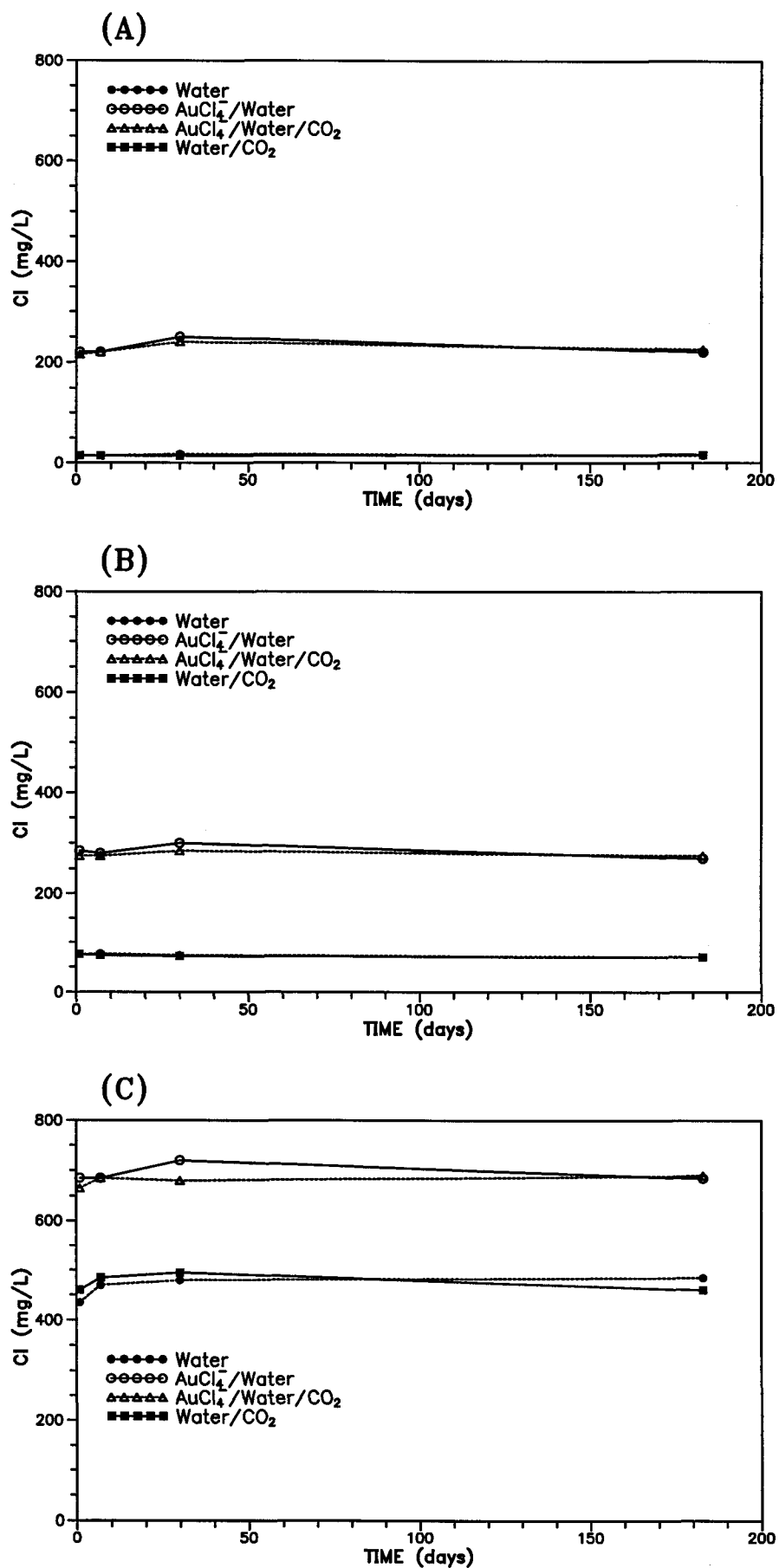
Figure 11: Cl⁻ vs. Time for (a) Sample 1467, (b) Sample 1468, and (c) Sample 1470.
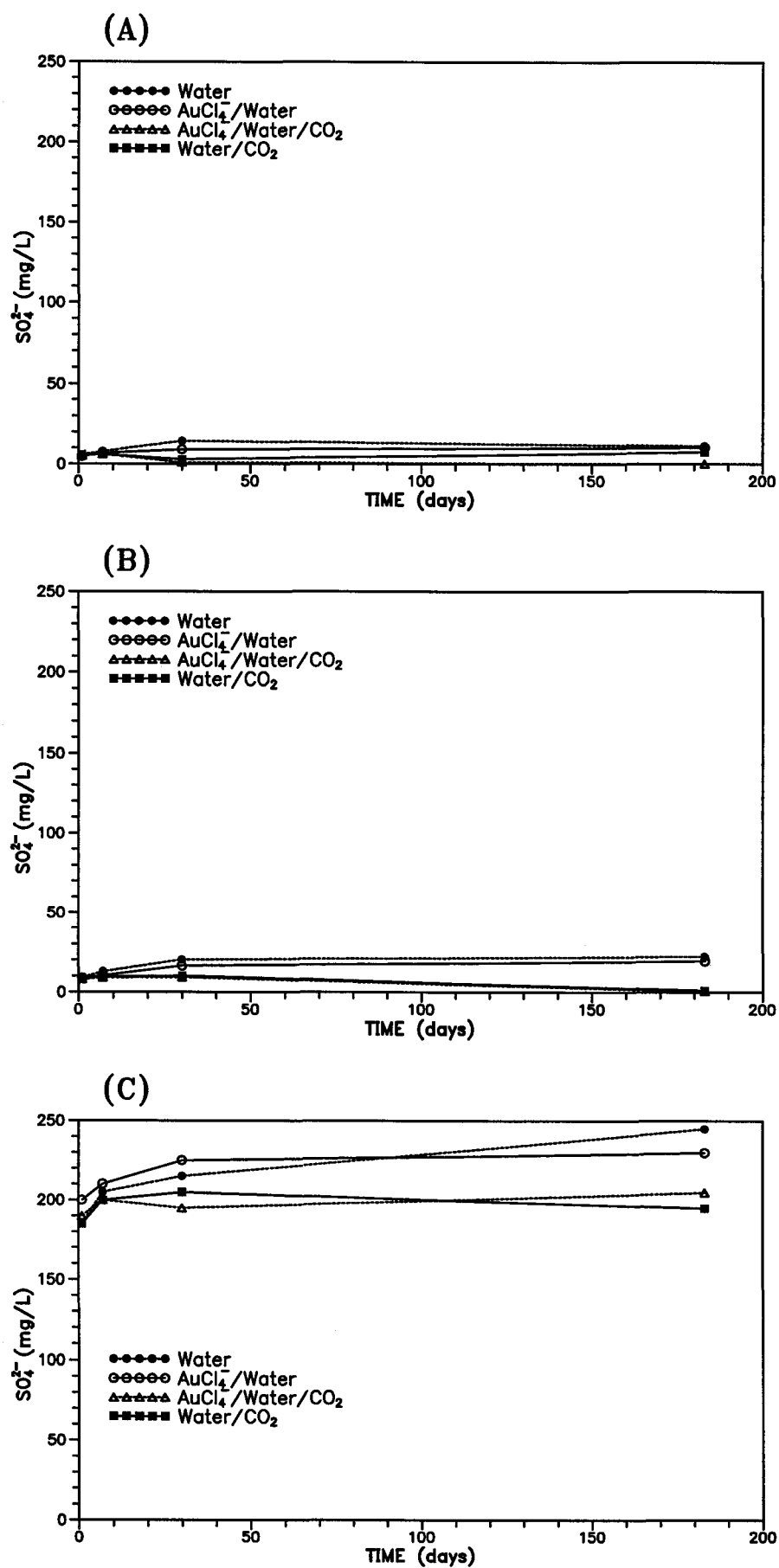
Figure 12: SO_4^{2-} vs. Time for (a) Sample 1467, (b) Sample 1468, and (c) Sample 1470.

(A)

(B)

(C)
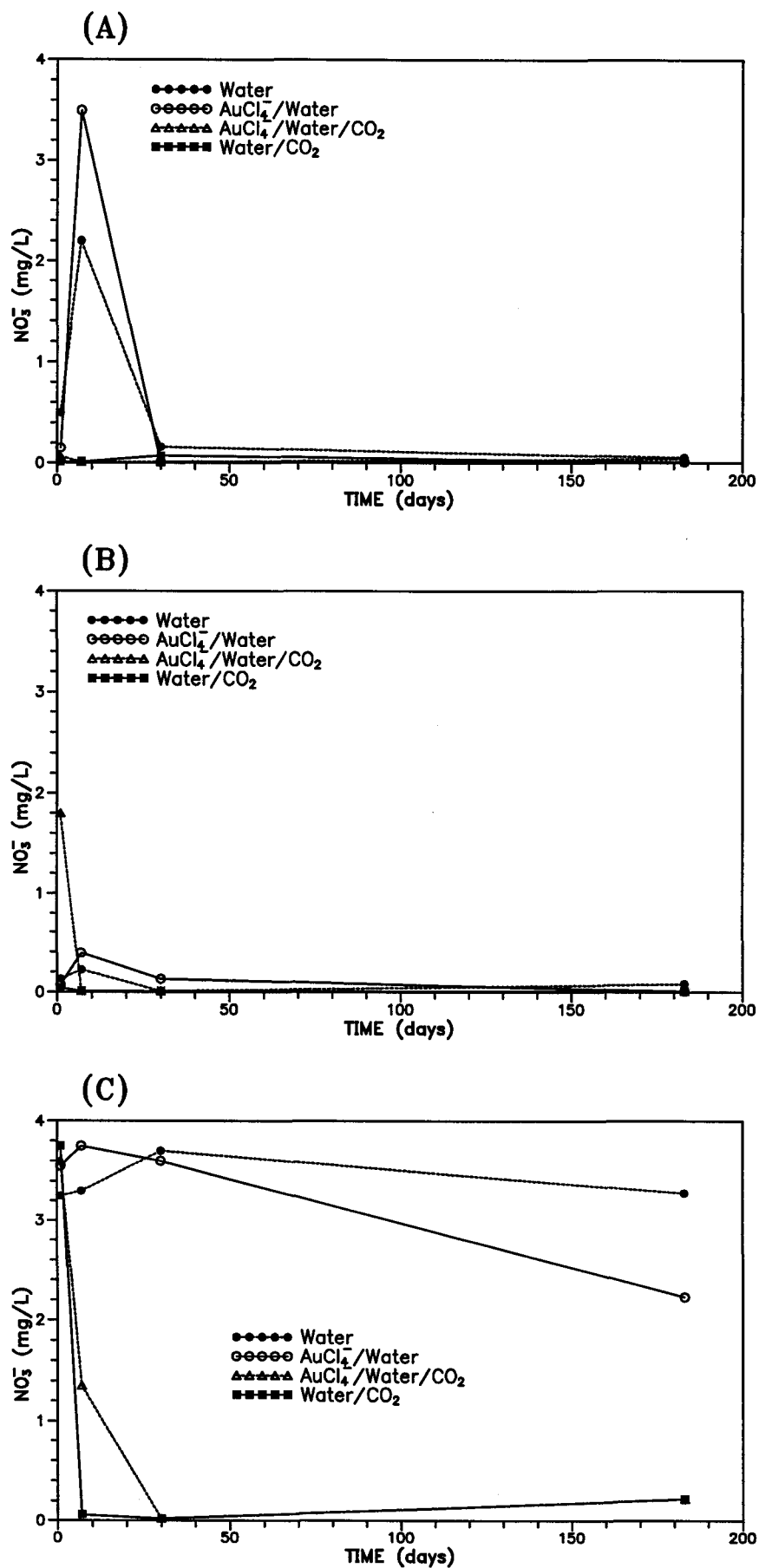
Figure 13: NO_3^- vs. Time for (a) Sample 1467, (b) Sample 1468, and (c) Sample 1470.
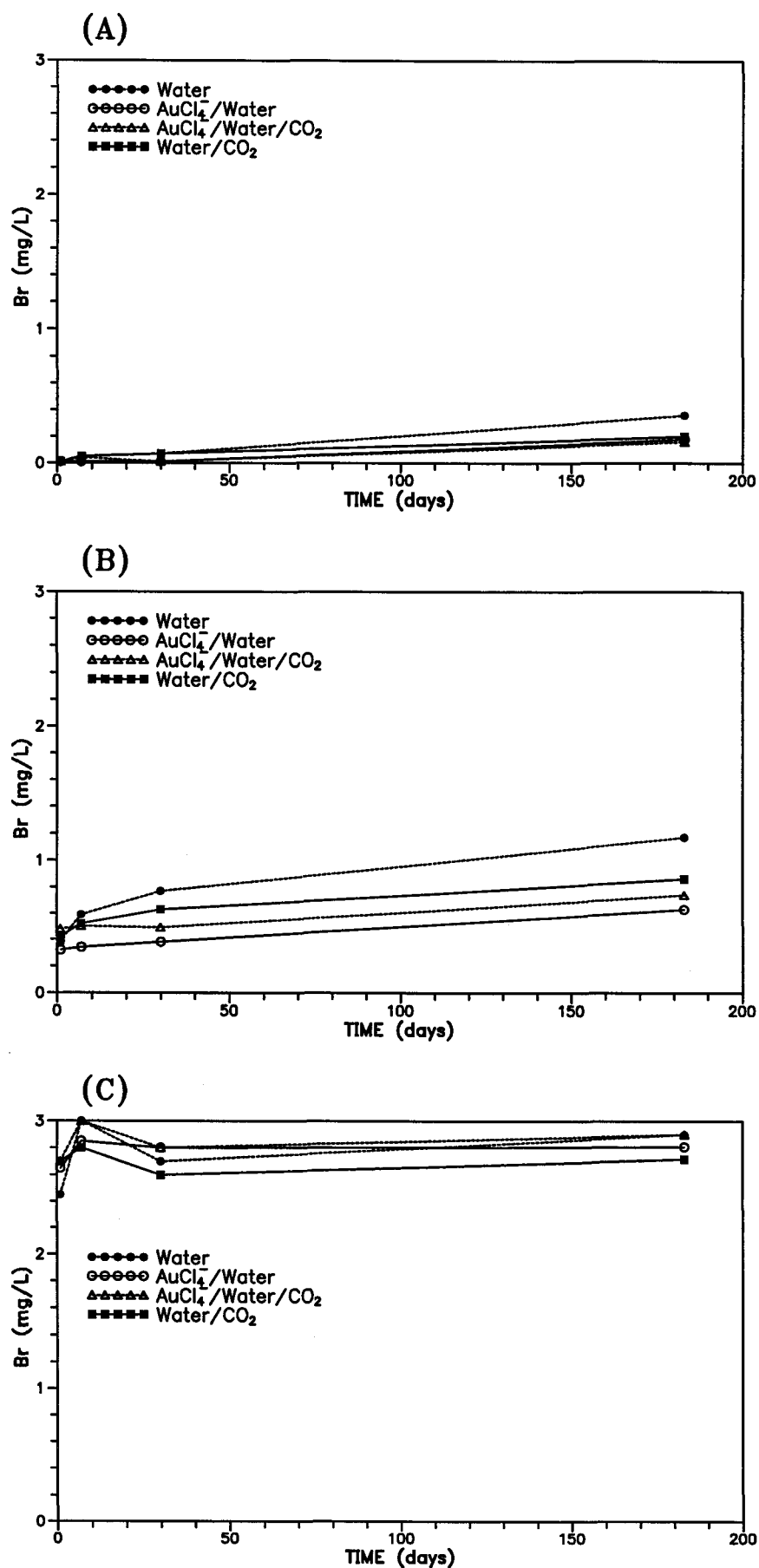
Figure 14: Br⁻ vs. Time for (a) Sample 1467, (b) Sample 1468, and (c) Sample 1470.

(A)

(B)

(C)
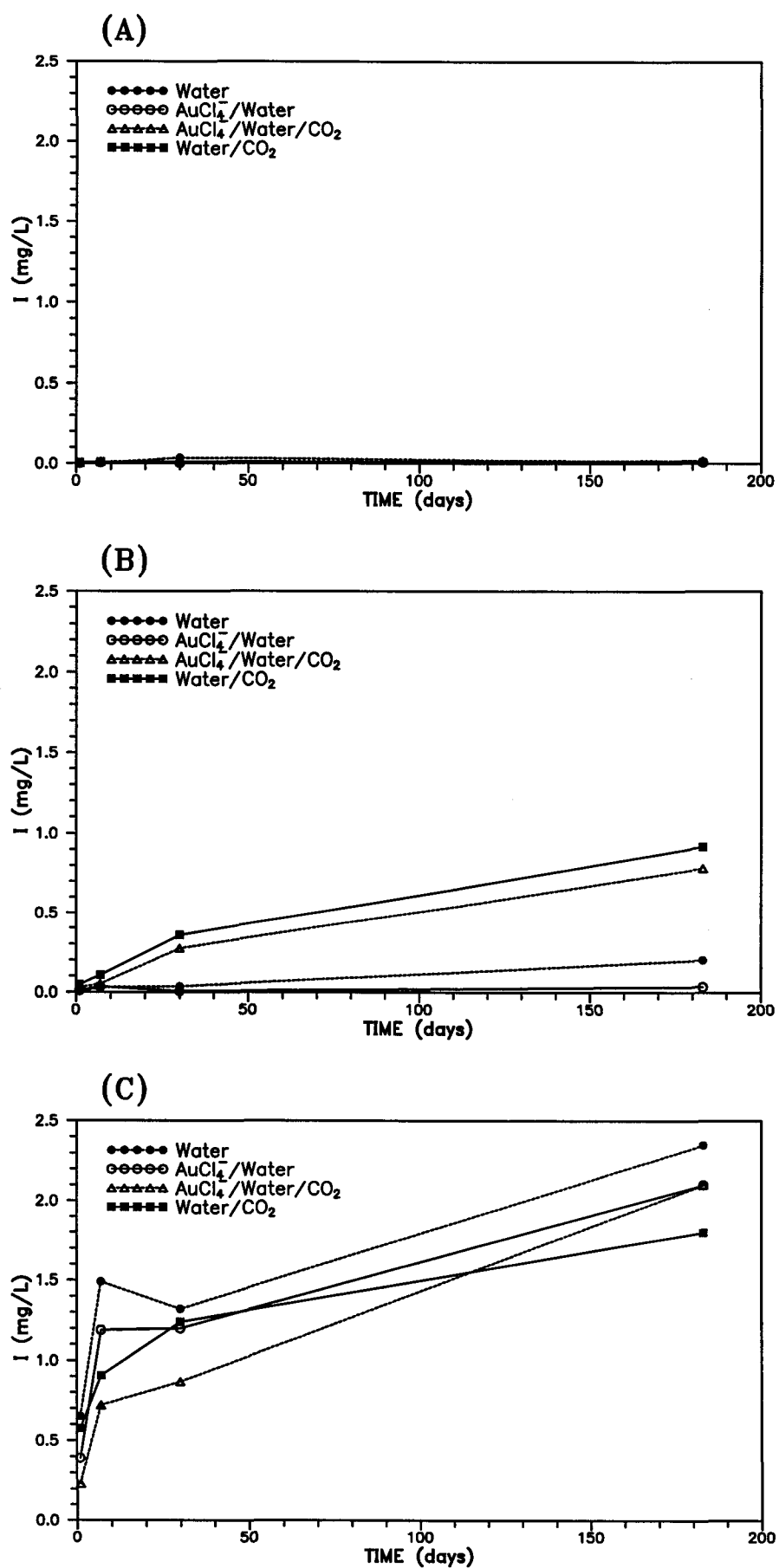
Figure 15: I$^-$ vs. Time for (a) Sample 1467, (b) Sample 1468, and (c) Sample 1470.

(A)

Water

○ AuCl$_4^-$/Water

△ AuCl$_4^-$/Water/CO$_2$

■ Water/CO$_2$

Mg^{2+}

Na$^+$ + K$^+$

— Ca^{2+} →

Water

○ AuCl$_4^-$/Water

△ AuCl$_4^-$/Water/CO$_2$

■ Water/CO$_2$

(B)

HCO$_3^-$

SO$_4^{2-}$

— Cl$^-$ →

Figure 16: Ternary Diagrams for Elemental Compositions of Sample 1467 Mixtures,
(a) cations, and (b) anions.

(A)

● Water
○ AuCl₄⁻/Water
△ AuCl₄⁻/Water/CO₂
■ Water/CO₂

(B)

● Water
○ AuCl₄⁻/Water
△ AuCl₄⁻/Water/CO₂
■ Water/CO₂

Figure 17: Ternary Diagrams for Elemental Compositions of Sample 1468 Mixtures, (a) cations, and (b) anions.

● Water
○ AuCl₄⁻/Water
△ AuCl₄⁻/Water/CO₂
■ Water/CO₂

(A)

Mg²⁺

Na⁺ + K⁺

Ca²⁺

● Water
○ AuCl₄⁻/Water
△ AuCl₄⁻/Water/CO₂
■ Water/CO₂

(B)

HCO₃⁻

SO₄²⁻

Cl⁻

Figure 18: Ternary Diagrams for Elemental Compositions of Sample 1470 Mixtures, (a) cations, and (b) anions.

There is also an increase in Ca and Mg levels with time (Figs. 5 and 6), presumably as an effect of acid production during organic matter decomposition. If Ca and Mg are considered in terms of molarity, the concentrations released to solution for soils 1467 and 1468 are about equal. This is indicated by the cation ternary diagrams (Figs. 16 - 18) which show the sample waters to lie along a line from the top apex to 50 % Ca. This is the line for [Ca] = [Mg], going from 0 % Ca and Mg and 100 % (Na+K) at the top, to 50 % Ca, 50 % Mg and 0 % (Na+K) at the bottom. This equivalence of dissolved Ca and Mg suggests that the source for the solution Ca and Mg is dolomite (or an amorphous mineral with similar stoichiometry) rather than calcite. This effect was observed even for sample 1467, for which no calcite or dolomite could be detected by XRD. The highest (Ca + Mg) dissolved for this soil was 12 mM/L, which corresponds to about 0.2 % dolomite. Such an amount of material is probably below the limits of detection for normal XRD analysis, but the analytical results suggest that even such small concentrations may dominate the solid/liquid equilibria.

Sample 1470 differs from the other samples (Fig. 18) in that dissolved Mg is higher than dissolved Ca. This would suggest an additional source for the Mg, such as magnesite or Mg on clay exchange sites. An alternative explanation is that Ca has precipitated during sampling. It is expected that dissolved CO_2 would be very high in the sealed bottles which contained soil 1470, due to the high concentrations of carbonate minerals in this sample. Thus, degassing of the solutions following opening of the bottles for sampling is expected to have caused major increases in alkalinity, in the range of one pH unit. Under these conditions, precipitation of calcite could well be significant, and fast, causing the observed high level of Mg, relative to Ca.

Whatever the interpretation of the higher level of Mg for sample 1470, the critical observation is that dissolved Mg is always greater than or equal to dissolved Ca. This strongly suggests that these elements are dissolving from dolomite alone, while little or no calcite dissolution is occurring. Thermodynamically, both calcite and dolomite have almost identical solubilities under the conditions of this experiment. Therefore, there must be some kinetic control over dissolution of these minerals, that effectively stops calcite dissolution. Dolomite may have formed as a late stage precipitate or as an alteration of calcite equilibrating with Mg rich waters, and may therefore tend to coat the calcite. In such circumstances dolomite would readily dissolve, whereas calcite would be effectively kept away from the solution. Other possible, though considered less likely, explanations are biological preference to dissolving dolomite, an inert material preferentially coating the calcite, or the calcite being held within impermeable nodules.

The other major elements (Na, K, Cl⁻, SO_4^{2-}), and the minor elements NO_3^- and Br⁻, all showed similar chemical behaviour (Figs. 7, 8, 11 - 14). The concentrations of these elements increased slightly down the profile from 1467 t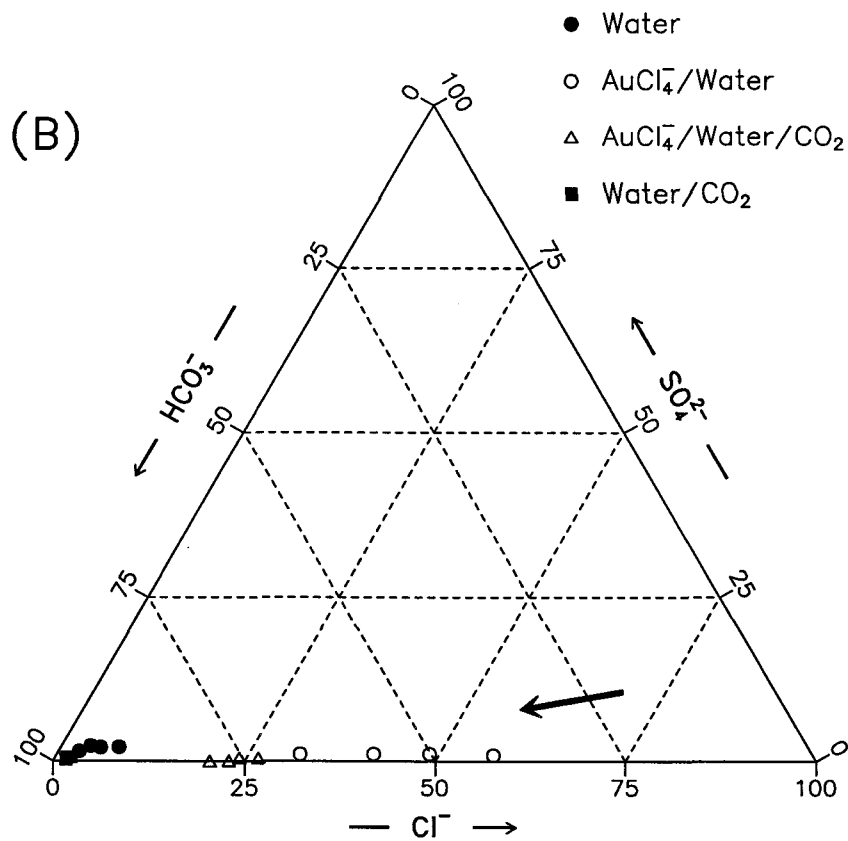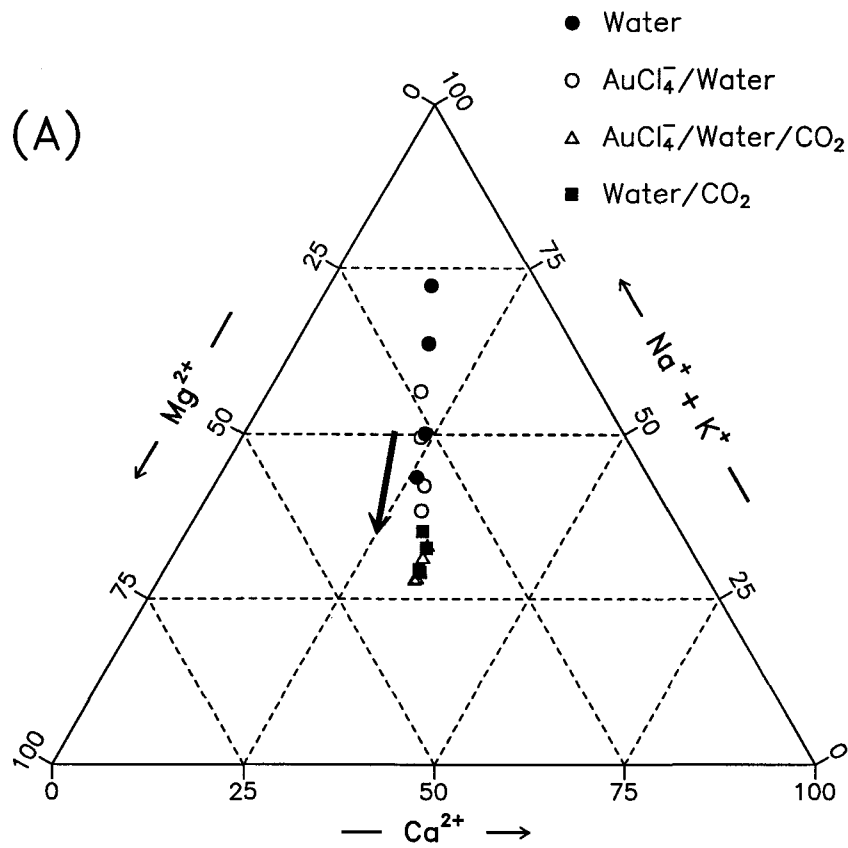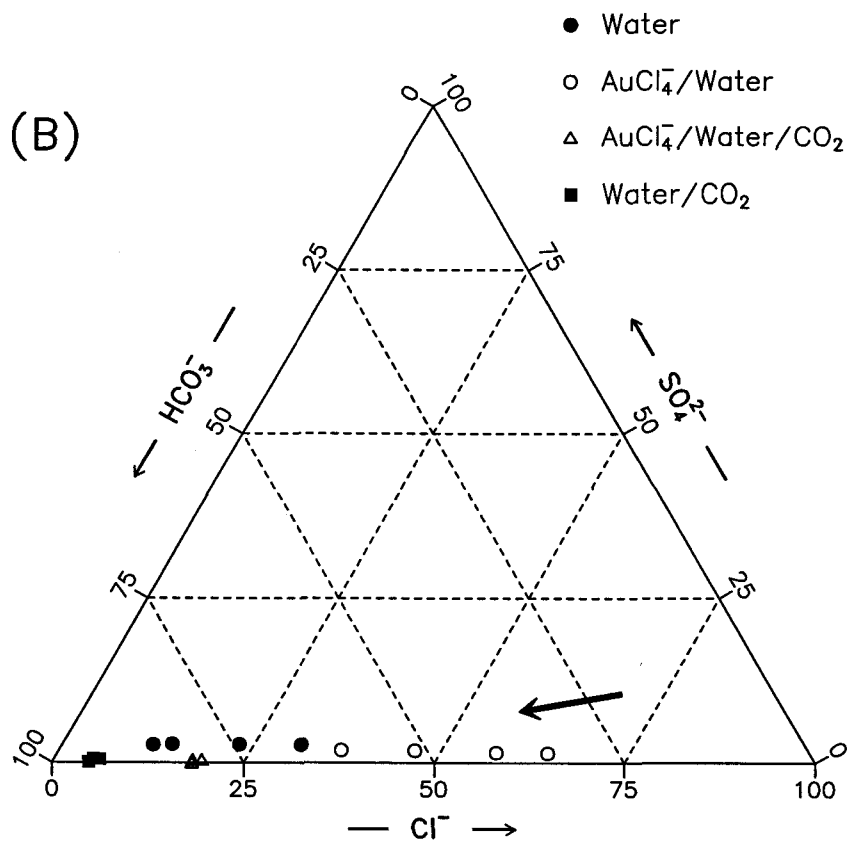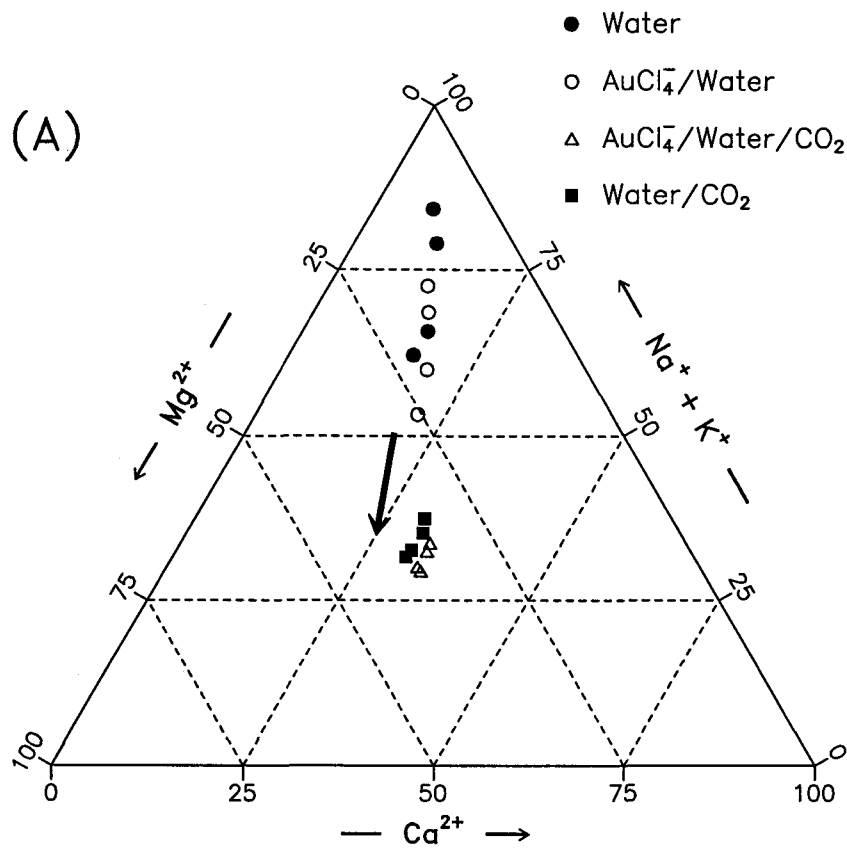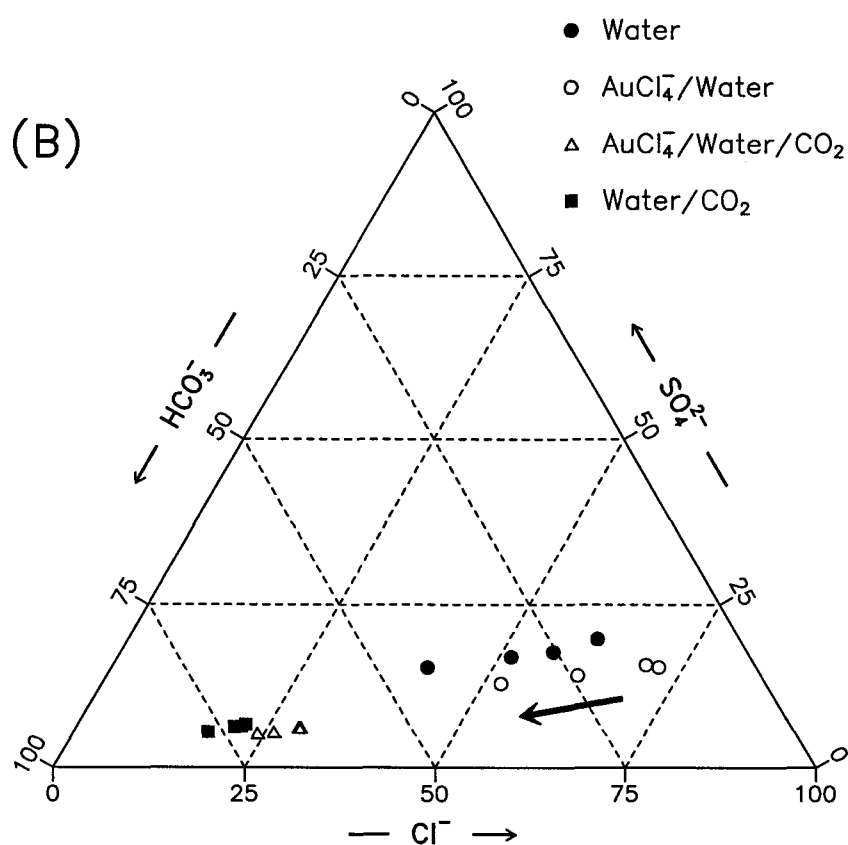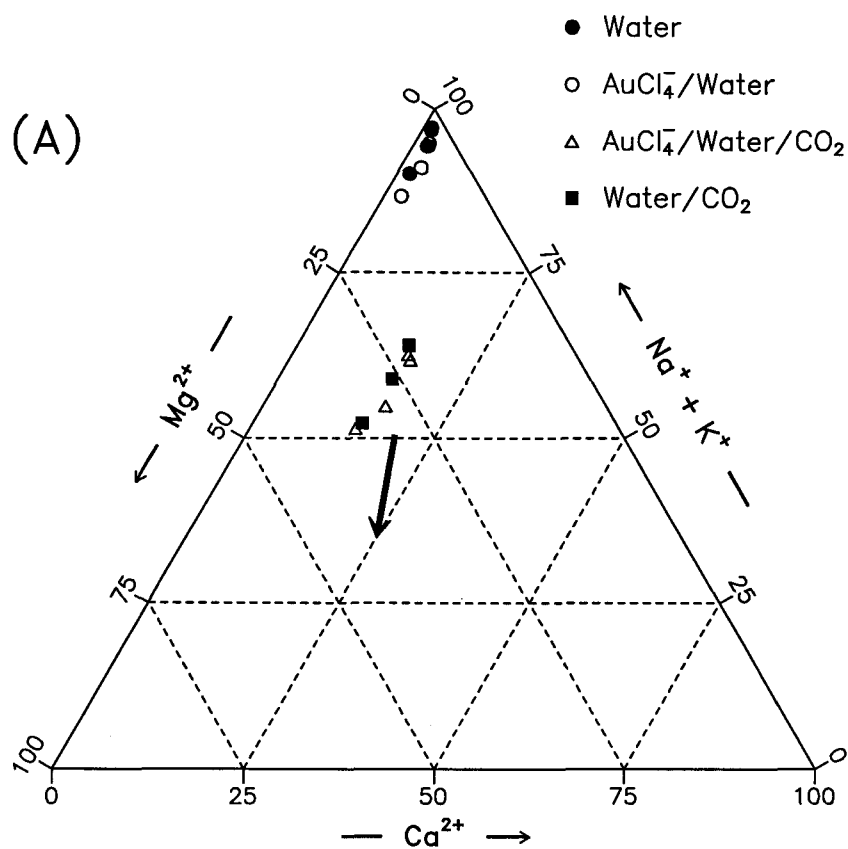o 1468, then increased dramatically for the deeper, carbonate-rich, sample 1470. This implies that the carbonate rich horizon is more saline than the overlying soil horizons and is an evaporative zone.

Dissolved Na and Cl⁻ increased very little over six months (Figs. 7 and 11), implying that they occurred in the solid as soluble components such as NaCl (halite) or $NaHCO_3$. The major increase in dissolved K with time (Fig. 8) indicates that a significant proportion of K is in slowly dissolving components such as carbonates or as slowly exchangeable K in illite.

Both Br⁻ and I⁻ showed increased concentrations with time (Figs. 14 and 15). Work on groundwaters and soils in Western Australia (Gerritse and George, 1988) has shown that Br⁻ and I⁻ are released during oxidation of organic matter. Bromide was dissolved with time in samples 1467 and 1468, but had a high, and generally constant concentration, in sample 1470 mixtures (Fig. 14). Iodide concentration was very low in the uppermost sample 1467, and showed increased levels with time in samples 1468 and 1470. Thus, Br⁻ showed a greater tendency to dissolve from the shallower samples and I⁻ from the deeper samples. In addition, dissolution of I⁻ from sample 1468 was

significantly higher in the CO_2-bubbled mixtures than in the other aerated mixtures. The reasons for this effect are not known, but it is of interest to note such a significant difference in the chemistry of these two halides.

Under normal aerated conditions, organic matter is oxidized over time, with atmospheric oxygen providing the ultimate electron sink (*i.e.*, oxidant). However, in sealed bottles, and particularly in the CO_2-bubbled mixtures, O_2 will be quickly used up and other oxidants will be required. The order in which different oxidants will be reduced (Berthelin, 1988) is:

$$O_2 + 4H^+ + 4e^- \Leftrightarrow 2H_2O \qquad ...(4)$$
$$2NO_3^- + 12H^+ + 10e^- \Leftrightarrow N_2 + 6H_2O \qquad ...(5)$$
$$MnO_2 + 4H^+ + 2e^- \Leftrightarrow Mn^{2+} + 2H_2O \qquad ...(6)$$
$$Fe(OH)_3 + 3H^+ + e^- \Leftrightarrow Fe^{2+} + 3H_2O \qquad ...(7)$$
$$SO_4^{2-} + 10H^+ + 8e^- \Leftrightarrow H_2S + 4H_2O \qquad ...(8)$$

Thus, once dissolved oxygen is depleted, NO_3^- may be used by soil organisms to oxidise organic matter, then Mn and Fe oxides, and then SO_4^{2-}. The change in concentration in the relevant species with time in the various mixtures can be related to this sequence. Samples 1467 and 1468 behaved in virtually the same manner and are discussed together. However, there were sufficient differences in the chemistry of sample 1470 for it to be treated separately.

Sample 1467 contains the highest levels of organic matter (Table 1). Nitrate shows a dramatic increase in concentration over the first week (up to approximately 3 mg/L) for the mixtures that were not bubbled with CO_2 (Fig. 13). Oxidation of ammonia or organic nitrogen in the presence of O_2 will result in high concentrations of NO_3^-, as observed:

$$R\text{-}NH_3^+ + 2O_2 \Rightarrow R\text{-}OH + NO_3^- + 2H^+ \qquad ...(9)$$

However, bubbling with CO_2 will remove O_2 from the system and will disallow this reaction. This explains why the CO_2-bubbled mixtures showed no NO_3^- production. This pattern was repeated for sample 1468 (Fig. 13), though the NO_3^- production in the CO_2-free mixture was much lower (approximately 0.3 mg/L). This lower level suggests a lesser level of oxidizable N, consistent with the lower level of organic matter in this deeper sample. The high initial concentration of NO_3^- in the one day sample with Au added and CO_2 bubbled is not understood (and may represent contamination of that sample).

After one week NO_3^- concentration started to decline in the mixtures and reached levels at or below the detection limit (0.02 mg/L) by six months (Fig. 13). This indicates that the mixtures were depleted in O_2. Nitrate then becomes the electron acceptor, according to eqn. 5. After one month NO_3^- is also depleted from the system and other electron acceptors, such as the variable oxidation state metals Mn and Fe (eqns. 6 and 7), are necessary. The sample/water mixtures for 1467 and 1468 (Fig. 9) without Au or CO_2 initially contained a small amount of Fe. All the other treatments strongly reduced the initial concentration of Fe. Presumably addition of Au reduced the concentration of soluble Fe via an oxidation reaction:

$$3Fe^{2+} + AuCl_4^- + 9H_2O \Rightarrow 3Fe(OH)_{3(S)} + Au_{(S)} + 9H^+ + 4Cl^- \qquad ...(10)$$
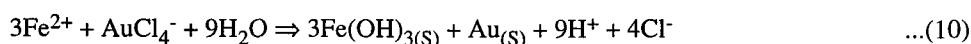
It is not understood why bubbling with CO_2 reduced soluble Fe. One possible reaction would be precipitation of siderite:

$$Fe^{2+} + CO_2 + H_2O \Rightarrow FeCO_{3(S)} + 2H^+ \qquad ...(11)$$

However, speciation calculations indicate this mineral should be soluble under the experimental conditions. In addition, dissolved Fe concentration in the CO_2-bubbled samples increased significantly over time, despite changes in the solution chemistry that would make siderite solubility lower rather than higher.

The higher level of Fe in the sample/water mixtures for 1467 and 1468 was lost after one week, possibly via oxidation:

$$4Fe^{2+} + O_2 + 10H_2O \Rightarrow 4Fe(OH)_{3(S)} + 8H^+ \qquad\qquad ...(12)$$
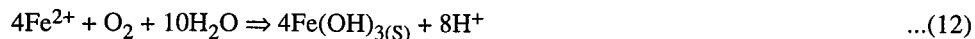
Following this, there was a small increase in dissolved Fe between one and six months (Fig. 9), possibly due to solid Fe oxides acting as an oxidant after the loss of all of the NO_3^- (eqn. 7). However, this increase was small (< 0.5 mg/L) and does NOT represent a significant contribution of oxidative capacity. The increase in dissolved Fe was even lower for the samples with Au added, possibly due to Au oxidizing Fe and thus rendering it insoluble. It may be that Fe is not dissolving in these materials for a similar reason to why calcite is not dissolving: *i.e.*, the Fe oxides are occluded by dolomite and/or other late stage precipitates.

In the absence of Fe playing a significant role in maintaining oxidative conditions, the next electron acceptor in the sequence (eqns. 4 - 8) is SO_4^{2-}. Sulphate concentrations in the 1467 and 1468 mixtures appear to plateau for the sample/water and the sample/water/Au mixtures after one month (Fig. 12). The lack of any significant decrease in SO_4^{2-} for these mixtures indicates that they have remained oxidizing. On the other hand, mixtures bubbled with CO_2 show major decreases in SO_4^{2-} concentrations, down to virtually zero by six months. Presumably the SO_4^{2-} has acted as an electron acceptor and been reduced to one of a number of partially or totally reduced species, such as thiosulphate ($S_2O_3^{2-}$), elemental sulphur [$S_{(S)}$], or hydrogen sulphide (HS^-).

With the removal of SO_4^{2-}, any further oxidation of remaining organic matter will be slow, and will possibly depend on Fe. As discussed previously, the dissolution and reduction of Fe oxide is very slow.

Sample 1470 differs from the other samples in that it is carbonate-rich, has a high initial concentration of NO_3^- (consistent with it being a zone of accumulation of soluble ions, as discussed above), and a lower organic carbon content (Table 1). The sample/water and sample/water/Au mixtures showed only minor reductions in NO_3^- (Fig. 13), indicating that the original dissolved oxygen concentration was sufficiently high to maintain reasonably oxidizing conditions. There was little or no NO_3^- production (compare the 1467 plots with the 1470 plots in Fig. 13), suggesting little organic N. In comparison, the CO_2-bubbled mixtures showed major reductions in NO_3^-. Thus, in the absence of O_2, nitrate is being removed from the system via reduction.

A similar effect is observed for Fe (Fig. 9). The highest initial concentration is observed for the sample/water mixture, possibly for the same reasons as discussed for 1467 and 1468. This initial concentration did decline over time, but at a slower rate than in samples 1467 and 1468. The CO_2-bubbled mixtures showed an increase in dissolved Fe with time, again suggesting that solid Fe oxides are behaving (weakly) as electron acceptors. Sulphate is also reduced in the CO_2-bubbled mixtures, suggesting that this ion is behaving as an electron acceptor, in a similar manner to 1467 and 1468. However, only a minor portion of the sulphate is consumed, so that the CO_2-bubbled mixtures will still be weakly oxidizing for the 1470 sample, while the 1467 and 1468 samples, as discussed previously, have become highly reduced.

A summary of relevant observations on the observed reactions of the samples over time are:

(i)   Ca and Mg dissolve from the soils with equimolar concentrations, suggesting dissolution of dolomite (or a more amorphous mineral with similar stoichiometry) rather than calcite;

(ii) the very small amounts of dissolution of calcite and Fe oxide could be due to these minerals being covered by late-stage precipitates such as dolomite;

(iii) dissolved HCO_3^-, Ca, Mg, and K increase significantly over time, presumably in response to acid production during oxidation of organic matter;

(iv) the readily soluble ions Na, K, Cl^-, Br^-, SO_4^{2-} and NO_3^- showed much higher concentrations in the 1470 mixtures, indicating that this carbonate-rich horizon is also the zone for accumulation of normally soluble ions, *i.e.*, this horizon represents an evaporative zone;

(v) Br^- and I^- concentrations increased over time, probably due to release from decomposed organic matter;

(vi) The CO_2-bubbled samples were anaerobic and by six months all of the SO_4^{2-} in the 1467 and 1468 mixtures was consumed, presumably via reduction. The 1470 sample had lower organic matter and higher NO_3^- and SO_4^{2-} and therefore not all of the SO_4^{2-} was consumed;

(vii) Fe initially present in solution was removed over time in the sample/water mixtures, possibly via oxidation/hydrolysis. Both the CO_2 and Au treatments decreased the initial concentration of Fe;

(viii) the concentration of dissolved Fe showed a small increase over time, possibly due to reduction of Fe oxides. For samples 1467 and 1468, this increase was least for the Au-treated mixtures, possibly due to oxidation of Fe by ionic Au. For sample 1470, dissolved Fe after six months was highest for the CO_2-bubbled mixtures.

3.3.3.   Gold Chemistry

<u>Mixtures without added Au.</u>

As with the general redox chemistry (Section 3.3.2), the Au dissolution chemistry was very similar for samples 1467 and 1468, whereas 1470 behaved quantitatively differently. Shaking sample 1467 with deionized water caused a dissolution of Au to about 8 µg/L after one week (Fig. 19), *i.e.*, a significantly high Au concentration: in comparison, groundwaters sampled from areas of Au mineralization in the Yilgarn contained Au at concentrations from <0.05 to 4 µg/L (Gray 1990a, b). Subsequently, Au concentration decreased to below analytical detection limits at one month, *i.e.*, Au dissolved from the solid, and then reprecipitated. Bubbling with CO_2 strongly reduced the amount of dissolution, though there was still a minor amount of dissolution after one week.

Though data for dissolution of gold from the irradiated samples were only obtained after three months and six months incubation, it is clear that irradiating the soil has a dramatic effect on the concentration of Au in the aqueous phase (Fig. 19). Gold levels are dramatically enhanced, relative to the unirradiated sample, with a more or less linear increase over time. After the three month mixture was sampled, it was "inoculated" with one gram of untreated dry sample and the solution sampled again after a further three months. This has caused a significant lowering in soluble Au, relative to the sample that was irradiated and left sealed for six months.

It is not certain what has caused these dissolution effects for Au. One feasible hypothesis is that, for the sample/water mixture, Au is dissolved by the action of various biologically-generated ligands (Gray, 1988), and then removed from solution by an effect involving the presence of significant concentrations of biota, such as adsorption on bacterial cell walls, or biologically-catalysed decomposition and precipitation of the Au complex. Prior to the experiment the soils were air-dry, with bacteria presumably present as spores. Development of significant biological activity would only occur after the addition of water and a "lag" period of hours or days, during which time bacteria would be multiplying to a significant mass. Thus, the initial high dissolution (8 µg/L over one week) of Au occurred while biological activity was relatively low. With the increase in biological activity, the Au was then removed from solution. For the samples in which the soils were irradiated, Au dissolution occurred over the entire period, with a rate approximately that indicated by the initial dissolution in the corresponding non-irradiated sample. Where the bottles were opened after 3 months and 'inoculated', the high levels of dissolved Au were then reduced by biological activity in a similar manner to the corresponding non-irradiated sample.

Bubbling with CO_2 de-oxygenates the soil, which could decrease dissolved Au if the Au was present in a reduced form in the solid and oxidation was required for dissolution. Other ways that CO_2 bubbling could conceivably affect Au dissolution is by reducing the pH or by bubbling out ligands such as cyanide or sulphide as gaseous HCN or H_2S.

Results for Au dissolution from sample 1468 were (as observed for the major elements) very similar to the results for sample 1467 (Fig. 19). However, the solubility of Au in the sample/water mixture was more sustained over time, possibly as a result of the lesser organic matter content of the sample (Table 1).

(A)

(B)

(C)
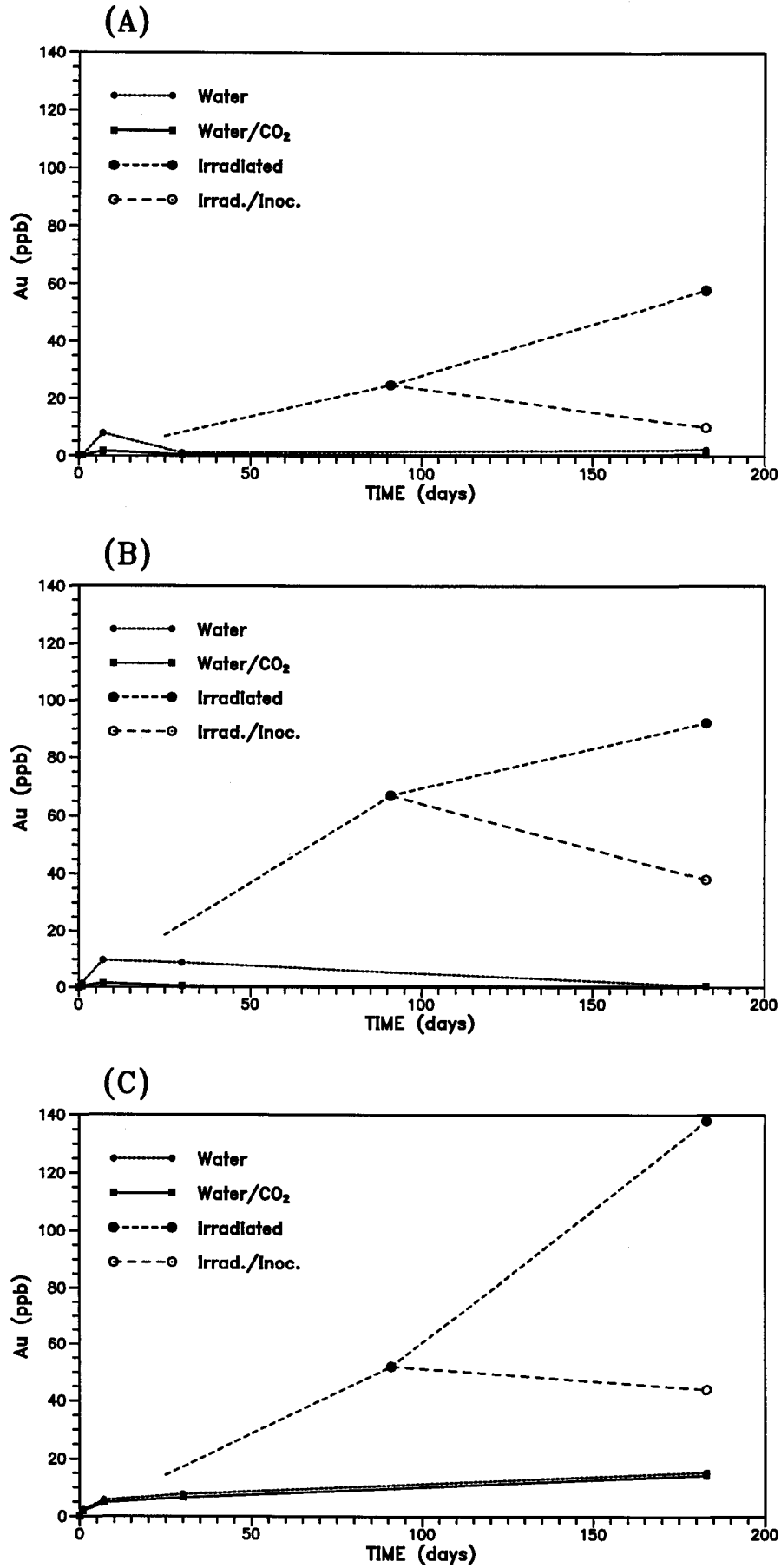
Figure 19: Au vs. Time for (a) Sample 1467, (b) Sample 1468, and (c) Sample 1470, without Au added.

As for the major elements (Section 3.3.2), the Au dissolution characteristics of sample 1470 were significantly different from the other two samples. Thus, dissolved Au concentration increased over time, in comparison with the other samples, though still significantly lower than for the irradiated mixtures. In addition, CO_2 bubbling had virtually no effect. This may be due to sample 1470 having higher NO_3^-, and lower organic matter, and thus maintaining strongly oxidizing conditions and having less biological activity than the other samples over the experimental period.

Mixtures with Au added.

The results for Au addition (Fig. 20) indicated similar processes are occurring for samples 1467 and 1468, with sample 1470 behaving distinctly differently.

In the sample/water/Au mixtures for 1467 and 1468 (Fig. 20) the added Au was removed from solution within the first day (possibly immediately on addition to the mixture). Following this, Au slowly dissolved over the next few days (reaching about 20 µg/L after one week), and then rapidly increased to levels of about one mg/L after one month. Sample 1467 showed a minor decrease for the six month sample, whereas dissolved Au reached 2.3 mg/L for sample 1468, *i.e.*, almost half of the added Au was re-dissolved. Bubbling with CO_2 completely suppressed this redissolution.

Irradiation of the 1467 and 1468 sample/water/Au mixtures reduced redissolution of the Au. Inoculation of the three month sample increased the level of dissolution, though only marginally for the 1468 mixture.

The results for the Au addition experiments showed significantly different phenomena to the case where Au was not added. Instead of a small amount of Au being dissolved and then reprecipitated over time, the redissolution of the added Au accelerated after one week. It is of relevance for the discussion of these results (but not immediately apparent due to the different concentration scales in Figs. 19 and 20) to note that over the first week redissolution of the added Au (Fig. 20) proceeded at a rate similar (2-3 times faster) to that for the Au dissolution (Fig. 19). In addition, Au redissolution was lower for the irradiated samples.

It is feasible that the differences observed between the Au dissolution and the Au addition experiments may be due to the mixtures having different bacteria present. At high concentrations Au could possibly act as a poison towards some of the soil organisms. Thus, the bacteria that in normal circumstances would act to reprecipitate or adsorb any dissolved Au (Fig. 19) might be killed by the high levels of Au in the Au added mixtures. (Indeed, any bacteria that adsorbed Au might be expected to be more susceptible to poisoning by Au, because they may be immobilizing Au by adsorbing or ingesting it). It is feasible that different bacteria may be present in the mixtures to which Au was added, and that these bacteria act to dissolve rather than precipitate Au, possibly via complexing of Au into forms less toxic to themselves. Thus, Au redissolution over the first few days will be due to ligands already in the soil solution and will occur at a similar rate as that observed for the Au dissolution (Fig. 19). Then, after a lag, there will be a phase of accelerated Au dissolution (Fig. 20), due to the production of complexing species such as amino acids, CN^- or thiosulphate (Gray, 1988). Irradiation will stop this phase occurring and decrease the amount of redissolution of Au. More experimentation is required to test this mechanism, but it is included here as a plausible explanation of the observed phenomena.
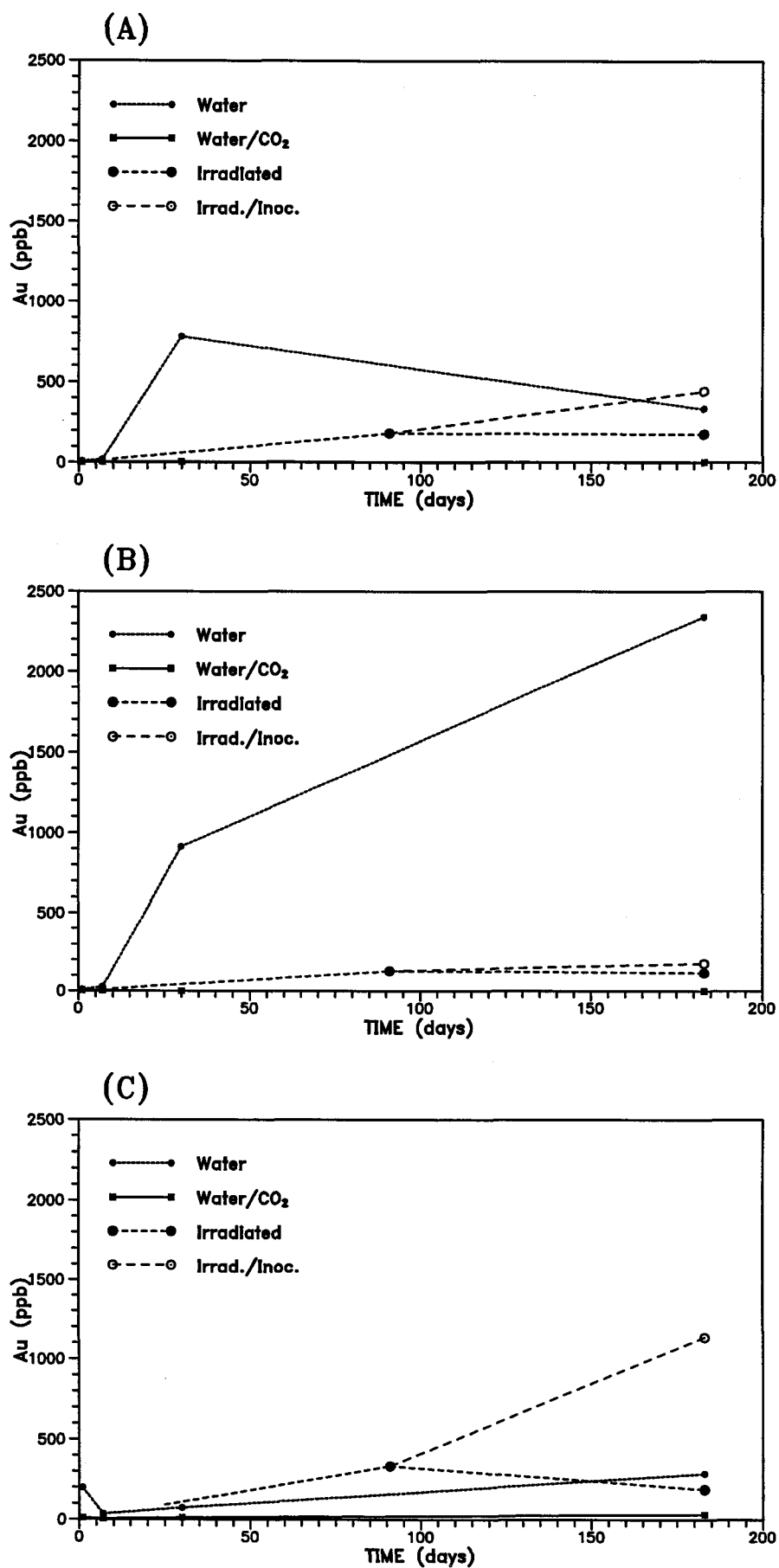
Figure 20: Au vs. Time for (a) Sample 1467, (b) Sample 1468, and (c) Sample 1470, with 5 mg/L Au added.

Results for mixtures for sample 1470 to which Au was added (Fig. 20) were significantly different from those of the other samples, and are compatible with the results for the Au dissolution (Fig. 19). Firstly, the added Au did not all immediately precipitate; some remained in solution so that the concentrations of dissolved Au only reached a minimum at about one week. Following this, Au redissolved at an approximately linear rate, suggesting chemical, rather than biological, control. Secondly, bubbling with CO_2 decreased, but did not entirely repress, redissolution of the Au. Close inspection of Fig. 20c shows that the CO_2-bubbled mixtures had the same trend in dissolved Au with time as the non-CO_2-bubbled samples, though reduced by an order of magnitude. Thus, both for dissolution of Au already present, and for redissolution of added Au, sample 1470 differed from the other samples in that CO_2 bubbling did not completely retard Au dissolution. As suggested previously, this may be due to sample 1470 having lower organic matter, and high levels of NO_3^-, thus maintaining oxidizing conditions.

Irradiation of the 1470 sample/water/Au mixture did not appear to significantly increase or decrease the concentrations of dissolved Au (Fig. 20). Irradiation, and then inoculation at three months, caused a significant increase in dissolved Au, for reasons that are not clear.

3.4. Discussion

The previous sections have discussed the results from the soil incubation experiments in terms of the hypothesized chemistry of the processes involved. In this section, results are interpreted in terms of changes in the soil properties within the soil profile. The correlation of soil Au with the elements Ca, Mg and Na has been investigated for soil profiles at a number of sites in the southern Yilgarn (Lintern, 1989; Lintern and Scott, 1990). The soil samples used here are considered to be generally representative of these soil profiles. However, it should be noted that further work is certainly required in order to verify that the conclusions drawn below are general.

Element concentration data (Table 1) and mineralogical determinations (Table 2) indicate Profile A to have increased concentrations of the "evaporites" with depth: $i.e.$, sample 1470 is enriched in Ca, Mg, Na and also Ba, Be and Cu. The incubation experiments indicated that solutions in contact with sample 1470 are enriched in Na, NO_3^-, SO_4^{2-}, Cl$^-$, Br$^-$, and I$^-$. The absence of enrichment in Ca, Mg, K and HCO_3^- is probably because these ions dissolve from dolomite and other carbonates, and their concentrations are limited by the solubility of these minerals (Fig. 3).

The most critical observation from this experiment is the high mobility of Au in surface soils. Shaking soil samples with deionized water (Fig. 19) has resulted in up to 15 μg/L of the Au (equivalent to 0.7% of the total Au in the solid phase) dissolving over 6 months. When irradiated, dissolution of Au was even more sustained, with up to 140 μg/L Au dissolved. It is calculated that, for the sample/water mixtures that were irradiated and shaken for six months, 6% of the Au was dissolved from samples 1468 and 1470, and 13% from sample 1467.

Gold is concentrated in the carbonate horizon in this profile. An initial expectation would be that this association is due to minerals in the carbonate horizon adsorbing and/or holding onto Au more strongly than in the other horizons. Results from this experiment suggest the converse to be the case. Gold was dissolved as readily, if not more so, from sample 1470 than from 1467 or 1468 (Fig. 19). Bubbling with CO_2, which was expected to simulate the high CO_2, low O_2 conditions expected to commonly occur close to actively respiring roots, strongly suppresses Au dissolution in the upper soil samples, but had little effect for sample 1470 (Fig. 19). Even shaking sample 1470 with water for only one day resulted in 2 μg/L Au dissolution. Finally, Au added to sample 1470 (with or without CO_2 bubbling) did not precipitate immediately, as was the case for 1467 and 1468, but instead took about one week to reach a minimum concentration of approximately 35 μg/L (Fig. 20).

Thus, in terms of dissolution of pre-existing Au and of the sorption and final redissolution of added Au, the experimental evidence for this soil profile suggests that Au in the carbonate horizon should be more mobile than elsewhere, and therefore that the carbonate horizon should be depleted rather than enriched with Au. This would suggest that the cause of the Au enrichment can not be primarily chemical. One hypothesis for the cause of the Au-carbonate association is that Au mobility is controlled in a manner similar analogous to relatively mobile elements such as Ca and Mg. Gold can have a high solubility when complexed with organically derived species such as CN^-, thiosulphate, amino acids or humic acids (Gray, 1988). Thus, in soil horizons, Au may be brought into solution by organically generated ligands, and precipitated in "evaporitic" horizons, *i.e.*, in the carbonate-rich zone. Clearly, describing Au as an evaporitic element would seem in most instances as incongruous. However, in the presence of large concentrations of ligands the Au may be considered a soluble element. This aspect will be discussed further in Section 7.

It was considered that, following this in-depth study on three samples, it was important to determine how general the conclusions are. In order to do this shorter experiments were developed, using more samples. These tests are described in the following sections.

4.   Soil Dissolution Tests

4.1.   Introduction

Previous incubation experiments (Section 3) indicate that, for Profile A, the sample representing the zone of major carbonate precipitation is also strongly enriched in the soluble "evaporitic" ions, namely Na^+, Cl^-, Br^-, I^-, NO_3^- and SO_4^{2-}. This section describes a simple dissolution experiment used to test this hypothesis on other soil profiles.

4.2.   Methodology and Results

Pulverized samples (< 75 μm) from Profiles A and B were shaken with water in a 1:5 soil:water ratio for one hour. The suspension was then centrifuged and filtered through 0.45 μm membrane filter. A sub-sample was analysed by Ion Chromatography, for Cl^-, Br^-, SO_4^{2-} and NO_3^-, using a DIONEX AS4A column under standard eluent conditions with a conductivity detector, and for I^- using a DIONEX AS5 column under standard eluent conditions with an electrochemical detector (Dionex, 1985). Another sub-sample was acidified and analysed for Na, K, Ca and Mg by flame AAS on a Varian AA875. Bicarbonate was calculated by difference.

Results are shown in Tables 8 and 9. Bromide was analysed for, but was not detected.

Table 8: Dissolution of Major ions from Profile B Samples, with the Comparative Composition of Sea Water.

Sample	Depth (m)	TDS mg/L	Ratio of ion/(total cations) - Measured in milli-equivalents/Litre								
			Mg	Na	K	Ca	Cl	NO_3^-	SO_4^{2-}	HCO_3^-	I⁻ (x 1000)
1214	0.005	452	0.21	0.19	0.06	0.55	0.23	0.014	0.09	0.66	0.00
1202	0.025	319	0.21	0.14	0.1	0.55	0.1	0.004	0.04	0.86	<0.01
1203	0.075	327	0.2	0.21	0.09	0.5	0.14	0.002	0.04	0.82	<0.01
1204	0.125	536	0.17	0.59	0.08	0.15	0.66	0.001	0.04	0.3	0
1205	0.175	786	0.12	0.76	0.05	0.06	0.76	0.002	0.06	0.18	0.01
1206	0.25	925	0.07	0.87	0.04	0.03	0.73	0.003	0.11	0.16	0.07
1207	0.35	836	0.06	0.88	0.03	0.02	0.67	0.002	0.13	0.2	0.23
1208	0.45	1094	0.04	0.92	0.03	0.01	0.68	0.002	0.17	0.15	0.23
1209	0.6	1200	0.04	0.93	0.02	0.01	0.66	0.001	0.19	0.15	0.16
1210	0.8	1051	0.03	0.93	0.02	0.01	0.63	0	0.19	0.17	0.17
1211	1	1025	0.05	0.92	0.02	0.02	0.62	0	0.19	0.19	0.09
1212	1.45	712	0.05	0.92	0.03	0	0.62	0	0.19	0.19	0.14
1213	1.8	641	0.03	0.94	0.02	0	0.66	0.001	0.2	0.14	0.41
Sea Water	-	34400	0.19	0.76	0.02	0.03	0.90		0.09	0.004	0.0008

Table 9: Dissolution of Major ions from Profile C Samples.

Sample	Depth (m)	TDS mg/L	Ratio of ion/(total cations) - Measured in milli-equivalents/Litre								
			Mg	Na	K	Ca	Cl	NO_3^-	SO_4^{2-}	HCO_3^-	I⁻ (x 1000)
1239	0.025	32	0.24	0.28	0.15	0.32	0.19	0.078	0.55	0.19	0.3
1241	0.125	22	0.30	0.27	0.15	0.28	0.22	0.062	0.51	0.20	2.1
1243	0.25	17	0.35	0.34	0.13	0.17	0.29	0.034	0.47	0.21	10.4
1245	0.45	17	0.37	0.34	0.13	0.17	0.38	0.015	0.57	0.03	4.8
1247	0.65	15	0.42	0.38	0.09	0.11	0.57	0.031	0.46	0.00	2.2
1249	0.85	19	0.48	0.36	0.08	0.07	0.47	0.019	0.50	0.01	4.0
1251	1.3	27	0.50	0.32	0.05	0.12	0.49	0.027	0.62	0.00	4.9

4.3. Discussion

As described previously (Section 3.3.2), the amounts of Ca and Mg dissolved from carbonate-rich materials such as the Profile A samples (Table 8) are not directly related to the amounts of Ca or Mg carbonates, but instead tend to reflect the equilibrium concentrations, for a particular pH and HCO_3^- concentration. For the solutions from Profile B, Mg and K are strongly correlated (Fig. 21), with a K:Mg ratio (when expressed in milli-equivalents) of 0.5:1, suggesting, as observed previously (Section 3.3.2), that available K is primarily incorporated in carbonates. Dissolved Ca and Mg (Fig. 22) show a bimodal distribution. When expressed in milli-equivalents, the upper line, which represents the upper, calcite-rich samples 1214, 1202 and 1203, has a Ca:Mg ratio of approximately 2.5:1, and the lower line, which represents the lower, dolomite-rich samples 1204 - 1213, has a Ca:Mg ratio of approximately

0.5:1. These results differ from those for Profile A, for which the Ca:Mg ratio was 1:1 (Figs. 16 - 18). Data are generally consistent with dolomite formation occurring in environments enriched in soluble Mg, relative to soluble Ca.
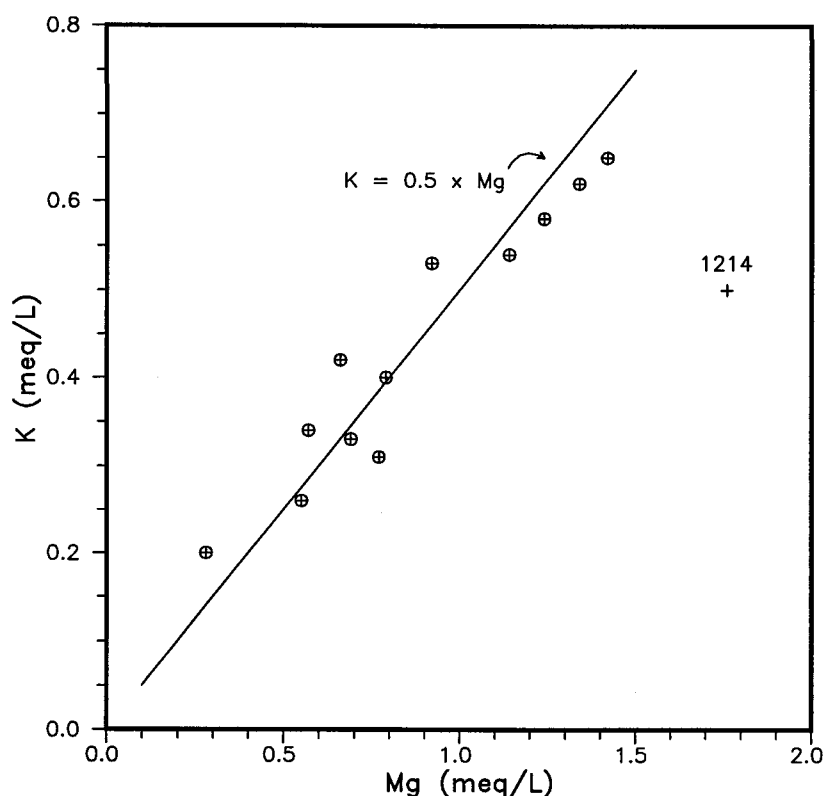
Figure 21: K vs. Mg for Soil Solutions from Profile B.

The chemistry of the soil solution for the Profile B samples (Table 8) changes dramatically at about 0.1 m, which is where the soil changes from calcite-dominated to dolomite-dominated (Table 4; Fig. 1). Solutions of the top three samples contain more than 50% Ca bicarbonate, with smaller concentrations of Mg and Na bicarbonate (Table 8). In comparison, all the deeper sample solutions contain 60% or more Na chloride, with up to 20% Na sulphate. In addition, the total salinity is also significantly increased below 0.1 m (Fig. 23). This is consistent with the soil below 0.1 m being enriched in evaporites, possibly due to the soil being of low permeability, thus retaining percolating waters and becoming enriched in salts as they evaporate.

Comparison with the composition of sea water (Table 8) indicates that the soil solutions are similar to sea water in that they are NaCl dominated. The soil waters differ mainly in that they are depleted in Mg (which may have been precipitated as dolomite) and enriched in SO_4^{2-} and HCO_3^-.

These results are consistent with those from the incubation experiments (Section 3.3.2), which indicated that the carbonate-rich sample was most enriched in evaporites, consistent the generally accepted hypothesis that the carbonate formation in these soils is an evaporitically driven process.
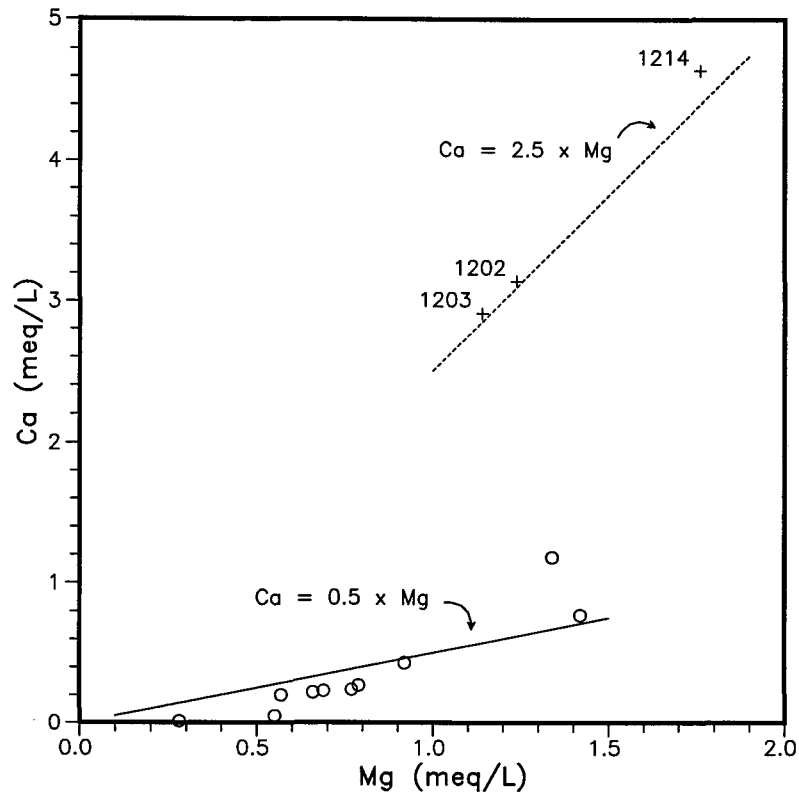
Figure 22: Ca vs. Mg for Soil Solutions from Profile B.
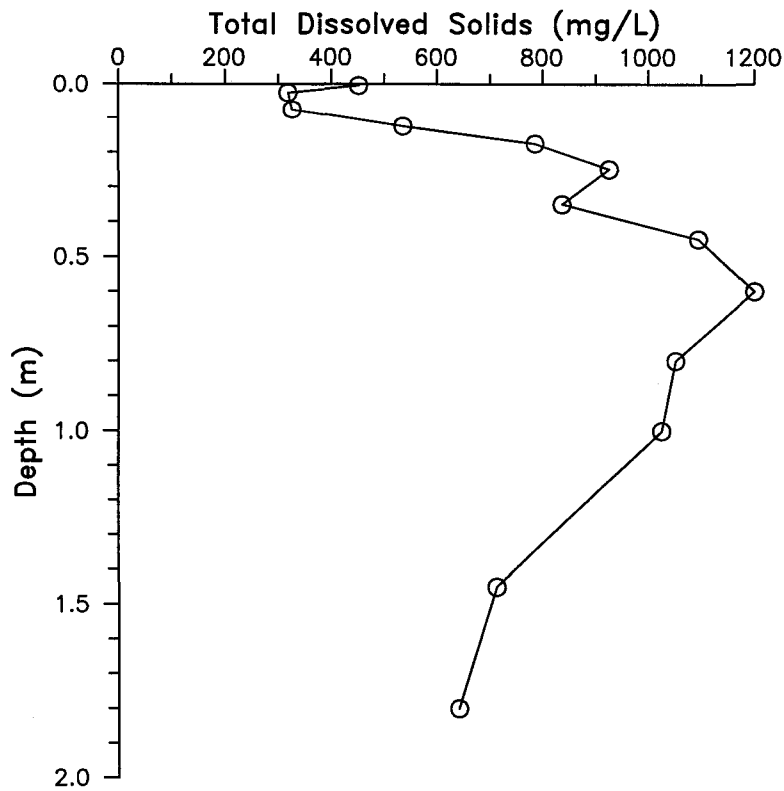
Figure 23: Total Dissolved Solids for Soil Solutions from Profile B.

The salinities, measured as total dissolved solids (TDS), of the Profile C solutions (Table 9) are 10 to 50 times lower than the Profile B solutions (Table 8), and the compositions have little resemblance to sea water (Table 9). This is consistent with Profile C representing a well drained soil profile, in which the effects of evaporation are less pronounced.

5. Gold Sorption Tests

5.1. Introduction

The incubation tests (Section 3) indicated that, contrary to expectations, initial adsorption (*i.e.*, after one day) of dissolved Au was weakest for the carbonate-rich sample 1470. The possible general nature of this phenomenon is of importance and has been tested, as described below.

5.2. Methodology and Results

Pulverized soil samples (< 75 μm) from Profiles B and C were shaken with a solution containing 5 mg/L Au and 5 mM hydrochloric acid (HCl) in a 1:2 soil:water ratio [*i.e.*, identical to the first batch experiment - mixture (iii) in Section 3.2] for 24 hours. The suspension was then centrifuged and filtered through 0.45 μm membrane filter. The solution was mixed with a solution of 0.2% potassium cyanide (KCN)/saturated CaO, in order to stabilize any Au in solution, and analysed for Au by ICP-MS. Results from this experiment are given in Tables 10 and 11.

Table 10: Sorption of Gold onto Profile B Samples.

Sample	Depth (m)	Au (μg/kg) relative to solid	% remaining in solution
1214	0.005	34	0.7
1202	0.025	8	0.2
1203	0.075	10	0.2
1204	0.125	10	0.2
1205	0.175	12	0.2
1206	0.25	58	1.2
1207	0.35	780	15.6
1208	0.45	344	6.9
1209	0.6	288	5.8
1210	0.8	420	8.4
1211	1	26	0.5
1212	1.45	16	0.3
1213	1.8	8	0.2

Table 11: Sorption of Gold onto Profile C Samples.

Sample	Depth (m)	Au (µg/kg) relative to solid	% remaining in solution
1239	0.025	<4	0.0
1241	0.125	36	0.4
1243	0.25	36	0.4
1245	0.45	16	0.2
1247	0.65	8	0.1
1249	0.85	12	0.1
1251	1.3	16	0.2

5.3. Discussion

The plot of Au remaining in solution after one day for the Profile B samples (Fig. 24), indicates very specific controls over Au sorption. Above 0.2 m and below 0.9 m, Au is effectively adsorbed, whereas in the zone between 0.2 and 0.9 m up to 16 % of the Au still remains in solution after one day. Data for OC content (Fig. 1) indicate that the top 0.2 m, as expected, has a distinctly higher OC content, and this may explain the strong adsorption of Au in this zone. The concentrations of carbonate minerals are particularly low in the two deepest samples (1.45 and 1.8 m; Fig. 1). Thus, it could be hypothesized that the area of least Au sorption is the zone of carbonate (in this case dolomite) dominance (i.e., where concentrations of carbonates are high, and organic carbon is low). These observations are consistent with the incubation experiments (Section 3), in which sample 1470 (which was enriched in dolomite and had low organic carbon; Tables 1 and 2) adsorbed Au only slowly (Fig. 20). In both cases, Au was added as a diluted standard (Cl^- concentration < 1000 mg/L) into a neutral mixture, and in such circumstances Au should have an extremely low solubility (Gray, 1988, 1990c).

The Profile C samples differed dramatically from the Profile B samples in that Au was strongly immobilized (Table 11), with a maximum of 0.4 % of the added Au remaining in solution after one day. Profile C differed from Profile B in that it contained no carbonates (Tables 1 - 4). Thus, these results are consistent with the hypothesis that Au is slowly adsorbed in soils dominated by carbonate, whereas environments rich in solid organic matter or low in carbonates tend to immobilize Au rapidly.

The inference that Au is particularly poorly adsorbed in carbonate-dominated horizons is surprising, particularly given the good correlation between Au and carbonate in soil profiles at a number of sites (Lintern, 1989; Lintern and Scott, 1990). It is feasible that poor adsorption onto dolomite is due to Au commonly being present as an anion [e.g., $AuCl_4^-$, $Au(OH)_2^-$, $Au(S_2O_3)_2^{3-}$] which would be expected to adsorb onto dolomite poorly. However, even in the absence of a proven explanation of the effect at this point, the poor sorption of Au of the dolomite dominated samples is clearly observed and obviously may be relevant in terms of modelling Au mobilization within these profiles.
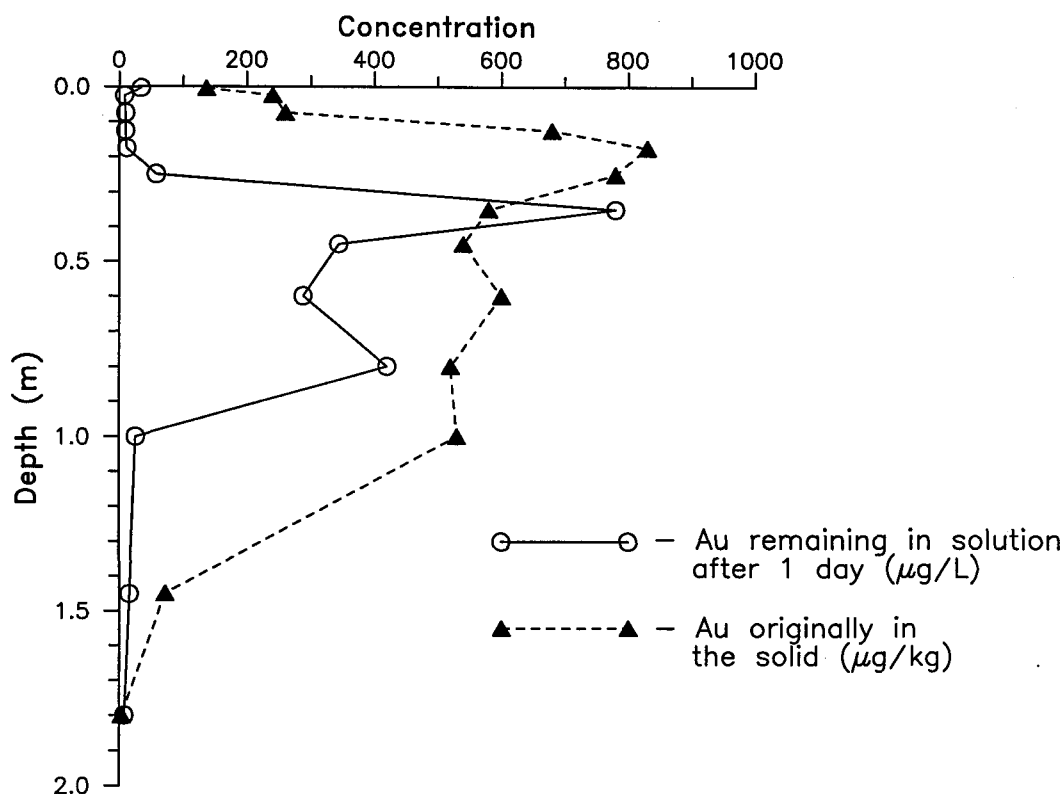
Figure 24: Gold Remaining in Solution after 1 day Equilibration with 5 mg/L AuCl$_4^-$ solution, with original Au concentration in the solid given for comparison.

6.   Soil Extraction Tests

6.1.   Introduction

The incubation studies (Section 3) showed Au dissolution effects that were presumably dependant on a number of factors such as the form of the Au, the presence of ligands and biological activity. In order to set up an experimental method that would give a rapid test of the chemical form of the Au in the soils, a number of selective extraction techniques were developed.

6.2.   Cyanide Extraction

Cyanide is the most commonly-used extractant for Au, but this reagent contains concentrated CN$^-$, thus ensuring very quick dissolution, and is buffered at pH 10, which may strongly affect the sample. A diluted, unbuffered CN$^-$ solution could offer a method of distinguishing the bonding of Au in soil. In the experiment described below the kinetics of Au dissolution from samples by CN$^-$ were investigated.

Eighty gram quantities of (non-pulverized) samples 1467, 1468 and 1470 were shaken with 400 mL of 100 mg/L KCN solution. Twenty mL aliquots were collected at specified time intervals, and analysed for Au. Results were calculated to a concentration of Au dissolved from the solid (with a correction for the Au removed from solution by each 20 mL aliquot removal), as shown in Table 12.

Table 12: Gold Dissolved (and measured pH) from Profile A Samples using dilute Cyanide.

Time	Au extracted (μg/kg)		
(days)	1467 (pH)	1468 (pH)	1470 (pH)
0.25	360 (8.5)	1350 (8.8)	2350 (9.3)
1	490 (8.9)	2250 (9.0)	3800 (9.3)
2	630 (8.6)	2500 (9.0)	3870 (9.7)
4	670	2780	4250
8	830	3300	4730

As the cyanide solutions were unbuffered their pH values were reduced by contact with the samples. The measured pH values are shown in brackets in Table 12. The pK_a of HCN is 9.22. Samples with pH less than 9.22 will have cyanide present as HCN, whereas solutions with pH greater than 9.22 will have cyanide present as CN^-. Thus, under these pH conditions the cyanide will be predominantly present as HCN in the 1467 and 1468 slurries and as CN^- in the 1470 slurry.

The dissolved Au at each collection time (Table 12) was calculated as the (Au extracted)/(Au extracted after 8 days), and the results plotted in Fig. 25. The extraction data for each sample approximately fitted a logarithmic curve. The curves for samples 1467 and 1468 were virtually co-incident, whereas sample 1470 showed a higher initial rate of dissolution, suggesting that the Au in sample 1470 is in a more available form than in the other samples, as found by the incubation experiments (Section 3.3.3). However, the difference is small, and could conceivably be due to the higher pH of the 1470 CN^- mixture (Table 12). Thus, although the results of the cyanide extraction suggests higher solubility of Au in sample 1470, they are not sufficiently discriminating to offer a useful selective extraction procedure for distinguishing the strength of bonding of Au. Buffer solutions could be used to ensure that the cyanide mixtures were maintained at constant pH, but the fast kinetics of the reaction (Fig. 25) and the poor distinction between the samples suggested that the cyanide extraction technique did not provide a useful method for development, and other (weaker) extractants were investigated.

6.3. Investigation of Selective Extractants

In the first experiment, six different extractants were tested:

(i)   0.1 $\underline{M}$ thiosulphate ($S_2O_3^{2-}$);
(ii)   0.1 $\underline{M}$ thiocyanate (SCN^-);
(iii)   0.1 $\underline{M}$ iodide (I^-);
(iv)   buffering the soil-solution mixture at pH 10 with sodium hydroxide (NaOH);
(v)   deionized water;
(vi)   0.2 % KCN / Saturated CaO.

Extractions (i), (ii), (iii) and (v) were all done at pH 7, using either HCl or NaOH to adjust pH.
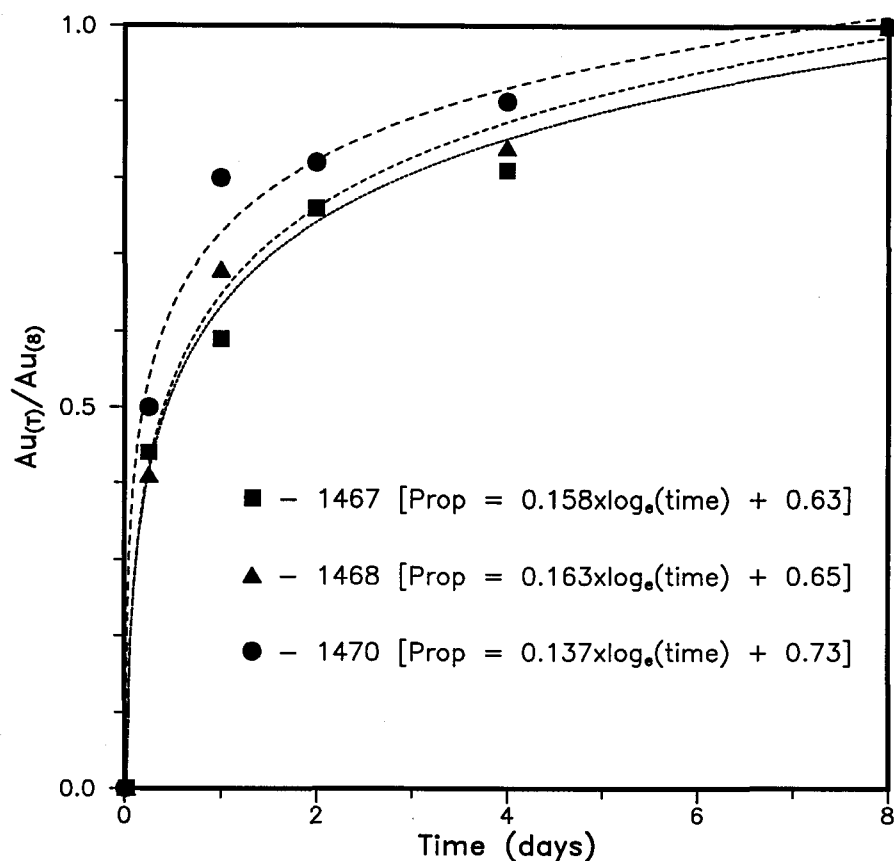
Figure 25: Proportion Au dissolved (relative to Au dissolved after 8 days) by Dilute Cyanide vs. Time, for Samples 1467, 1468 and 1470, with derived best fit logarithmic curves.

The solid materials used were:

(i)	Sample 1467:	Organic rich;
(ii)	Sample 1468:	Iron oxide rich;
(iii)	Sample 1470:	Carbonate rich;
(iv)	Std. 7:	Iron oxide rich;
(v)	Std. 11:	Iron oxide rich;
(vi)	TMF:	Saprolite.

Details on the chemistry, mineralogy and origin of these samples are given in Tables 1, 2 and 7. As with the other experiments, the Profile A samples were not pulverized.

Each of the solid materials was shaken with the six different extracting solutions (in plastic bottles) at a 1:2 soil:solution ratio. Water samples were taken at one day and seven days. These samples were filtered through 0.45 μm membrane filter, the filtrate then digested with aqua-regia, and analysed for Au by ICP MS. Results are given in Table 13.

Table 13: Effect of Various Extractants on Au Dissolution.

Extractant	Time (days)	Gold Extracted (µg/L)					
		1467	1468	1470	Std. 7	Std. 11	TMF
$S_2O_3^{2-}$	1	60	135	60	25	70	45
	7	85	110	170	30	20	60
SCN⁻	1	45	105	105	15	60	20
	7	35	145	270	20	40	50
I⁻	1	15	65	500	5	395	140
	7	20	105	655	<5	960	90
pH 10	1	50	<5	10	20	<5	5
	7	45	<5	15	10	<5	10
Water	1	<5	<5	<5	<5	<5	<5
	7	<5	<5	<5	<5	<5	<5
CN⁻	1	175	1150	1950	105	1500	4300
	7	290	540	1965	110	1275	4270

The results from this experiment were then normalized for each sample by dividing the Au from each solution by the maximum Au dissolved by CN⁻ for that sample. These relative results are given in Table 14.

Table 14: Relative Au Dissolution by Various Extractants.

Extractant	Time (days)	Proportion Gold Extracted					
		1467	1468	1470	Std. 7	Std. 11	TMF
$S_2O_3^{2-}$	1	0.21	0.12	0.03	0.23	0.05	0.01
	7	0.29	0.10	0.09	0.27	0.01	0.01
SCN⁻	1	0.16	0.09	0.05	0.14	0.04	0.005
	7	0.12	0.13	0.14	0.18	0.03	0.01
I⁻	1	0.05	0.06	0.25	0.05	0.26	0.03
	7	0.07	0.09	0.33	<0.05	0.64	0.02
pH 10	1	0.17	<0.004	0.01	0.18	<0.003	0.001
	7	0.16	<0.004	0.01	0.09	<0.003	0.002
Water	1	<0.02	<0.004	<0.003	<0.05	<0.003	<0.001
	7	<0.02	<0.004	<0.003	<0.05	<0.003	<0.001

All samples except TMF showed significant (> 10%) Au dissolution by one or more of the reagents. The poor extractability of the Au from TMF could be because this sample is from saprolite and the Au is present as medium- or large-grained native Au. The higher extractability of Au in samples 1467, 1468, 1470, Std. 7 and Std. 11 suggests that at least some of the Au in these samples is present as what might loosely be described as "chemical Au". This term could include very small-grained Au, adsorbed Au, or Au present as salts. However, the different extractants also differ dramatically in which samples they most effectively dissolve Au from, suggesting that this "chemical Au" exists in varying forms.

As would be expected, water alone is very poor at dissolving Au. Observed Au was < 5 µg/L for samples 1467, 1468 and 1470, in comparison with the analogous experiment described in Section 3, in which up to 8 µg/L Au was dissolved over seven days. The experiment described in Section 3 was conducted in glass bottles, whereas the experiment described here was conducted in plastic, and had higher analytical detection limits.

At pH 10, water extracted up to 20% of the Au from the organic-rich samples 1467 and Std. 7, with minimal dissolution from other samples. This effect may be due to the alkaline conditions resulting in dissolution of a normally insoluble Au compound, rather than formation of new bonds for the Au. For example, the Au in 1467 and Std. 7 may be present as organic complexes, which are solubilized in alkaline conditions.

The $S_2O_3^{2-}$ and SCN^- reagents are both expected to complex Au via the S group, and therefore to have similar relative activities. The reagents were moderately effective at dissolving Au from samples 1467, 1468, 1470 and Std. 7, weakly extracted Au from Std. 11, and were very poor for TMF (Table 14). In general the $S_2O_3^{2-}$ and SCN^- reagents appear to show some ability to distinguish "chemical Au" from native Au.

The I^- reagent differed dramatically from either alkaline extraction, or from $S_2O_3^{2-}$ and SCN^- (Table 14). It particularly extracted Au from Std. 11 (which was weakly extracted by the other reagents) and 1470. The Au extracted from TMF was higher than that dissolved by the other reagents.

In summary, the experiments indicate that Au in soils (as represented by samples 1467, 1468, 1470, Std. 7 and Std. 11) is much more soluble than Au in saprolite (sample TMF), in which it is possibly present as native Au. This is of course compatible with assertions that some Au in soils is present as "chemical Au". The major variations in the degrees of solubilities of the Au from the various samples in differing reagents suggest that this chemical Au category could represent at least two different forms: namely alkaline soluble (humic complexed?), and I^- soluble (chemically adsorbed?).

Iodide and pH 10 solutions were chosen as the most effective reagents and were used for all subsequent tests. The pH 10 reagent was modified for further extraction tests (as detailed in Section 6.4), for experimental simplicity. Results from these experiments are described in Sections 6.4.

6.4.   Iodide and Alkaline Extractions

Iodide extractions were done on the samples from Profiles B and C. The samples and their properties are listed in Tables 3 to 6. The extracting reagent was 0.1 $\underline{M}$ KI / 1 $\underline{M}$ NaHCO$_3$, which was taken to pH 7 with HCl. This reagent was shaken with 25 g of sample (pulverized to < 75 µm) for one day at a soil:solution ratio of 1:2. Following this, 10 mL of solution was removed, filtered through 0.45 µm membrane filter, mixed with 10 mL 0.2 % CN solution, and analysed for Au by ICP-MS. The results for this extraction could then be compared with previous total Au determinations by CN$^-$ extraction (Lintern, 1989).

An additional experiment was conducted on the same sample set, using the same reagent conditions, except that samples were merely crushed to < 10 mm. This was done in order to test for any effect of inclusion of Au in impermeable aggregations. Following the I^- extraction, 10 mL of 2 % KCN in saturated CaO was added to the mixture (giving a final solution concentration of 0.2 % KCN) and the bottles shaken for a further 3 days. Solution was then removed, filtered and analysed as previously. This experiment was done in duplicate in case of sample heterogeniety because of the large particle sizes of some of the samples. Results from the extractions of both the pulverized and crushed samples are shown in Tables 15 and 16. For simplicity, the duplicate analyses have been

averaged. Variability between duplicate samples was always less than 10%, and commonly less than 5%, except where the total Au concentration was less than 20 μg/kg, in which case variability was considerably higher, presumably due to lower precision.

Table 15: Iodide and Cyanide Dissolution from Profile B Samples.

Sample No.	Depth (m)	Fe_2O_3 (%)	CaO (%)	$Au_{(I)}$* (μg/kg) <75 μm	$Au_{(CN)}$# (μg/kg) <75 μm	$Au_{(I)}/$ $Au_{(CN)}$ <75 μm	$Au_{(I)}$ (μg/kg) <10 mm	$Au_{(CN)}$ (μg/kg) <10 mm	$Au_{(I)}/$ $Au_{(CN)}$ <10 mm
1214	0.005	6.2	3.2	44	136	0.32	10	77	0.13
1202	0.025	6.0	5.3	72	240	0.30	16	191	0.08
1203	0.075	5.7	7.5	64	260	0.25	16	250	0.06
1204	0.125	4.0	11.2	84	680	0.12	50	507	0.10
1205	0.175	4.3	13.2	64	830	0.08	76	640	0.12
1206	0.250	4.1	13.0	76	780	0.10	144	547	0.26
1207	0.350	4.9	9.1	52	580	0.09	106	431	0.25
1208	0.450	5.3	8.6	116	540	0.21	106	370	0.29
1209	0.600	5.5	7.4	64	600	0.11	106	380	0.28
1210	0.800	5.5	6.3	88	520	0.17	96	400	0.24
1211	1.000	6.1	3.2	68	530	0.13	70	320	0.22
1212	1.450	6.5	0.1	32	72	0.4	18	50	0.36
1213	1.800	5.9	0.06	<20	<5	nd	3	42	≈0.07

*   Au extracted using KI
#   Au extracted using KCN

Table 16: Iodide and Cyanide Dissolution from Profile C Samples.

Sample No.	Depth (m)	Fe_2O_3 (%)	CaO (%)	$Au_{(I)}$* (μg/kg) <75 μm	$Au_{(CN)}$# (μg/kg) <75 μm	$Au_{(I)}/$ $Au_{(CN)}$ <75 μm	$Au_{(I)}$ (μg/kg) <10 mm	$Au_{(CN)}$ (μg/kg) <10 mm	$Au_{(I)}/$ $Au_{(CN)}$ <10 mm
1239	0.025	20.4	0.06	116	170	0.68	10	181	0.06
1241	0.125	32.1	0.06	84	240	0.35	6	138	0.04
1243	0.250	30.6	0.05	88	160	0.55	5	77	0.06
1245	0.450	36.3	0.04	60	221	0.27	6	89	0.07
1247	0.650	37.5	0.05	52	170	0.31	8	124	0.06
1249	0.850	36.3	0.04	44	490	0.09	10	210	0.05
1251	1.300	48.9	0.05	48	990	0.05	12	570	0.02

*   Au extracted using KI
#   Au extracted using KCN

Alkaline extractions were also performed on the samples from Profiles B and C. The extracting reagent was 0.1 M $NaHCO_3$ taken to pH 10 with NaOH solution. This reagent was shaken with 25 g of sample (pulverized to < 75 μm) for one day at a soil:solution ratio of 1:2. Following this, 10 mL of solution was removed, filtered through

0.45 μm membrane filter, mixed with 10 mL 0.2 % CN solution, and analysed for Au by ICP-MS. The results for this extraction could then be compared with previous total Au determinations by CN⁻ extraction (Lintern, 1989).

An additional experiment was conducted on some selected samples, using the same reagent conditions, except that samples were crushed to < 10 mm rather than pulverized to < 75 μm. Results from the extractions of both the pulverized and crushed samples are shown in Tables 17 and 18.

Table 17: Alkaline and Cyanide Dissolution from Profile B Samples.

Sample No.	Depth (m)	Fe_2O_3 (%)	CaO (%)	$Au_{(OH)}$* (μg/kg) <75 μm	$Au_{(CN)}$# (μg/kg) <75 μm	$Au_{(OH)}/Au_{(CN)}$ <75 μm	$Au_{(OH)}$ (μg/kg) <10 mm	$Au_{(CN)}$ (μg/kg) <10 mm	$Au_{(OH)}/Au_{(CN)}$ <10 mm
1214	0.005	6.2	3.2	32	136	0.24	14	77	0.18
1202	0.025	6.0	5.3	12	240	0.05	4	191	0.02
1203	0.075	5.7	7.5	32	260	0.12	<4	250	<0.02
1204	0.125	4.0	11.2	24	680	0.04	<4	507	<0.01
1205	0.175	4.3	13.2	208	830	0.25	650	640	1.01
1206	0.250	4.1	13.0	240	780	0.31	110	547	0.20
1207	0.350	4.9	9.1	20	580	0.03	16	431	0.04
1208	0.450	5.3	8.6	12	540	0.02	8	370	0.02
1209	0.600	5.5	7.4	36	600	0.06	8	380	0.02
1210	0.800	5.5	6.3	64	520	0.12	<4	400	<0.01
1211	1.000	6.1	3.2	28	530	0.05	8	320	0.03
1212	1.450	6.5	0.1	36	72	≈0.5	<4	50	<0.08
1213	1.800	5.9	0.06	36	<5	nd	<4	42	<0.1

*   Au extracted using pH 10 reagent
#   Au extracted using KCN

The extraction of Au from the pulverized Profile B samples is generally more effective by I⁻ than alkaline extraction (Fig. 26). These extractions were very mild, both in terms of the reagents used and the short extraction time (one day), and that these results may therefore represent Au that could be reasonably expected to be mobilized by reagents produced during weathering or biological activity, over a longer time period. The ratio of I⁻ extractable Au to CN⁻ extractable Au for the pulverized samples $[Au_{(I)}/Au_{(CN)}$-pulv] is about 15 ± 5 % below 0.1 m depth (Table 15), which is the carbonate dominated zone (Fig. 1) and greater than 25 % in the upper organically dominated 0.1 m, whereas $[Au_{(OH)}/Au_{(CN)}$-pulv] is generally less than 10 % down the profile (Table 17). The percentage extracted by alkaline extraction is increased above 20 % in two zones: in sample 1214, which is highly organic; and in samples 1205 and 1206 (Table 17). The high $[Au_{(OH)}/Au_{(CN)}$-pulv] values for 1205 and 1206 are marked (Fig. 26). The solutions were clean and hence not contaminated. In summary, for the pulverized samples from Profile B about 20 % of the Au is generally extractable by I⁻, and about 10 % extracted by alkaline solution, except for the high Au zone at 0.2 m from which about 30 % of the Au is extracted at pH 10.

Table 18: Alkaline and Cyanide Dissolution from Profile C Samples.

Sample No.	Depth (m)	Fe_2O_3 (%)	CaO (%)	$Au_{(OH)}$* (μg/kg) <75 μm	$Au_{(CN)}$# (μg/kg) <75 μm	$Au_{(OH)}$/ $Au_{(CN)}$ <75 μm	$Au_{(OH)}$ (μg/kg) <10 mm	$Au_{(CN)}$ (μg/kg) <10 mm	$Au_{(OH)}$/ $Au_{(CN)}$ <10 mm
1239	0.025	20.4	0.06	68	170	0.40	28	181	0.15
1241	0.125	32.1	0.06	60	240	0.25	40	138	0.29
1243	0.250	30.6	0.05	20	160	0.13	<4	77	<0.05
1245	0.450	36.3	0.04	56	221	0.25	8	89	0.09
1247	0.650	37.5	0.05	16	170	0.09	32	124	0.26
1249	0.850	36.3	0.04	8	490	0.02	32	210	0.15
1251	1.300	48.9	0.05	24	990	0.02	20	570	0.04

*   Au extracted using pH 10 reagent
\#   Au extracted using KCN

Figure 26: Au extracted by Various Reagents vs. Depth using Pulverized (< 75 μm) Profile B Samples.

The samples that were crushed to < 10 mm had less Au extracted by CN^- over three days (Fig. 27) than when the samples were pulverized (Fig. 26). However I^- extractable Au was **HIGHER** in the crushed samples than in the pulverized samples, between 0.15 and 1 m depth (Fig. 27; Table 15). A possible explanation is that, in the crushed samples, Au associated with the carbonates is being readily extracted (as was also observed for the carbonate-rich sample 1470; Table 14). This Au associated with carbonate may be in a surface adsorbed form and therefore accessible to the solution. Thus, pulverizing the solid would not enhance Au extraction by I^-. Indeed, by exposing the surfaces of minerals such as Fe oxides, which could re-adsorb the dissolved Au (Gray, 1990c), pulverizing may reduce the I^- extractable Au, as is observed. The high concentration of alkaline-extractable Au in the pulverized samples could occur because, unlike Au in the I^- solution, the extracted Au would be very poorly

adsorbed by any exposed Fe oxide at pH 10, due to the surface becoming anionic at higher pH levels. Conversely, Au extractable by both I⁻ and by alkaline extraction is significantly reduced for the crushed samples, relative to the pulverized samples, for the top 0.1 m (Tables 15 and 17). This is the zone of high organic matter (Fig. 1). It is possible that Au in the "interior" of a humic particle or a decaying piece of twig would become more extractable following pulverization of these particles.
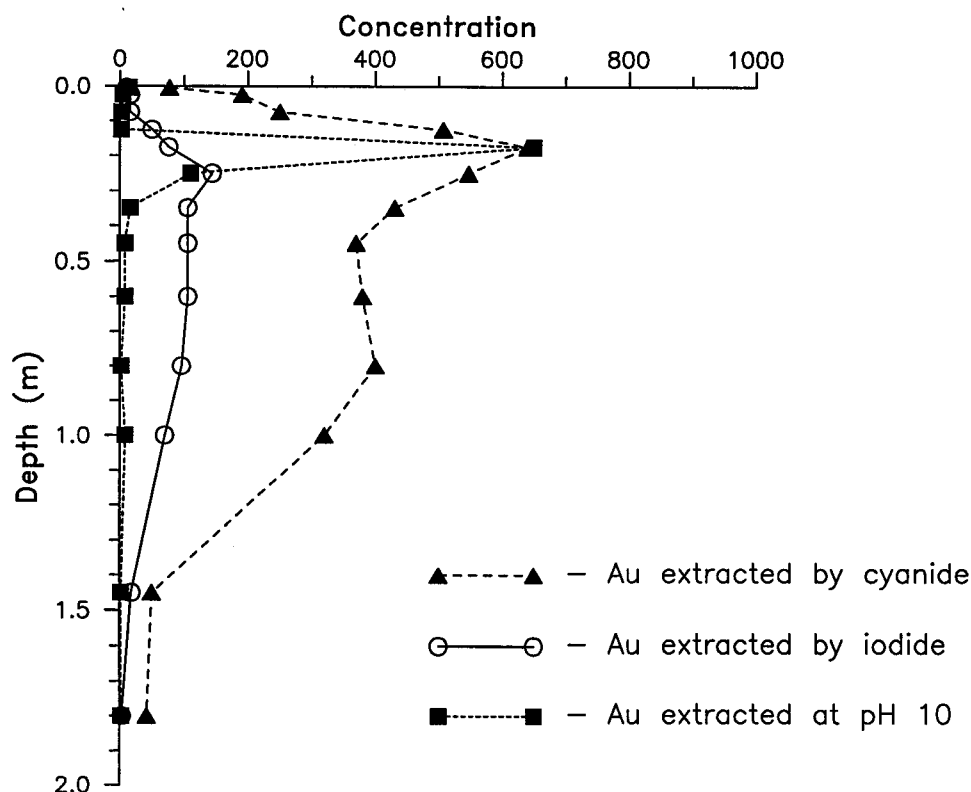
Figure 27: Au extracted by Various Reagents vs. Depth using Crushed (< 10 mm) Profile B Samples.

The extraction results do NOT suggest that the Au contained in the Au-rich carbonate horizon in Profile B is LESS extractable than in other horizons. Indeed, the evidence, though not yet clearly understood, suggests that Au associated with the carbonate is MORE chemically extractable than in the upper organic-rich zone or in the lower carbonate poor clay.

Cyanide extractable Au in the pulverized Profile C samples (Fig. 28) is approximately 200 μg/kg for the samples from the upper 0.6 m of the profile. Below this it increases sharply to about 990 μg/kg at 1.3 m depth. Iodide extractable Au shows a very different pattern, being highest at the very top of the profile [where $Au_{(I)}/Au_{(CN)}$-pulv = 0.68; Table 16], and steadily decreasing with depth. A similar pattern is also observed for alkaline extractable Au (Fig. 28; Table 18).
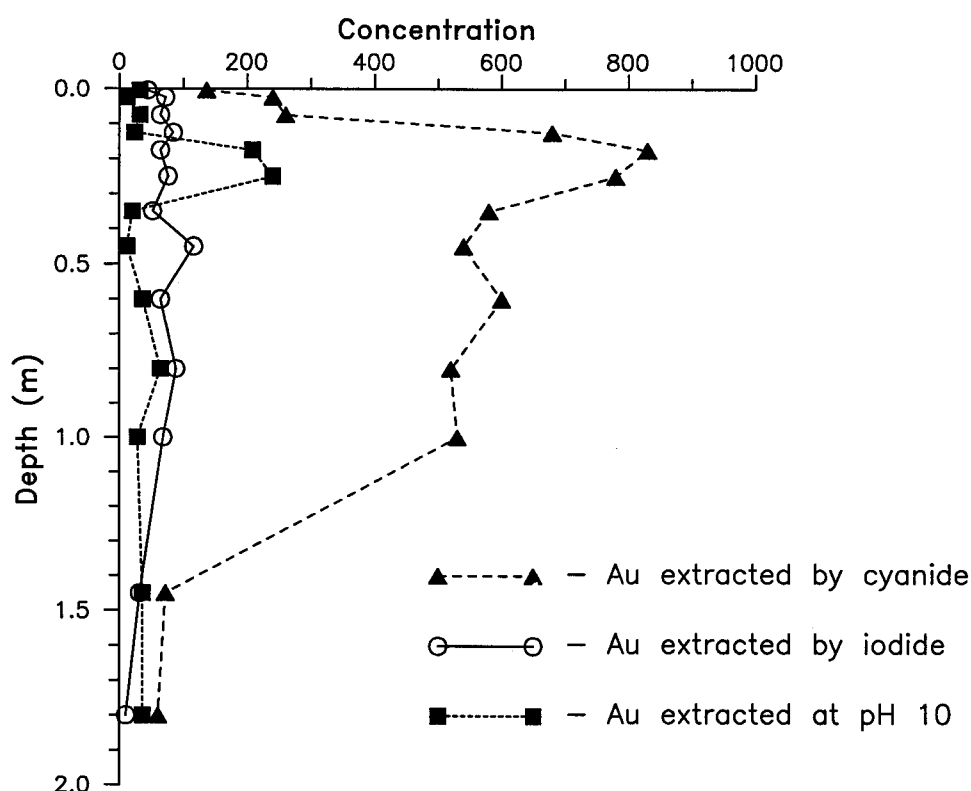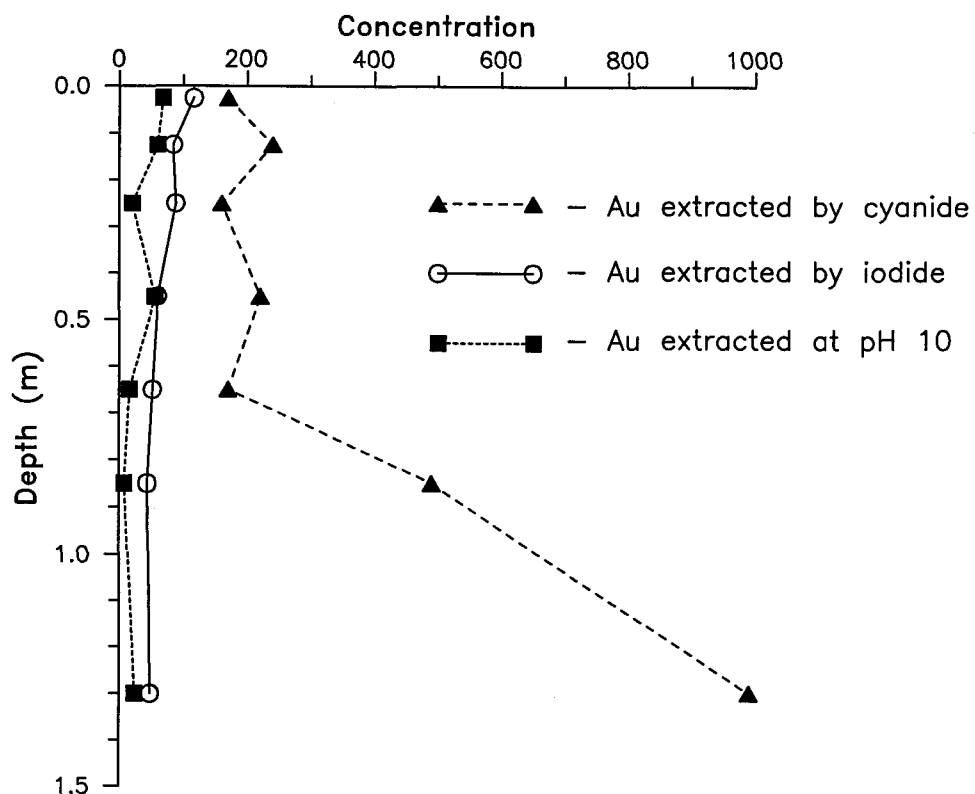
Figure 28: Au extracted by Various Reagents vs. Depth using Pulverized (< 75 μm) Profile C Samples.

In samples that were only crushed prior to extraction, CN⁻ extractable Au is reduced by about half (Fig. 29), except for the uppermost organic-rich sample, in which similar amounts of Au were extracted for both sample treatments. Iodide-extractable Au was significantly reduced in the crushed samples (compare Fig. 29 with Fig. 28), implying that Au is incorporated within minerals, rather than just being on an external surface, as may be the case in the Profile B samples.

Thus, the lower part of Profile C (which is richer in Au) corresponds with the zone where Au is least extractable, and the upper 0.6 m of the profile (which is poorer in Au) corresponds to the zone where Au is readily extractable. This is in contrast with Profile B, which shows totally opposite behaviour.

Concentration
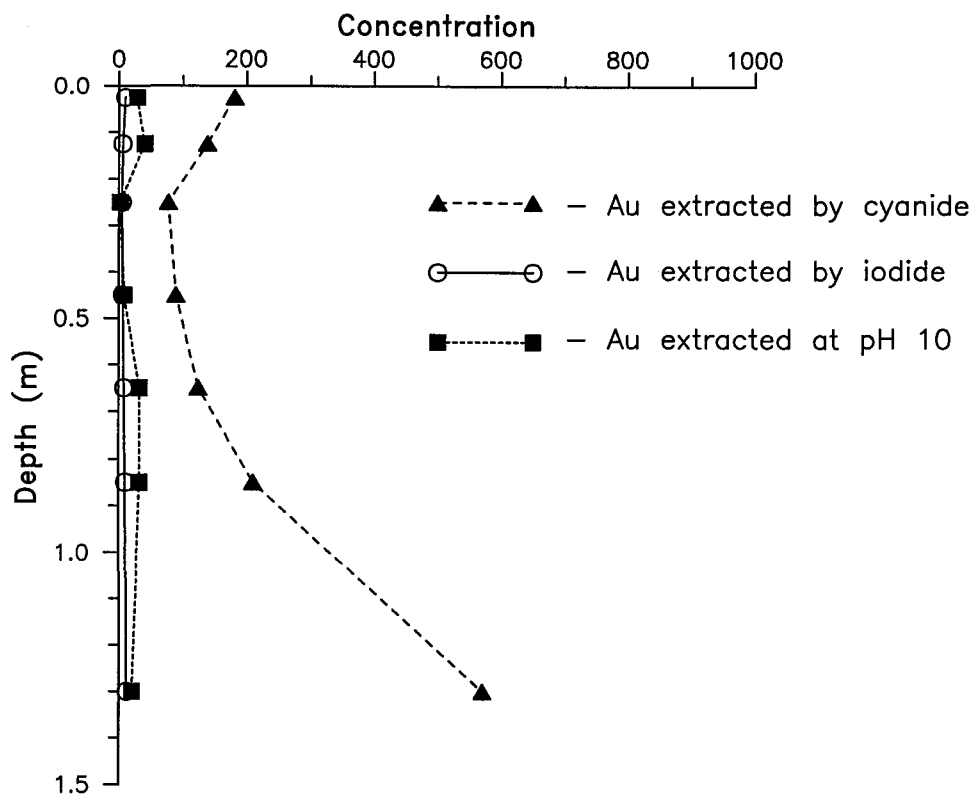
Figure 29: Au extracted by Various Reagents vs. Depth using Crushed (< 10 mm) Profile C Samples.

7.   General Discussion

7.1.   Chemistry of Relevant Solid Phases

Certain results (Sections 3, 5 and 6) suggest that the chemistry of Au is strongly affected by the presence of particular mineral phases, such as dolomite or organic matter. It is therefore important to understand the processes controlling the distribution of these mineral species.

Several authors have pointed to lateritic zones as important in gold redistribution (Evans, 1981; Mann 1984b; Freyssinet *et al.*, 1987; Butt, 1989), and gold is often found intimately associated with iron oxides in many profiles (Foster *et al.*, 1978; Crone *et al.*, 1984; Mann, 1984a; Smith and Keele, 1984; Wilson, 1983, 1984). The chemical reason for this is not certain, but the redox reaction of Fe^{2+} with dissolved gold (Eqn. 10) does result in precipitation of both metals. Additionally, near the surface of lateritic zones, oxidation of Fe^{2+} can cause highly acid conditions which can destabilize thiosulphate and other ligands (Gray, 1988), resulting in precipitation of the complexed gold. Iron oxide strongly adsorbs gold from solution (Nechaev, 1984), as would be expected, as these oxides generally have positively charged surfaces at neutral and low pH.

All of the soils tested contained minor (approximately 5%) to major (up to 50%) concentrations of Fe oxides. These oxides may be very old, having been formed by lateritization processes during a more humid period. In profiles which have not become carbonate-enriched (*i.e.*, Profile C), processes such as adsorption may still be primarily controlled by Fe oxides (particularly below the upper zone of organic matter enrichment).

The major carbonate minerals in the soils investigated are calcite and dolomite. Carbonate minerals are common in soils in semi-arid regions of the Yilgarn Block south of the Menzies Line (Butt *et al.*, 1977), and may be actively forming at present. Calcite is commonly observed in soils and in general will readily dissolve or precipitate from solution. Dolomite is much more difficult to form (Drever, 1982), and waters are commonly observed that are supersaturated with respect to dolomite (*i.e.*, in theory dolomite should be precipitating, but this is not occurring due to kinetic constraints). It is possible that the clue to the formation of dolomite in these soils are the highly saline conditions within the carbonate horizon (Sections 3.3.2 and 4). This saline sub-surface moisture is primarily enriched in Na, but is also strongly enriched in Mg (Fig. 6; Table 9). Thus, the dolomite could be occurring as a result of the long-term interaction of calcite with such high-Mg waters. The strong association of K with carbonates, both for Profile A (Fig 8; Section 3.3.2) and for Profile B (Fig. 21), suggests that potassian carbonates are also being generated by the interaction of saline waters with carbonate.

The 1:1 relationship for dissolved Mg and Ca for the Profile A incubations (Figs. 16 - 18) indicates that dolomite is being dissolved, with little or no calcite dissolution. This implies some kinetic constraint to calcite dissolution, which would be unlikely, or more probably that the dolomite, having formed later, has "coated" the calcite. Given the high abundances of Mg in Profiles A and B (Tables 1 and 3), this is not an unreasonable hypothesis. The implication of this is that the only surfaces exposed within the upper carbonate-rich zone of a soil will be the dolomite, and/or any other recently formed carbonate (such as the K-containing carbonate discussed in the last paragraph). The chemistry of Au may therefore be strongly controlled by these minerals.

The other soil phase expected to be of recent origin is organic matter, formed via the decomposition of plant debris. Data for Profile A are given in Table 1, and depth profiles for Profiles B and C are shown in Figs. 1 and 2. In general, organic matter concentration is particularly high within the top 0.2 m of the profiles. It should also be recognized, though this has not been tested, that the nature and composition of the organic matter may change with depth, possibly going from a "mull" type material at the top of the surface, towards a more fine grained material at depth. As organic matter is expected to be the most recently formed phase in the upper soil, it is presumably the most surface active. Thus, at the top of the soil profile, it is highly likely that Au distribution may be strongly controlled by the organic matter.

Research conducted at a number of sites within the southern Yilgarn area (Lintern, 1989; Lintern and Scott, 1990) has indicated a strong association between Au and carbonate. A natural assumption would be to assume that there is a chemical tendency towards Au enrichment in this zone, such as a strong adsorption of Au by carbonate, or a lessened tendency for Au to dissolve from carbonate, than from other phases within the soil, such as Fe oxides or organic matter. All available chemical studies, as described in this report and summarized below, appear to contradict this assumption.

7.2.   Sorption of Gold

Shaking of Au solutions with samples from Profiles A, B and C (Fig. 20 and 24; Table 12) unambiguously showed that the samples least likely to adsorb Au chloride strongly from solution over the short term (one day to one week) are those enriched in carbonates, with low levels of organic matter: *i.e.*, those samples whose SURFACES are dominated by carbonates. Other samples which are expected to have available organic matter or Fe oxide surfaces adsorb Au very strongly.

There are three important ways in which these sorption experiments may not accurately mirror true soil processes, these are:

(i)   gold is presumably not being transported as the Au chloride complex;

(ii) where Au is being transported in solution, it is presumably not occurring at concentrations of 5 mg/L;

(iii) the experimental soil/water ratio is lower than would occur in a natural soil.

The second and third objections may have some validity, and experiments could be repeated at lower Au concentrations, though increasing the soil/water ratio would severely complicate any experimentation. Analytical sensitivity problems may preclude scaling the Au concentration down beyond two orders of magnitude. It is suggested that these experiments will probably show similar results. A more important concern is the expected form of the Au complexes in natural conditions. Unfortunately, this is not presently known, but it is possible that the low sorption of the Au is due to a poor tendency of these carbonates to adsorb anions. Most important soluble complexes of Au are expected to be anionic [e.g., $AuCl_2^-$, AuI_2^-, $Au(S_2O_3)_2^{3-}$] and may therefore show similar tendencies to those demonstrated in the sorption experiments. In addition, work described in another report (Gray, 1990c) indicates that $Au(S_2O_3)_2^{3-}$ is more poorly adsorbed by sample 1470 than by any of the other samples (which represented a range of organic, Fe oxide, and Mn oxide rich soils) tested.

Other experiments that would be valuable, are sorption tests on pure minerals, and tests on the sorption of Au by soils from solutions generated by incubation experiments (Section 3.3.3). Of course, even the latter experiment represents a somewhat artificial environment, but it may still offer a closer approximation to "soil solution Au".

Thus, further work on the sorption may still be warranted, in order to validate the conclusions drawn here. However work done to date indicates the poor tendency of carbonate-rich samples to adsorb Au, either when present as the chloride complex (Sections 3.3.3 and 5), or as the thiosulphate complex (Gray, 1990c).

7.3.   Selective Extraction

Various selective extraction procedures (Section 6) can be used to gain information on the form of the Au already present in the soils. The two treatments considered most useful were I^- and alkaline extraction. Gold in the carbonate-rich horizon was easily extracted by an I^- or pH 10 reagent, for both Profile A (Table 15) and Profile B (Tables 16 and 18; Figs. 26 and 27). The high extractability of Au even when the samples were merely crushed (indeed, from 0.175 m to 1 m depth I^- extractable Au was higher in the crushed material, relative to the pulverized material; Table 16) suggests that a significant proportion of the Au associated with the carbonate is present in a form that is readily accessible to the solution.

Extractable (and total) Au was considerably lessened above and below the carbonate zone, and was also very low for the Au-rich regions of the Fe-rich Profile C (Figs. 28 and 29). The only zone in Profile C that had high values of extractable Au was in the uppermost organic-rich zone, probably due to dissolution of Au associated with organic matter. This extractable Au was considerably reduced in the samples that were merely crushed (Fig. 29), as also occurred for the upper, organic rich, samples from the top 0.1 m of Profile A (Table 16; Figs. 26 and 27).

In summary, the extraction experiments for the three Profiles, and for the other single samples, suggest that Au may exist in a number of different forms. These predicted forms, and the extraction behaviour attributed to them, are:

(i) Gold associated with organic matter in the upper part of the soil. This Au is particularly extractable when the soil material is crushed, suggesting that the Au is occluded. In the crushed material, alkaline-extractable Au is greater than I⁻ extractable Au, possibly because the alkaline conditions act to solubilize the organic material.

(ii) Gold associated with the Fe oxides or other, non-carbonate material, as observed in the lower part of Profile C. This Au has a moderate extractability in I⁻ or in alkaline solution (Fig. 28). This is considerably lowered for the samples that are merely crushed (Fig. 29), suggesting that the Au occurs within solid phases.

(iii) Gold associated with carbonates. This Au has a strong extractability in I⁻ or in alkaline solution, PARTICULARLY in the samples that are merely crushed, suggesting that a substantial part of the Au is on surfaces or in environments that are readily accessible to the solution.

The extraction results imply that Au in carbonates is readily accessible to the solution, and is also relatively easily dissolved. Some of the results from the incubation experiments (Section 3), which were initially highly surprising, can now be seen to be consistent with this hypothesis.

7.4. Incubation Experiments

The effects of the incubation of the normal and irradiated soils on the dissolution of Au already present in the samples, and on Au added at the beginning of the experiment are discussed in detail in Section 3.3.3, and only a general overview of the results are given here. In general, the dissolution of the Au already present was highest for the samples that were irradiated (Fig. 19): *i.e.*, biological activity reduces the dissolution of Au. Dissolution from irradiated mixtures was highest for the carbonate-rich sample 1470. Mechanisms for the suppression of Au dissolution could be decomposition of potential ligands or adsorption of Au by bacteria. This effect was most strongly marked for samples 1467 and 1468, which are higher in the profile, and are more enriched in organic matter. In addition, bubbling with CO_2 strongly suppressed Au dissolution in these samples. Sample 1470 differed in that Au dissolution increased with time even for the non-irradiated samples, and there was little effect from CO_2 bubbling.

Thus, the Au dissolution results yield two important conclusions:

(i) Gold is potentially highly soluble in all three of the samples tested, but tends to be immobilized by biological action. However, the high concentrations of soluble Au after one week shaking (approximately 10 μg/L in all three mixtures; Fig. 19) implies that Au could be extensively mobilized in a profile by a large rain-fall event.

(ii) For the normal, CO_2-bubbled, and irradiated treatments, Au was most extensively dissolved from the most carbonate-rich sample (1470), consistent with the selective extraction experiments (Section 6) described above.

When Au was added to the soils (Fig. 20), it precipitated from solution (though, as discussed above, only slowly in the case of sample 1470), but then, following a lag of about one week for sample 1467 and 1468, began to redissolve. This lag period suggests a biological control, and indeed, irradiation strongly suppressed the dissolution of the added Au. Additional work done on this phenomenon (Gray, 1990c, and other unpublished data) suggests that this redissolution of Au is a general effect for surface soils containing significant amounts of organic matter, but is not observed for organic-poor soils, nor for other metals such as Ag. Sample 1470 differed from the other samples in that the dissolution was nearly linear with time, that the CO_2-bubbled treatment also showed a linear, though slower, dissolution, and that irradiation had less effect, suggesting that the dissolution was chemically controlled. Thus, the conclusions drawn from the incubation of the Au added treatments are that:

(i)   gold added to the carbonate-rich sample 1470 is more soluble than that added to samples 1467 and 1468;

(ii) long term (greater than one week) incubation of the organic-rich samples 1467 and 1468 results in the formation of solution species with a strong ability to dissolve Au.

7.5.   Conclusions

The general hypothesis to be made from all of the experimental data available to date is that Au may be strongly mobilized by biologically-controlled species, can also be immobilized by biological processes, and generally appears to be most chemically mobile within carbonate-rich zones. Why then is Au most strongly correlated with carbonate, for a large number of carbonate profiles across the southern Yilgarn area? At the present time the only viable hypothesis is that Au distribution is at least partially controlled by evaporative processes. Thus, Au, as discussed above, can be highly mobile in soil horizons, as a result of biologically generated ligands. Gold is known to be adsorbed into plants, both in the southern Yilgarn study areas (Lintern 1989; Lintern and Scott, 1990) and elsewhere (Shacklette et al., 1970; Kaspar et al., 1972; Girling et al., 1979; Warren, 1982; Smith and Keele, 1984; Erdman and Olson, 1985). As the humus decomposes, Au-organic complexes are formed that then percolate down the soil profile. As demonstrated in Fig. 20, such Au-organic complexes may be very stable against adsorption or precipitation. However once these complexes reach the carbonate horizon, they will be immobilized, not necessarily by chemical means, but by the very fact that these horizons are an evaporative zone. As the soil solution evaporates, forming additional carbonate, and precipitating halite and other salts, the Au must also precipitate with the carbonate zone. Thus, the primary controls on Au distribution in these soils are biological and physical, rather than chemical, as first expected.

What are the implications of this hypothesis? In general, if Au is strongly correlated with carbonate within soils in the southern Yilgarn, as has been generally observed, then for these soils the mechanism is not as significant, from an exploration stand-point, than the very fact that the correlation occurs. Possibly of more significance are the implications of this hypothesis for the distribution of Au in soils outside the area of extensive carbonate formation in soils (i.e., north of the Menzies line) or in non-carbonate soils within the southern Yilgarn. It is highly possible that the formation of carbonates is a strong indicator of an 'evaporitic' horizon, and its absence would indicate well-drained soils, which according to the above hypothesis would not have such a late-stage Au soil enrichment as observed for the carbonate soils. Work is particularly required north of the Menzies line, to check other soil types and see whether their characteristics are compatible with this theory for Au redistribution in soils, and to find out the implications for Au exploration using soils in other weathering environments.

Acknowledgements

References.

Anon., (1981). The climate and meteorology of Western Australia. Western Australian Year Book 1981 (New Series): 49-65. Australian Bureau of Statistics.

Berthelin, J. (1988). Microbial weathering processes in natural environments. *In.* "Physical and Chemical Weathering in Geochemical Cycles". (Eds. A. Lerman and M. Meybeck). ISBN 90-277-2821-6. (Kluwer Academic Publishers, Dordrecht, The Netherlands)

Butt, C.R.M, Horwitz, R.C. and Mann, A.W. (1977). Uranium Occurrences in Calcrete and Associated Sediments in Western Australia. CSIRO Miner. Research Lab., Div. Mineralogy. Rep. No. FP16.

Butt, C.R.M, (1989). Genesis of supergene gold deposits in the lateritic regolith of the Yilgarn Block, Western Australia. *In* "The Geology of Gold Deposits: the Perspective in 1988." (Eds. R.R. Keays, W.R.H. Ramsay and D.I. Groves). Economic Geology Monograph 6, Economic Geology, New Haven, pp. 460-470.

Crone, W., Larson, L.T., Carpenter, R.H., Chao, T.T. and Sanzolone, R.F. (1984). A comparison of iron oxide-rich joint coatings and rock chips as geochemical sampling media in exploration for disseminated gold deposits. J. Geochem. Explor., 20: 161-178.

Dionex, (1985). Technical Note 16. (PO Box 3603 Sunnyvale, California, USA).

Drever, J.I. (1982). "The Geochemistry of Natural Waters." (Prentice-Hall, Inc., Englewood Cliffs, N.J. USA). 388 p.

Erdman, J.A. and Olson, J.C. (1985). The use of plants in prospecting for gold: a brief overview with a selected bibliography and topic index. J. Geochem. Explor., 24: 281-309.

Evans, D.L. (1981). Laterization as a possible contribution to gold placers. Eng. Mining. Jour., 182(8): 86-91.

Foster, R.L., Foord, E.E. and Long, P.E. (1978). Mineralogy and composition of Jamison Creek particulate gold, Johnsville Mining District, Plumas County, California. Econ. Geol., 73: 1175-1183.

Freyssinet Ph., Zeegers, H. and Tardy, Y. (1987). Neoformation d'or dans les cuirasses lateritiques: dissolution, migration, precipitation. C.R. Acad. Sci. Paris, t. 305, Serie II, p 867-874.

Gerritse, R.G. and George, R.J. (1988). The role of soil organic matter in the geochemical cycling of chloride and bromide. J. Hydrology, 101: 83-95

Girling, C.A., Peterson, P.J. and Warren, H.V. (1979). Plants as indicators of gold mineralization at Western Bar, British Columbia, Canada. Econ. Geol., 74: 902-907.

Gray, D.J. (1988). The Aqueous Chemistry of Gold in the Weathering Environment. (AMIRA P240/P241). CSIRO Division of Exploration Geoscience Restricted Report EG 4R.

Gray, D.J. (1990a). Hydrogeochemistry in the Mount Gibson Gold District. (AMIRA P240: Laterite Geochemistry). CSIRO Division of Exploration Geoscience Restricted Report 120R.

Gray, D.J. (1990b). Hydrogeochemistry of the Panglo Gold Deposit. (AMIRA P241: Weathering Processes). CSIRO Division of Exploration Geoscience Restricted Report 125R.

Gray, D.J. (1990c). The Sorption of Gold and Silver on Soil Minerals. (AMIRA P241: Weathering Processes). CSIRO Division of Exploration Geoscience Restricted Report 127R.

Kaspar, J., Hudec, I., Schiller, P., Cook, G.B., Kitzinger, A. and Wolfl, E. (1972). A contribution to the migration of gold in the biosphere of the humid mild zone. Chem. Geol., 10: 299-305.

Lintern, M.J. (1989). Study of the Distribution of Gold in Soils at Mt. Hope, Western Australia. (AMIRA P241: Weathering Processes). CSIRO Division of Exploration Geoscience Restricted Report 125R.

Lintern, M.J. and Scott, K.M. (1990). The Distribution of Gold and other Elements in Soils and Vegetation at Panglo. (AMIRA P241: Weathering Processes). CSIRO Division of Exploration Geoscience Restricted Report 129R.

Mann, A.W. (1984a). Mobility of gold and silver in lateritic weathering profiles: some observations from Western Australia. Econ. Geol., 79: 38-49.

Mann, A.W. (1984b). Redistribution of gold in the oxidized zone of some Western Australian deposits. A.I.M.M. Perth and Kalgoorlie Branches, Regional Conf. on "Gold Mining, Metallurgy and Geology", Oct 1984.

Nechaev, Ye.A. (1984). The effects of solution composition on the adsorption of gold(III) complexes on hematite. Geochem. Int., 21(4): 87-93.

Parkhurst, D.L., Thorstenson, D.C. and Plummer, L.N. (1980). PHREEQE, a computer program for geochemical calculations. U.S. Geol. Surv. Water Resources Investigations 80-96, 210p.

Shacklette, H.T., Lakin, H.W., Hubert, A.E. and Curtin, G.C. (1970). Absorption of gold by plants. U.S. Geol. Surv. Bull. 1314-B, 23 p.

Smith, B.H. and Keele, R.A. (1984). Some observations on the geochemistry of gold mineralization in the weathered zone at Norseman, Western Australia. J. Geochem. Explor., 22: 1-20.

Warren, H.V. (1982). The significance of a discovery of gold crystals in overburden. *In* "Precious Metals in the Northern Cordillera". A Symposium held by the Association of Exploration Geochemists, April 13-15 1981, Vancouver, British Columbia, Canada. pp 45-51.

Wilson, A.F. (1983). The economic significance of non-hydrothermal transport of gold, and of the accretion of large gold nuggets in laterites and other weathering profiles in Australia. Spec. Publ. geol. Soc. S. Afr., 7: 229-234.

Wilson, A.F. (1984). Origin of quartz-free gold nuggets and supergene gold found in laterites and soils - a review and some new observations. Aust. J. Earth Sci., 31: 303-316.

Appendix 1: Chemical Compositions of Solutions From Incubation Experiments.

All concentrations in mg/L, except Au in µg/L

A. Sample 1467

Addition	Time	pH	Au	Fe	Mg	Na	K	Ca	Cl⁻	Br⁻	I⁻	NO₃⁻	HCO₃⁻	SO₄²⁻	S₂O₃²⁻
	1 day	7.67	<0.2	0.39	10	91	2.5	15	15	<0.02	<0.001	0.5	306	5.7	<0.002
	1 wk	7.67	7.9	0.06	17	108	3.8	26	14	0.05	0.002	2.2	440	7.8	
	1 mth	7.05	1.1	0.15	39	137	9	59	17	0.07	0.034	0.16	744	14.3	
	6 mth	7.97	2.2	0.27	57	148	8	79	15	0.36	0.010	0.05	912	11.1	<0.002
Au	1 day	7.27	7.3	0.05	29	130	4.4	41	220	<0.02	<0.001	0.15	277	4.7	
Au	1 wk	7.25	18.9	0.03	40	137	5.7	58	220	<0.02	0.004	3.5	390	6.8	
Au	1 mth	7.12	781	0.08	58	148	8.2	87	250	<0.02	<0.001	<0.02	598	9	
Au	6 mth	7.94	333	0.12	77	167	10.5	114	220	0.18	0.008	<0.02	801	10.2	<0.002
Au,CO₂	1 day	6.08	2.4	0.03	93	167	7.8	147	215	<0.02	0.003	0.06	1017	5.1	
Au,CO₂	1 wk	6.3	3.3	0.05	109	174	9.6	164	220	0.04	0.009	<0.02	1187	6.1	
Au,CO₂	1 mth	6.24	3.3	0.05	133	178	12.3	193	240	<0.02	0.011	<0.02	1391	0.9	
Au,CO₂	6 mth	7.25	<1	0.23	145	189	17.1	207	225	0.16	0.017	0.04	1510	<0.1	<0.002
CO₂	1 day	6.05	0.2	0.03	83	159	7.5	125	15	<0.02	0.007	<0.02	1225	5.7	<0.002
CO₂	1 wk	6.49	1.8	0.03	97	167	9.5	150	14	0.05	0.009	<0.02	1466	5.9	
CO₂	1 mth	6.63	<1	0.09	118	167	10.8	175	15	0.07	0.011	0.07	1571	2.8	
CO₂	6 mth	7.48	<1	0.58	136	193	18.2	200	16	0.2	0.008	<0.02	1741	7.4	<0.002

B. Sample 1468

Addition	Time	pH	Au	Fe	Mg	Na	K	Ca	Cl⁻	Br⁻	I⁻	NO₃⁻	HCO₃⁻	SO₄²⁻	S₂O₃²⁻
	1 day	8.2	1.5	1.04	6	126	0.7	10	76	0.38	0.004	0.13	277	9.0	
	1 wk	8.07	9.7	0.17	11	163	1.5	19	77	0.59	0.029	0.22	426	12.7	
	1 mth	7.74	8.8	0.08	31	211	3.1	46	74	0.77	0.035	<0.02	741	20.1	
	6 mth	8.44	<1	0.23	44	237	4.0	55	70	1.17	0.200	0.08	872	22.1	<0.002
Au	1 day	7.78	9.0	0.04	21	200	1.9	31	285	0.32	0.012	0.07	262	8.8	
Au	1 wk	7.82	26.4	0.03	26	204	2.3	39	280	0.34	0.034	0.39	345	10.4	
Au	1 mth	7.48	913	0.06	43	234	3.6	66	300	0.38	0.007	0.13	572	16.3	
Au	6 mth	8.17	2343	0.15	65	252	8.0	89	270	0.63	0.034	<0.02	772	19.2	<0.002
Au,CO₂	1 day	6.49	4.0	0.03	154	289	4.5	247	275	0.48	0.030	1.8	1965	7.9	
Au,CO₂	1 wk	6.54	3.5	0.02	169	297	5.2	264	275	0.50	0.050	<0.02	2126	9.0	
Au,CO₂	1 mth	6.44	<1	0.06	196	297	7.1	286	285	0.49	0.272	<0.02	2201	9.2	
Au,CO₂	6 mth	7.15	<1	0.15	229	338	13.0	343	275	0.74	0.780	<0.02	2129	0.6	<0.002
CO₂	1 day	6.47	0.4	0.05	136	293	4.2	207	76	0.42	0.046	0.04	2063	8.6	
CO₂	1 wk	6.73	1.5	0.03	154	300	5.2	232	74	0.52	0.105	<0.02	2293	9.7	
CO₂	1 mth	6.89	<1	0.08	178	297	6.5	247	72	0.63	0.354	<0.02	2285	10.1	
CO₂	6 mth	7.38	<1	0.23	217	338	9.5	289	70	0.85	0.915	<0.02	2408	1.0	<0.002

C. Sample 1470

Addition	Time	pH	Au	Fe	Mg	Na	K	Ca	Cl$^-$	Br$^-$	I$^-$	NO$_3^-$	HCO$_3^-$	SO$_4^{2-}$	S$_2$O$_3^{2-}$
	1 day	8.98	2.4	0.27	4	415	2.2	4	435	2.45	0.65	3.25	336	185	<0.002
	1 wk	8.91	5.7	0.27	5	464	2.6	5	470	3.00	1.49	3.3	245	205	
	1 mth	8.43	7.7	0.13	11	530	5.3	9	480	2.70	1.32	3.7	502	215	
	6 mth	nd	15.4	0.06	33	671	7.1	11	485	2.90	2.35	3.28	872	245	<0.002
Au	1 day	8.59	198	0.03	10	545	3.2	10	685	2.65	0.39	3.55	210	200	
Au	1 wk	8.48	35.2	0.05	11	564	3.5	11	685	2.85	1.20	3.75	241	210	<0.002
Au	1 mth	8.22	73.7	0.06	23	645	5.4	17	720	2.80	1.20	3.6	483	225	
Au	6 mth	8.62	286	0.08	49	720	9.3	16	685	2.81	2.10	2.23	784	230	<0.01
Au,CO$_2$	1 day	6.54	10.3	0.02	163	868	10.0	186	665	2.70	0.23	3.6	2513	190	
Au,CO$_2$	1 wk	6.62	5.7	0.05	169	883	11.4	200	685	3.00	0.72	1.35	2625	200	
Au,CO$_2$	1 mth	6.63	12.1	0.06	253	898	14.3	232	680	2.80	0.87	<0.02	3059	195	
Au,CO$_2$	6 mth	7.4	33	0.31	356	987	21.2	236	690	2.90	2.10	<0.22	3475	205	<0.008
CO$_2$	1 day	6.61	2.0	0.05	148	838	9.5	168	460	2.70	0.58	3.75	2663	185	<0.002
CO$_2$	1 wk	6.89	4.8	0.06	154	868	10.8	175	485	2.80	0.91	<0.06	2728	200	<0.002
CO$_2$	1 mth	6.62	6.6	0.08	211	898	12.8	200	495	2.60	1.24	<0.02	3023	205	
CO$_2$	6 mth	7.49	14.3	0.31	317	927	21.2	225	460	2.72	1.80	<0.22	3465	195	<0.01